AD NUMBER
AD282297
NEW LIMITATION CHANGE
TO Approved for public release, distribution unlimited
FROM Distribution authorized to U.S. Gov't. agencies and their contractors; Administrative/Operational Use; JUN 1962. Other requests shall be referred to Army Signal Research and Development Laboratory, Fort Monmouth, NJ.
AUTHORITY
USAEC ltr, 25 Apr 1973

UNCLASSIFIED

AD 282 297

Reproduced
by the

ARMED SERVICES TECHNICAL INFORMATION AGENCY
ARLINGTON HALL STATION
ARLINGTON 12, VIRGINIA

UNCLASSIFIED

PAGES _____
ARE
MISSING
IN
ORIGINAL
DOCUMENT

SOLUBLE CARBONACEOUS FUEL-AIR

FUEL· CELL

Report No. 1

Contract No. DA 36-039   SC-89156

ARPA Order No. 247-62

Task No. OST 760200471

FIRST Semi-Annual Report, 1 Jan. 1962 - 30 June 1962

U.S. Army Signal Research and Development Laboratory

Fort Monmouth, New Jersey

ESSO RESEARCH AND ENGINEERING COMPANY

LINDEN, NEW JERSEY

NOTICE

Qualified requestors may obtain copies of this report from ASTIA.

ASTIA release to OTS not authorized.

SOLUBLE CARBONACEOUS FUEL-AIR FUEL CELL

REPORT NO. 1

CONTRACT NO. DA 36-039 SC-89156
ARPA ORDER NO. 247-42
TASK NO. OST 760200471

FIRST SEMI-ANNUAL REPORT, 1 JAN. 1962-30 JUNE 1962

OBJECT: CONDUCT RESEARCH AIMED TOWARD DEVELOPING
A SOLUBLE CARBONACEOUS FUEL-AIR FUEL CELL

Carl E. Heath
Barry L. Tarmy
Eugene L. Holt
Duane G. Levine
Andreas W. Moerikofer
Joseph A. Shropshire
Charles H. Worsham

CONTENTS

ILLUSTRATIONS

TABLES

APPENDIX ILLUSTRATIONS

APPENDIX TABLES

SECTION 1

PURPOSE

The purpose of these investigations is to perform research on the basic components of an electrolyte-soluble carbonaceous fuel - air fuel cell. The major emphasis of the program is on the simultaneous development of all components in order to optimize the performance of the entire cell and to take into account interactions between components.

This work is aimed toward the development of a practical fuel cell using a partially oxidized hydrocarbon as the fuel and air as the oxidant. The fuel must be capable of reacting completely to CO_2, be reasonably available, and pose no unusual corrosion, toxicity, or handling problems. In addition the cell must use a CO_2 rejecting electrolyte and operate at temperatures and pressures below 152°C. and 5 atm. Other objectives include high electrical output per unit weight and volume, high efficiency, long life, high reliability, reasonable cost, and ruggedness.

The program is divided into three parts. These are referred to as Tasks A, B, and C in this report. Tasks A and B are, respectively, the development of practical fuel electrodes, and the development of practical air electrodes. Included are studies on selecting the best fuel, optimizing such process variables as temperature and fuel concentrations, and establishing long term performance with air. Task C includes work carried out on establishing the basic cell design, especially with regard to the operation of all components in a single cell.

SECTION 2

ABSTRACT

Research on the soluble carbonaceous fuel - air fuel cell has concentrated on improving the performance of individual cell components and on translating these results into compatible electrode-electrolyte systems. These efforts encompass work carried out in three areas, namely the development of the fuel electrode, the development of the air electrode, and their combination into a total cell.

2.1 Task A, Fuel Electrode

A number of noble and base metals were codeposited with platinum either by electrodeposition or reduction with $NaBH_4$. Incorporating these metals improved the catalyst activity of platinum. Particularly beneficial were iron and molybdenum. The improvements, which were large at low current densities, were small at practical current densities. However, they indicate that methanol can be electrochemically oxidized at appreciable current densities with significantly lower polarizations than are possible with platinum. Other studies included the addition of MoO_3 and various surfactants to the electrolyte. The addition of MoO_3 improved the performance at low current densities, while the addition of surfactants was harmful.

Studies were also carried out to select the most suitable carbonaceous fuel or fuels for use in the fuel cell. Methanol proved to be the best overall because it gave the lowest polarization under long term operation and could be used at sufficiently low concentrations to minimize vaporization losses and to reduce its effect on air electrode performance.

2.2 Task B, Air Electrode

The air electrode being developed is a redox system based on the electrochemical reduction of a small quantity of HNO_3 dissolved in the electrolyte. Air is used indirectly for chemically regenerating HNO_3. Its advantage lies in its prospects for low polarization and long life. Its major problems are ensuring efficient HNO_3 regeneration and establishing the compatibility of HNO_3 and its reduction products with the fuel electrode.

Mechanism studies showed that the air electrode reaction rate is limited by an initial chemical reduction of undissociated HNO_3 to HNO_2, the electrochemically active species. Regeneration was limited by oxidation of NO with air to NO_2, which hydrolyzes to reform HNO_3.

Studies also were made of the effects of the major operating variables on the performance of the redox air electrode. Sulfuric acid was found superior to H_3PO_4. Increasing temperature and HNO_3 and H_2SO_4 concentrations improved performance, while increasing flow rate of oxidant proved harmful at the limiting current. Catalyst activity did not limit performance, since a number of catalysts gave similar results.

Efficient regeneration of HNO_3 is necessary for practical operation of the redox electrode and a preliminary target of 5 regenerations has been set. The effects of the main operating variables on regeneration efficiency were studied to see how this target may be achieved. It was found that regeneration varies little

3

with the flow rates of air or O_2, current density, or HNO_3 concentration. As expected O_2 gives better efficiency than air. Significant improvements in the regenerating efficiency were achieved by incorporating suitable foaming surfactants into the electrolyte or covering the electrolyte surface with glass wool.

2.3 Task C, The Total Cell

Tests were made of the effects of HNO_3 on fuel electrode performance and of CH_3OH on air electrode performance. In the absence of HNO_3 reduction products, the fuel electrode could tolerate as much as 1.8 wt.% HNO_3 when operated with CH_3OH, but failed at 0.8 wt.% or lower when reduction products were present. With ethylene glycol, only about 0.2 wt.% HNO_3 could be tolerated at the fuel electrode. Air electrode polarization increased appreciably above about 0.1 M CH_3OH.

Mathematical analysis, confirmed by experimental results, showed that the steady state CH_3OH concentration at the air electrode can be reduced to as little as 33% of that at the fuel electrode. This is accomplished by addition of the fuel to a chamber on the side of the fuel electrode facing away from the air electrode. This causes most of the CH_3OH to react on the electrode walls before reaching the bulk electrolyte.

A complete fuel cell was assembled to evaluate the operability of a CH_3OH electrode and an HNO_3 redox air electrode each in the presence of the other. Two membranes were employed to prevent bulk mixing of fuel and oxidant. Performances of both electrodes were in agreement with previously obtained half-cell data. Chemical oxidation by HNO_3 was found to be unimportant. Two problems which arose during total cell operation were a higher ohmic loss due to CO_2 flowing over the fuel electrode and a slow decline in fuel electrode activity caused by contaminants produced by acid attack on materials of construction.

These results demonstrate that a soluble carbonaceous fuel-air fuel cell is feasible. They show that cell components can be combined as a compact power cell without severe losses in efficiency due to their interactions. Of course problems still remain. The polarization occurring at the fuel electrode, the greatest source of voltage loss, must be reduced if large increases in efficiency are to be attained. In addition the fuel and air electrode performance must be demonstrated in a compactly designed cell during long term operation. However, the data obtained to date in screening new catalysts and in studying the electrodes indicate that these problems can be solved.

4

SECTION 3

PUBLICATIONS, LECTURES, REPORTS AND CONFERENCES

3.1 Lectures

Tarmy, B. L. - "The Soluble Carbonaceous Fuel-Air Fuel Cell"
Meeting of ARPA sponsored Fuel Cell Contractors,
Chicago, Illinois, February 14, 1962.

Tarmy, B. L. - "Methanol-Air Fuel Cell", 16th Annual Power
Sources Conference, Atlantic City, New Jersey,
May 23, 1962.

3.2 Conferences

January 24, 1962 - Fort Monmouth, New Jersey

Organizations Represented: United States Army Signal Research and Development
Laboratory
Esso Research and Engineering Company

The meeting was mainly a review of results obtained by Esso Research prior
to the inception of the contract. In addition, the complete program planned for the
next three months was discussed.

March 28, 1962 - Esso Research Center, Linden, New Jersey

Organizations Represented: Esso Research and Engineering Company
United States Army Signal Research and Development
Laboratory
Engelhard Industries

The purpose of the meeting was to brief Dr. H. Hunger, project engineer
for the U S. Army Signal Research and Development Agency, on our progress and future
plans in all aspects of the program. The meeting was held jointly with Engelhard
because they are working on developing fuel electrode catalysts.

May 4, 1962 - Engelhard Industries, Newark, New Jersey

Organizations Represented: Engelhard Industries
Esso Research and Engineering Company
United States Army Signal Research and Development
Laboratory

The main topic was a discussion of studies carried out by both Esso
Research and Engelhard on determining the mechanism of the reactions occurring at
the anode. It was concluded that more work is needed to determine the cause of the
large polarization loss and that this effort would be desirable.

May 21, 1962 - Esso Research Center

Organizations Represented: Esso Research and Engineering Company
California Research Corporation

Dr. L. R. Griffith of California Research visited the Esso Research Laboratory to discuss mutual interests in the field, particularly to discuss experimental techniques for assessing anode reactions.

3.3 Reports

This report is written in conformance with the detailed reporting requirements as presented in the Signal Corps Technical Requirement on Technical Reports (SCL-2101N, 14 July 1961) under the terms of our contract; these requirements differ from the usual requirements for reports issued within Esso Research and Engineering Company.

SECTION 4

FACTUAL DATA

4.1 Task A, Fuel Electrode

The use of a soluble carbonaceous fuel requires an acid electrolyte to permit rejection of the CO_2 product. This limits the selection of the catalyst to substances that are stable in acid. Although this requirement is met by several noble metals, they do not have sufficient catalyst activity. For example, although high current densities can be obtained with Pt, these are accompanied by high polarization losses. Thus studies have been carried out on developing catalysts composed of a noble metal, particularly Pt, to impart acid stability to the catalyst and a second metal, whose function is to increase the overall performance. These catalysts have been prepared by both electrodeposition and by reduction of metal salts with $NaBH_4$. Measurements have been made of the performance and physical characteristics of these catalysts. Studies were also carried out to select the most suitable partially oxygenated hydrocarbons as determined by evaluating their physical properties and by measuring their performance under a wide range of operating conditions. The final phase of this task includes studies to find the basic causes of the voltage loss at the fuel electrode.

Phase 1 - Catalysts Prepared
        By Electrodeposition

   Part a - Preparation of Fuel
           Electrodes By Electrodeposition

Electrodeposition was used to coat Pt sheet electrodes with the desired catalysts. The metals codeposited with Pt were Au, Pd, Rh, Cu, Pb, Ni, Co, and Fe. Other metals have been tried but either failed to deposit or else were chemically incompatible with Pt salt solutions.

All electrodepositions were carried out with solutions containing both H_2PtCl_6 and a salt of the other desired metal or metals. Plating conditions were determined from polarographic curves showing deposition potentials and currents for the metal species from the mixed solutions. Appendix A-1 discusses this method in detail. Prior to testing, all electrodes were cathodized in dilute H_2SO_4. Performance screening runs were carried out at 60°C. in 30 wt.% pre-electrolyzed H_2SO_4 electrolyte with 1 M spectroquality CH_3OH as fuel. The fuel electrode and the driven counter electrode were kept in separate compartments with a glass frit between to prevent H_2 evolved at the counter electrode from reaching the fuel electrode. Appendix A-2 describes the equipment used for the preparation and testing of these electrodes.

   Part b - Effect of Codeposition of
           Metals on Catalyst Activity

The incorporation of other metals into the Pt structure was found to alter its catalytic activity. In general those base metals more electropositive than H_2 improved activity while those less electropositive decreased it. In the case of noble metal adducts no trend was observed. The magnitude of the base metal effect generally depended on the electropositivity of the metal and also on the current density at which performance was measured. Thus the average Pt-Fe electrode

7

was polarized 0.070 V.[1] less than an average Pt electrode at 1 ma/cm^2, 0.030 V. less at 10 ma/cm^2, but was even at 50 ma/cm^2. Cobalt, less electropositive than Fe, caused a 0.030 V. decrease in polarization at 1 ma/cm^2 but was equal to pure Pt at 10 and 50 ma/cm^2. With the exception of Pb, the other base metals tested also exhibited activity proportional to their position in the electromotive series. In the case of noble metal adducts, Pt-Rh was superior to Pt while Pt-Au and Pt-Pd were inferior. A combination of Pt-Rh-Fe was second only to Pt-Fe at low current densities and was equivalent to Pt at high currents. Table A-1 summarizes these findings.

TABLE A-1

Activity Of Pt And Cocatalysts

Catalyst Composition	Polarization at Indicated ma/cm^2*			
	1	10	50	100
Pt-Fe	0.41	0.51	0.59	0.63
Pt-Rh-Fe	0.43	0.52	0.57	0.60
Pt-Ni	0.44	0.52	0.58	0.62
Pt-Co	0.45	0.54	0.60	0.63
Pt-Rh	0.46	0.53	0.58	0.60
Pt	0.48	0.54	0.59	0.61
Pt-Cu	0.48	0.55	0.59	0.64
Pt-Pb	0.49	0.56	0.62	0.65
Pt-Au	0.51	0.57	0.62	0.65
Pt-Pd	0.57	0.60	0.64	0.67

* Average values of all electrodes tested.

Appendix A-3 lists the deposition conditions and performances of all electrodes tested and Appendix Figure A-2 shows some performances graphically. It should be pointed out that one Pt-Fe electrode was greatly superior to any other, showing 0.11 V. less polarization than the best Pt electrode at 1 ma/cm^2, and 0.07 and 0.03 V. less at 10 and 50 ma/cm^2, respectively.

Part c - Effect of Added Metals on Tafel Slopes and Exchange Currents

In addition to variations of activity, the Tafel slopes and exchange currents were observed to be increased by those base metals which are more electropositive than H$_2$. Thus Pt-Fe had an average Tafel slope, the rate of change of polarization with the log of current, of 0.103 and an exchange current, the current density when the performance curve is extrapolated to zero polarization, of 10$^{-4.0}$ ma/cm^2. The noble metals all decreased both Tafel slope and exchange current while Pt-Rh-Fe was intermediate to Pt-Rh and Pt-Fe. These results are shown in Table A-2.

---

(1) Polarization, unless otherwise noted, is defined here and elsewhere as the difference between observed voltage and the voltage of a reversible electrode operating with the same reactant, temperature, pressure, and electrolyte. It is not the difference between observed and open circuit or standard reference electrode voltages.

TABLE A-2

Tafel Slopes And Exchange
Currents Of Pt And Cocatalysts

Catalyst Composition	-Log Exchange* Current (I_0)	Tafel* Slope(b)
Pt-Fe	4.0	0.103
Pt-Ni	4.3	0.109
Pt-Rh-Fe	5.4	0.081
Pt-Co	5.5	0.084
Pt-Pb	6.0	0.085
Pt	7.3	0.066
Pt-Rh	7.9	0.063
Pt-Cu	8.4	0.059
Pt-Au	8.8	0.058
Pt-Pd	21	0.033

* Average values of all electrodes tested.

The variations of Tafel slope and exchange current explain the improved performance of the more electropositive co-metals at lower current densities. Their higher exchange currents enable them to operate with lower polarizations at small current densities, but their higher slopes cause a more rapid decay in performance as current densities are raised.

Part d - Stability of Added Base Metals

To determine if the improved performance of Pt-Fe electrodes was due to contributions to the current density by anodic dissolution of the base metal, electrolytes from screening runs were analyzed for Fe content. In no case was the Fe equivalent to more than 0.01% of the number of coulombs passed nor did it exceed the concentrations of other metals present as trace impurities. In another test, a Pt-Fe electrode was anodically polarized in 30 wt.% H_2SO_4 in the absence of CH_3OH. The electrode could not deliver more than 0.01 ma/cm^2 before failure. Thus there was no significant dissolution of the Fe. Although other base metals were not similarly tested, their lower electropositivity will render them even less likely to dissolve than Fe.

Phase 2 - New Catalyst Techniques
and Physical Properties

Part a - Catalysts Prepared by
Reduction With NaBH$_4$

Preparation of catalysts by reduction of solutions of H_2PtCl_6 alone or mixed with salts of other metals was begun. Finely divided precipitates of Pt, Ru, Ir, and Ni or NiB as well as Pt-Fe, Pt-Co, Pt-Ni and Pt-Mo were coated onto Pt sheet electrodes by evaporation of their aqueous suspensions. A detailed description of these procedures is given in Appendix A-5.

The relative activities of Pt and Pt-Fe prepared by NaBH$_4$ were comparable to their electrodeposited counterparts, although absolute performance was somewhat reduced. Pt-Co, Pt-Ni and Ir were about equal to Pt in activity while Ru was worse.

9

The catalyst prepared by reduction of $NiCl_2$ alone, producing Ni or NiB, dissolved in the acid electrolyte. Pt-Mo had superior activity, especially at low current densities. For example, at 1 ma/cm^2, Pt-Mo was polarized only 0.22 V. after one hour of operation with 1 M CH_3OH in 30 wt.% H_2SO_4 at 60°C. Pt under the same conditions was polarized 0.48 V. and Pt-Fe, 0.41 V. Even after 72 hours the Pt-Mo electrode maintained a polarization of only 0.37 V. At higher current densities its activity approached that of Pt-Fe, although still maintaining a small advantage. Table A-3 shows these results.

TABLE A-3

Activity Of $NaBH_4$ Reduced Catalysts

Electrode	Polarization at Indicated ma/cm^2			-Log I_0	b
	1	10	50		
Pt	0.48	0.57	0.61	11.2	0.047
Pt-Co	0.55	0.59	0.65	9.4	0.058
Pt-Ni	0.55	0.61	0.68	9.1	0.060
Pt-Fe	0.41	0.55	0.60	6.5	0.073
Pt-Mo	0.22-.37	0.52	0.57	--	--
Ir	0.52	0.58	0.62	9.9	0.053
Ru	--	0.60	--	--	--

Appendix A-6 gives complete details of performance for all electrodes made by $NaBH_4$ reduction.

Part b - Analysis of CO_2 Production

An important consideration in developing an improved catalyst is whether methanol will react completely to CO_2 at polarizations less than 0.4 V. Such measurements are not possible with Pt because the current densities obtainable at low polarizations are too small. However the Pt-Mo catalyst permits such an evaluation.

The evolution of gas from the surface of Pt-Mo electrodes operating at 1 ma/cm^2 at initial polarizations as low as 0.2 V. was observed with 1 M CH_3OH in 30 wt.% H_2SO_4 at 60°C. This gas was collected over a 24 hour period in a fine glass tube initially filled with electrolyte. A funnel placed just above the electrode and joined to the lower end of the glass tube caught escaping bubbles which then rose to the top of the tube. A rubber septum at this end allowed withdrawal of samples with a hypodermic syringe.

During the 24 hour collection time, the Pt-Mo electrode decayed to 0.37 V. polarization. An average polarization of 0.32 V. was achieved during this time. Analysis was performed by gas chromatography and comparison with known samples showed the presence of CO_2 far in excess of the CO_2 content of air or the electrolyte. It is significant that no such gas evolution was observed on Pt electrodes until polarizations of over 0.5 V. were reached.

Part c - Physical Properties
of Catalysts

Measurements of electrode capacitance, X-ray fluorescence and diffraction, emission spectrum, and particle size were made in an effort to find the cause of performance variations produced by the addition of other metals to Pt.

Because insufficient catalyst samples were available for conventional surface area measurements, the areas of several Pt-black and Pt-Fe electrodes were determined by their relative double-layer capacities. The electrodes were prepared in the normal manner by electrodeposition from solutions containing H_2PtCl_6 or H_2PtCl_6 + $FeCl_3$. Constant current charging curves were measured oscillographically in 30 wt.% H_2SO_4 at 60°C. Comparison of the values obtained with the double-layer capacity of a bright Pt electrode allowed calculation of the surface area amplification factors for the deposited electrodes.

The experimental results showed both types of electrodes to have about the same surface areas. This similarity for Pt and Pt-Fe catalysts means that the observed differences in exchange current between Pt and Pt-Fe of about 10^4 is not due to a quantitative surface area effect. Table A-4 shows these catalysts compared with bright Pt.

TABLE A-4

Relative Areas Of Pt And Pt-Fe

Electrode	Capacitance Millifarads/cm^2	Surface Area Ampl. Factor
Bright Pt	0.85	1
Pt Black	47 ± 12	56 ± 14
Pt-Fe	53 ± 15	62 ± 18

X-ray fluorescence measurements indicated that the Pt-Fe catalyst has a much larger Fe content than the Pt catalyst. This was confirmed by emission spectroscopy which showed only about 10 ppm of Fe in the Pt catalysts, but about 1% in Pt-Fe. X-ray diffraction studies showed no difference in structure between Pt and Pt-Fe catalysts. However, this is expected since Pt-Fe alloys have almost exactly the same lattice constants as pure Pt.

Also, preliminary results from an electron microscopic study now under way indicate only slight differences in average particle size. Thus the differences in catalytic activity appear to be due to either electronic interaction between the elements or a difference in the number of active sites.

Part d - Addition of Metal
Ions to Electrolyte

Previous work has indicated that addition of polyvalent metal cations can improve fuel electrode performance by altering the double layer structure or by participating in catalytic redox reactions. Therefore 0.1 wt.% of $Al_2(SO_4)_3$, $MgSO_4$, and MoO_3 were added to 1 M CH_3OH solutions in either 30 wt.% or 4 wt.% H_2SO_4 at 82°C. The performances of these fuel-electrolyte mixtures were evaluated with an electrodeposited Pt black electrode.

It was found that only MoO_3 affected CH_3OH performance. In 30 wt.% H_2SO_4 it caused higher polarization at low current densities with no changes at the high

11

currents. Upon reimmersing the electrode in fresh electrolyte containing no added MoO_3, a decrease in polarization out to 2 ma/cm^2 was observed. In 4 wt.% H_2SO_4, MoO_3 addition resulted in less polarization out to 4 ma/cm^2. These results are shown more fully in Table A-5.

TABLE A-5

Effect Of Added MoO_3 On Fuel Electrode Activity

System	Polarization @ Ind. ma/cm^2				
	0	0.2	2	4	20
30 wt% H_2SO_4 - 1 M CH_3OH	0.23	0.42	0.51	--	0.57
30 wt% H_2SO_4 - 1 M CH_3OH - 0.1 wt% MoO_3	0.37	0.42	0.49	--	0.57
30 wt% H_2SO_4 - 1 M CH_3OH	0.11	0.15	0.38	--	0.57
4 wt% H_2SO_4 - 1 M CH_3OH	0.14	0.27	0.46	0.49	0.57
4 wt% H_2SO_4 - 1 M CH_3OH - 0.1 wt% MoO_3	0.11	0.15	0.30	0.38	0.57

This improvement could not have been caused by oxidation of Mo, since it is in its highest valence state. Apparently, a small amount of adsorbed MoO_3 lessens the polarization especially in the more concentrated acid.

Phase 3 - Fuel Variable Studies

Methanol represents only one of many possible partially oxygenated hydrocarbons that might be employed. However its low boiling point could result in significant fuel loss at the temperature required for water removal. Further it suffers from the fact that it cannot be prevented from migrating to and consequently affecting the cathode. Therefore studies were carried out to determine whether these problems could be eliminated and/or whether other fuels might be more suitable.

Part a - Fuel Selection

A survey was made to select the best fuel or fuels for further study. The possibilities included a wide variety of mono-and polyhydric alcohols, aldehydes, ketones, and acids. The selection was based upon a consideration of their physical properties, cost, chemical reactivity, and selectivity to CO_2.

The following criteria were used in making the selections:

Minimum Boiling Point to Prevent Fuel Loss   60°C.
Minimum Solubility in Water   5 Volume %
Minimum Specific Power at 70% Efficiency   1·KWH/Lb
Maximum Cost at 70% Efficiency   20¢/KWH
Minimum Limiting Current on Pt-Black   100 ma/cm^2
Selectivity to CO_2 Approximately 100%

The complete tabulation of the results of this survey are presented in Appendix A-7. The fuel costs used were obtained from the Chemical Engineering News Quarterly Report on Current Prices (October 30, 1961). Most of the data on reactivity and selectivity to CO_2 were obtained prior to the inception of the contract with the government.

12

Of the oxygenated hydrocarbons considered, three met all requirements. These are methanol, ethylene glycol, and glycerin. All are completely soluble in acid. Methanol boils at 65°C., yields 1.9 KWH/Lb at 70% efficiency, costs 2.3¢/KWH at this efficiency, and goes completely to CO_2 at all current densities. Ethylene glycol boils at 197°C., yields 1.7 KWH/Lb, costs 8¢/KWH, and produces CO_2 as the major product at all current densities. Finally, glycerin boils at 290°C., is completely soluble, yields 1.6 KWH/Lb, costs 15.3¢/KWH, and produces CO_2 as the main product at comparable current densities. Table A-6 summarizes the characteristics of these fuels.

TABLE A-6

Characteristics Of Fuels Selected For Further Study

Fuel	Boiling Point °C.	Solubility Gms/100 Ml 30 wt% H2SO4	Specific Power KWH/Lb	Cost ¢/KWH	Maximum ma/cm^2	% Selec. to CO$_2$
Methanol	65	∞	1.9	2.3	300+	97+
Ethylene Glycol	197	∞	1.7	8.0	300+	100[1]
Glycerin	290	∞	1.6	15.3	300+	100[1]

(1) Intermediates produced but reacted to CO_2 at about 50% overall conversion level in batch operation.

The remaining fuels considered failed to meet one or more of the criteria used in making the selection. On the basis of this survey, further studies were carried out with methanol, ethylene glycol, and glycerin.

Part b - Effect of H$_2$SO$_4$ Concentration on Methanol Performance

The electrochemical oxidation of 0.5 molar methanol was studied in 4 to 72 wt.% H_2SO_4 at 82°C. to determine the effect of acid concentration on electrical performance. These data, combined with air electrode performance and electrolyte resistivity measurements, are needed to predict optimum electrolyte composition for power production.

The performance data were obtained in a cell containing 10 cm diameter platinum sheet electrodes separated by a 1.9 cm electrolyte space contained in a pyrex glass spacing ring. The anode had a catalyst coating of 8 mg/cm^2 of electrodeposited platinum black. The cathode was driven with direct current and had no catalyst coating. The equipment is shown in more detail in Appendix A-8.

The study showed that fuel electrode polarization increased with higher acid strengths. Also, the higher the current density the greater the effect. At 10 ma/cm^2 increasing the H_2SO_4 concentration from 4 to 72 wt% resulted in 80 millivolts more polarization. Similarly, 50 ma/cm^2 and 100 ma/cm^2 currents resulted in 120 and 190 millivolt increases, respectively, as shown in Figure A-1.

13

Figure A-1

Effect Of H_2SO_4 Concentration On Methanol Performance

Fuel = 0.5 gm moles CH_3OH/liter
Temp. = 82°C.

100 ma/cm²

50 ma/cm²

10 ma/cm²

(Y-axis: Volts Polarization, 0.50 to 0.75)
(X-axis: Wt.% H_2SO_4, 0 to 80)

Wt.% H_2SO_4
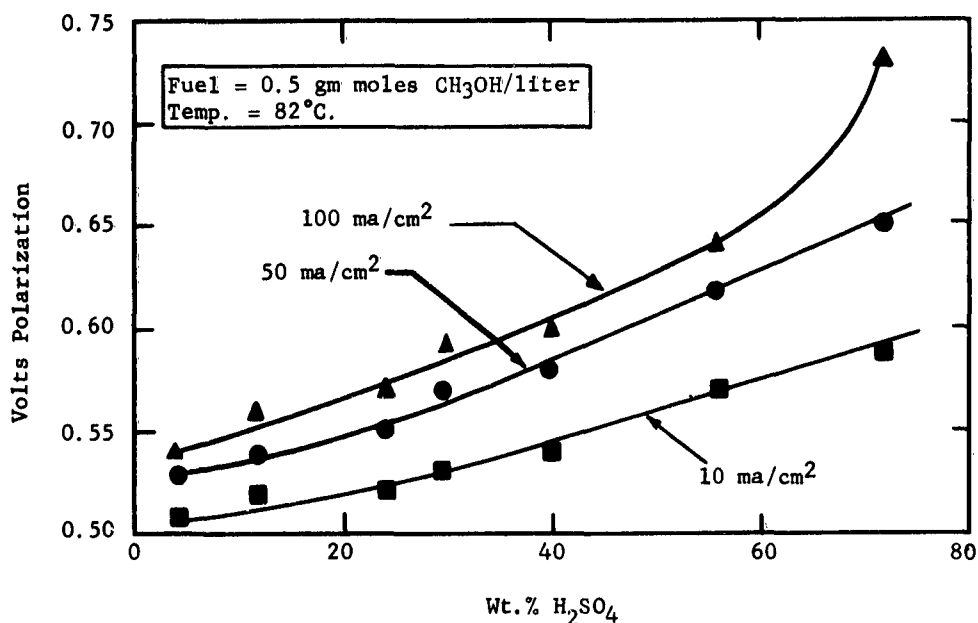
Complete data on these tests are given in Appendix A-9.

Part c - Effect of Methanol
        Concentration on Performance

There are two difficulties in the use of methanol as the fuel. First, its low boiling point, 65°C., could result in appreciable vaporization losses at the temperatures required to remove the product water and, secondly, methanol in concentrations above 0.5 vol.%*significantly decreases air electrode performance. Both problems might be circumvented if the concentration of methanol required at the fuel electrode could be sufficiently reduced without impairing performance.

Therefore tests were carried out to determine the effects of current density, acid concentration, and temperature on the concentration of methanol below which the polarization is increased by 20 mv. This was established by measuring at constant current the potential of the electrode as a function of methanol utilization. The experiments were carried out in 20 to 50 wt.% H_2SO_4 (2.4 to 7.2 molar) at 82 and 93°C. using initial methanol concentrations of 0.60, 2.0 and 12 volume %. The performances at these concentrations were very similar when tested in 30 wt.% H_2SO_4 at 82°C. for several currents as shown in Table A-7.

---

* Methanol concentration will be expressed in volume % whenever design problems are involved. One volume % is equivalent to 0.25 M.

Effect Of Methanol
Concentration On Performance

Methanol in 30 wt% H_2SO_4 at 82°C.			
Volume %	0.6	2.0	12.0
or Gm moles/liter	0.15	0.5	3.0
Volts Polarization at:			
10 ma/cm^2	0.49	0.53	0.55
50 ma/cm^2	0.55	0.57	0.57
100 ma/cm^2	0.60	0.59	0.58

The performance was relatively unaffected by variations in methanol concentrations within the range of 0.6 to 12 vol. %. At lower methanol concentrations, polarization rapidly increased and was dependent on the current density and acid strength used. The dependence on current density is illustrated in Figure A-2 in which the fuel electrode polarization is shown at current densities of 30 and 100 ma/cm^2 as a function of methanol concentration in 30wt% H_2SO_4 at 82°C. Current

Figure A-2

Effect Of Methanol Concentration
And Current Density On Polarization
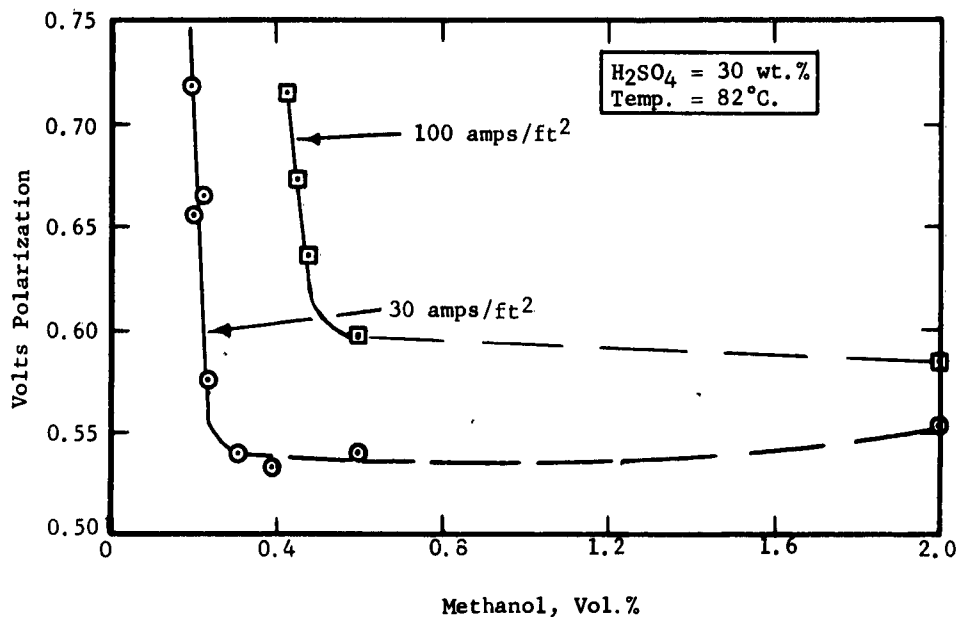
density was found to be the prime variable affecting the minimum methanol concentration, with temperature and acid concentrations below 20 wt.% H_2SO_4 having little effect. At 10 ma/cm^2 and 30 wt.% H_2SO_4 the minimum concentration was 0.14 vol. % while at 100 ma/cm^2 with the same electrolyte the minimum concentration had increased to only 0.52 vol. %. These data are summarized in Tables A-8, A-9, and A-10.

TABLE A-8

Effect Of Current Density On
Minimum Methanol Concentration

Current Density ma/cm^2 at 82°C.	Minimum Methanol Concentration to Avoid Severe Polarization in 30 wt.% H_2SO_4, Volume %
10	0.14
30	0.26
50	0.32
100	0.52

TABLE A-9

Effect Of H_2SO_4 Concentration On
Minimum Methanol Concentration

Wt.% H_2SO_4 at 82°C.	Minimum Methanol Concentration to Avoid Severe Polarization at ~50 ma/cm^2, Volume %
20	0.30
30	0.32
40	0.44
45	0.50
50	0.56

TABLE A-10

Effect Of Temperature On
Minimum Methanol Concentration

Temperature, °C. Using 30 wt.% H_2SO_4	Minimum Methanol Concentration to Avoid Severe Polarization at 50 ma/cm^2, Volume %
82	0.32
93	0.32

16

The conversion of methanol to CO_2 was measured in the foregoing tests and showed that the methanol reaction is essentially complete. At the current densities, acid strengths, and temperatures studied the measured oxidations to CO_2 accounted for 93 to 104% of the measured currents. These measurements are summarized in Appendix A-10.

Part d - Ethylene Glycol As a Fuel

The performance of ethylene glycol was measured at temperatures from 49 to 118°C. in 4 to 30 wt.% H_2SO_4 using electrodeposited platinum black catalyst. Ethylene glycol was added to the electrolyte in concentrations from 0.5 to 12.8 molar (2.8 to 71 vol.%) and reacted to fuel conversion levels ranging from 8 to 77%. Experiments were also carried out to determine the performance of glycolic acid, which was a major intermediate in the electrochemical oxidation of ethylene glycol. The tests were made in the cell previously described in Part b and shown in Appendix A-8.

The best performance was achieved with 6 molar ethylene glycol in 4 wt.% H_2SO_4 at 82°C. The polarization from theory at open circuit amounted to 0.08 volts while 0.63 volts polarization at 100 ma/cm^2 was obtained as long as glycol conversion was less than 2%. Ethylene glycol in 3 molar concentration showed very similar performance. Lower concentrations significantly increased polarization as shown in Table A-11.

TABLE A-11

Effect Of Ethylene Glycol
Concentration On Performance

4 wt.% H_2SO_4 at 82°C.

Ethylene Glycol, M/L	0.5	1.0	3.0	6.0
Volts Polarization at:				
10 ma/cm^2	0.59	0.57	0.55	0.56
50 ma/cm^2	1.15	0.67	0.61	0.59
100 ma/cm^2	--	0.74	0.63	0.63

Increasing acid strength, however, improves the performance of 0.5 molar ethylene glycol. At 82°C. and 50 ma/cm^2 the polarization was reduced from 1.15 to 0.64 volts on increasing the acid strength from 4 to 30 wt.% as shown in Table A-12.

TABLE A-12

Effect of Acid strength On Ethylene Glycol Performance
0.5 Molar Ethylene Glycol at 82°C.

H_2SO_4 Concentration, wt.%	4	24	30
Volts Polarization at:			
10 ma/cm^2	0.59	0.65	0.60
50 ma/cm^2	1.15	0.71	0.64
100 ma/cm^2	--	0.73	0.66

Increasing the temperature also reduced the polarization. At 50 ma/cm^2, 0.5 molar ethylene glycol in 30 wt.% H_2SO_4 showed a 0.19 volt reduction in polarization on increasing the temperature from 49 to 82°C. Under the same conditions, a further increase in temperature to 93°C. gave only a slight additional reduction in polarization as shown in Table A-13.

TABLE A-13

Effect Of Temperature On Ethylene Glycol Performance
0.5 Molar Ethylene Glycol in 30 wt.% H_2SO_4

Temperature,°C.	49	65	82	93
Volts Polarization at:				
10 ma/cm^2	0.69	0.63	0.60	0.60
50 ma/cm^2	0.82	0.68	0.64	0.62
100 ma/cm^2	--	0.73	0.66	0.63

The data on effects of ethylene glycol concentration, acid strength, and temperature on performance are shown more completely in Appendices A-11, A-12, and A-13.

The foregoing results were obtained at ethylene glycol conversion levels of less than 2%. Therefore, tests were made to determine the products of the reaction and the effect on performance at higher conversion levels. The only intermediates found were glycolic and formic acids, the remaining product being CO_2. With 1 molar ethylene glycol in 4 wt.% H_2SO_4 at 82°C., at about 50% coulombic conversion level, the rate of CO_2 production equaled the rate of glycol disappearance. Ethylene glycol in 3 molar concentration required about a 40% conversion level before CO_2 production equaled glycol disappearance. These data are summarized in Table A-14. In 30 wt.% H_2SO_4, an equivalence between CO_2 rejection and current could not be obtained at reasonable polarizations, as shown in Appendix A-14.

TABLE A-14

Effect Of Conversion On Glycol Performance
4 wt.% H_2SO_4 at 82°C.

Ethylene Glycol M/L	3.0
Current Density, ma/cm^2	115
% Coulombic Conversion for Current to Equal CO_2 Rejection	40

% Coulombic Conversion	Volts Polarization
0.0	0.56
3.3	0 58
10.7	0.79
18.1	0.91
33.0	1.02
40.4	1.16

These data show that the polarization increases sharply as the ethylene glycol is reacted and products are produced. Analysis of the run solution showed the presence of an amount of glycolic acid equivalent to about 25% of the current while the formic acid present accounted for 0.7%.

Since glycolic acid was found as an intermediate, it was tested for performance in 0.5 molar concentration in 30 wt.% H_2SO_4 at 82°C. The glycolic acid was unreactive; the limiting current was 0.3 ma/cm^2. Subsequent tests carried out with the same electrode using methanol as the fuel showed that the electrode had lost almost all its catalytic activity but could be restored by cleaning. These data suggest that the electrochemical oxidation of ethylene glycol may be adversely affected by the formation of glycolic acid as an intermediate.

Part e - Glycerin As a Fuel

The performance of glycerin was measured at 82°C. in 4 wt.% H_2SO_4 using electrodeposited platinum black catalyst. The glycerin was added to the electrolyte in concentrations of 1.0 and 3.0 molar. The cell used for the tests was the same as used for the ethylene glycol and methanol studies shown in Appendix A-8.

Glycerin exhibited a performance comparable to ethylene glycol. At 100 ma/cm^2, 1 M glycerin was polarized 0.63 volts and 3 M, 0.60 volts. These performance data are summarized in Table A-15.

19

TABLE A-15

The Electrical Performance Of Glycerin
4 wt.% H_2SO_4 at 82°C.

Glycerin, M/L	1.0	3.0
Current Density	Volts Polarization	
10 ma/cm^2	0.56	0.55
50 ma/cm^2	0.61	0.59
100 ma/cm^2	0.63	0.60

The coulombic conversion level for equal rates of CO_2 production and glycerin disappearance was only about 29% for 1 M glycerin. Product analysis of the run solution showed the presence of an amount of glyceric acid (identification not positive) equivalent to 34% of the current and of an amount of formic acid equivalent to 7%. However, as in the case of ethylene glycol, polarization became severe as conversion increased and intermediates built up. Propylene glycol was also tested and showed a performance similar to glycerin and ethylene glycol.

Part f - The Effect of Surfactants on Performance

Mechanism studies have indicated that inadequate H_2O adsorption on the fuel electrode surface may limit the rate of CH_3OH oxidation. Therefore a series of surfactants, which could influence H_2O adsorption, were tested for their effect on CH_3OH performance. This work also served to check the compatibility of the fuel electrode towards surfactants added to the air electrode. Those surfactants which appeared most promising for HNO_3 regeneration were tested using 0.1 wt.% concentrations. The tests were carried out in 30 wt.% H_2SO_4 and 1 M CH_3OH at 82°C. using a platinized Pt electrode. The equipment is described in Appendix A-15.

All the surfactants tested adversely affected the fuel electrode performance, particularly at higher current densities. For example, although a 1:12 tridecyl alcohol-ethylene oxide adduct decreased the open circuit polarization by 20 mv, it increased the polarization by 50 mv at 10 ma/cm^2 and by 150 mv at 30 ma/cm^2. The other compounds tested harmed performance even more. Therefore membranes would be required to prevent migration of surfactants from the air electrode to the fuel electrode. These results are summarized in Table A-16.

TABLE A-16

The Influence Of Surfactants On
Methanol Electrode Performance

Surfactant	Polarization @ Indicated ma/cm^2				
	0	1	10	30	50
None	0.15	0.43	0.51	0.58	0.62
T.D. 120	0.13	0.45	0.56	0.73	0.80
T.D. 150	0.18	0.55	0.61	0.74	0.83
R.S. 710	0.21	0.55	0.66	0.75	0.82
R.S. 610	0.24	0.51	0.59	0.68	0.75
Benax 2A1	0.19	0.56	0.66	0.81	0.91
D.M. 730	0.18	0.58	0.66	0.82	0.94
D.M. 880	0.23	--	0.62	0.72	0.76

These surfactants are described in detail in Task B.

Phase 4 - Mechanism Studies

The electrode reaction on platinized Pt, the catalyst best known to date, is characterized by an inability to produce significant currents at polarizations less than 0.4 to 0.5 volts from the calculated reversible potential for the reaction. In an effort to reduce the polarization, a study of the reaction mechanism has been initiated with the hope that a better understanding of the limiting reaction step can lead to the development of improved catalysts.

These experiments have centered about chronopotentiometric studies in which electrode polarization is recorded as a function of time at a constant appli·d current. The reactions of methanol and two possible reaction intermediates, formaldehyde and formic acid, were investigated by this technique. The experiments were carried out in pre-electrolyzed 30 wt.% H_2SO_4 at 25 and 8ℓ°C. The test electrode, a platinized Pt wire sealed in a glass holder, was pulsed with a constant current supplied by a high voltage source (30-200 volts D.C.). The transient potentials were measured against a reference electrode in the system, displayed on an oscilloscope, and photographed. In this study polarizations are reported versus the normal hydrogen reference electrode, which is designated as N.H.E. A diagram of the experimental arrangements is shown in Appendix A-15. Using this chrono-potentiometric technique investigations were made of the oscillatory behavior of the electrode previously found to occur above 1 ma/cm^2, and of the oxidation of adsorbed single layers of fuel.

Part a - Oscillatory Behavior of
Oxygenated Hydrocarbons

Initial attempts to observe potential transients occurring with 1 M methanol in 30 wt.% H_2SO_4 at 25°C. indicated the existence of a voltage oscillation phenomenon. At a high constant current (e.g., 160 ma/cm^2) the polarization increased to 0.86 volts, then, after a few seconds, decreased to 0.60 volts. Thereafter, a spontaneous oscillation in the voltage developed between these levels and continued with a frequency of 0.29 cycles/sec. The amplitude and frequency of the oscillations could be varied by changing the current, the frequency increasing with current. Formaldehyde and formic acid also exhibited similar phenomena, the oscillations being more easily excited with these fuels. The low polarization region of the oscillation wave with formic acid was in general of much greater duration than with formaldehyde or methanol. Using formaldehyde at current densities of 1000 ma/cm^2, amplitudes of 0.5 volts and frequencies as high as 15 cycles/sec were obtained. Existence of the

21

oscillations is temperature dependent, the oscillations occurring most easily at low temperatures. Typical natural oscillatory behaviors for methanol, formaldehyde, and formic acid are shown in Appendix Figures $\overline{A}$-3, $\overline{A}$-4, and $\overline{A}$-5.

In an effort to understand the causes of these voltage oscillations and to define the conditions under which they occur, a series of experiments was carried out in which the electrode was loaded and open circuited repetitively. The duration of the respective conditions was controlled by a mercury relay operated either manually or by a variable frequency pulse generator. Using this arrangement, conditions were found where single oscillation waves were reproduced artifically. These conditions are typified by the following example using 1 M formaldehyde at a current density of about 80 ma/cm^2. The electrode was polarized to about +0.92 volts vs N.H.E. Upon open circuiting, the voltage was allowed to rise to +0.4 volts vs N.H.E. Under these conditions, application of the next load resulted in a voltage-time wave similar to the natural oscillation. If, however, the open circuit voltage was allowed to rise to less positive values than 0.4, no oscillation wave was observed on the subsequent loading. Methanol and formic acid gave similar behavior. With methanol and formic acid, the potential could be decreased to less than +0.3 volts for short periods of time with evidence of the oscillation wave remaining upon loading again. With proper timing of the open circuit pulse it was possible to obtain a time averaged polarization which was less than the normal polarization of the electrode. Typical oscillographs of this behavior for the three fuels are shown in Appendix Figures $\overline{A}$-6, $\overline{A}$-7, $\overline{A}$-8, and $\overline{A}$-9.

The shapes of the naturally occurring oscillation waves, of methanol, formaldehyde, and formic acid are suggestive of diffusion limited waves as shown in Figures $\overline{A}$-3, $\overline{A}$-4, and $\overline{A}$-5. Therefore the wave shape was analyzed in terms of the effect of voltage on $\log (1 - (t/\tau)^{1/2})$. Here t is the time in seconds at which the potential is measured and τ is the transition time of the wave, as detailed in Appendix A-16. Delahay[1] has indicated that for a diffusion controlled irreversible reaction, this would plot as a straight line. For methanol and formic acid it was found that the E vs $\log (1 - (t/\tau)^{1/2})$ plot had a slope approximately 0.12 volts/decade. Assuming a charge transfer coefficient of one-half, this would correspond to a one electron-charge transfer limited reaction. In contrast, formaldehyde did not produce a significantly straight line. Figure A-3 shows the plots for all three materials.

---

[1] Delahay, P. "New Instrumental Methods In Electrochemistry", p. 187, Interscience 1954.

22

**Determination Of Kinetic Parameters
For Natural Oscillation Wave**

1 M Fuels   30 wt.% H2SO4   T = 25°C.

Figure legend:
- ■ = CH3OH; slope = 0.111
- ▲ = HCOOH; slope = 0.126
- ● = CH2O; slope --

Y-axis: $1 - (t/\tau)^{1/2}$

X-axis: Volts
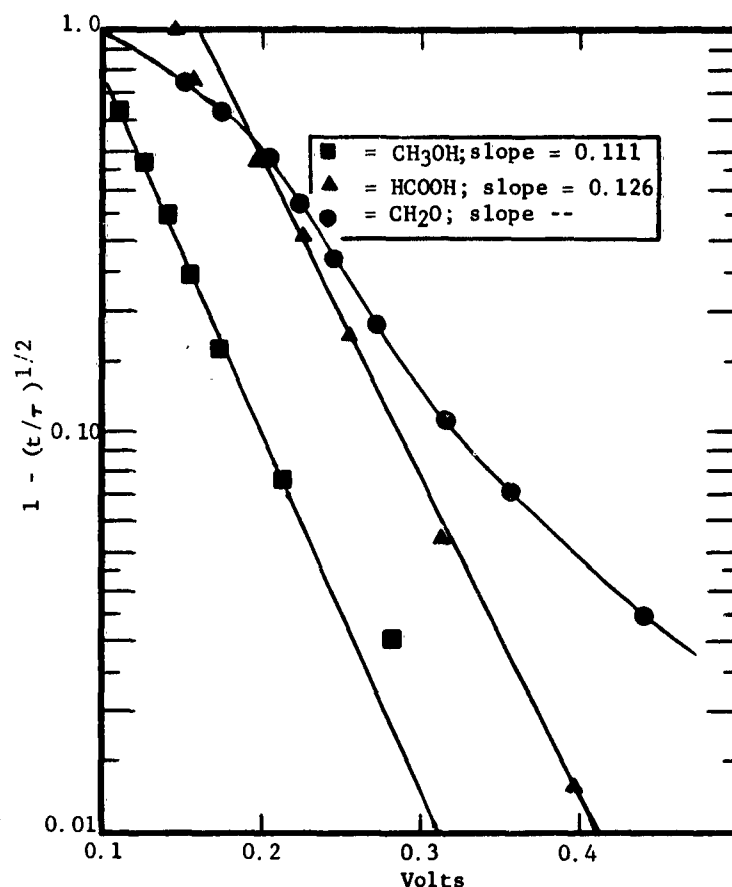
A series of experiments was also carried out in which anodic current pulses in excess of the limiting current were applied to the electrode. Analysis of the potential transients produced can often dictate the choice between diffusion and kinetic control. The product of current times the square root of the wave transition time should remain constant for simple diffusional control but would vary with current density if kinetic or adsorption limitations exist. (see Appendix A-16). It was found that $i\tau^{1/2}$ was a relatively stable constant for 1 M formaldehyde fuel, but decreased with increasing current for methanol and formic acid, as shown in Figure A-4. Thus it appears that the maximum current is diffusion controlled for formaldehyde but not for the other two fuels. As indicated in a later section, the slow adsorption of methanol may account for its behavior.

Dependence Of $i \tau^{1/2}$ On Current Density

25°C.   1 M Fuels   30 wt.% H_2SO_4
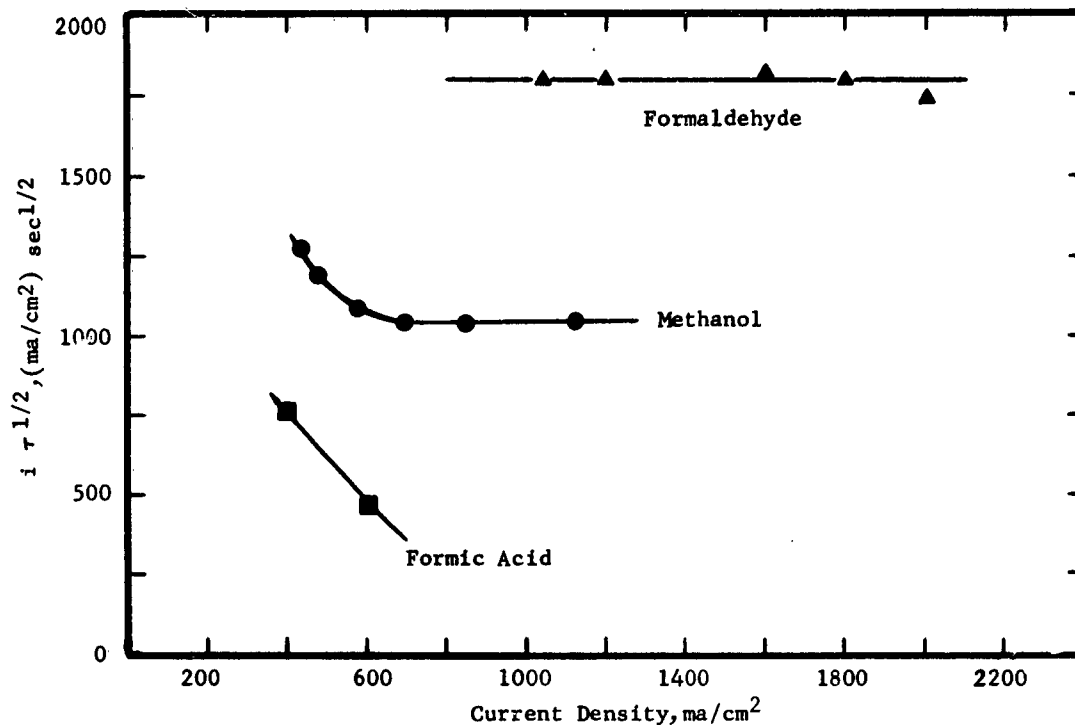
Part b - Single Layer Experiments

    Experiments were carried out in which the adsorption of fuels on platinized Pt was studied by anodic stripping of preadsorbed fuel layers. Anodic stripping is the removal of substances present on the electrode by electrochemical oxidation at constant current. In this technique the electrode was first polarized to a predetermined potential in degassed 30 wt.% H_2SO_4. It was then removed and placed in the fuel solution for a given time. At the end of the specified time it was removed, rinsed quickly in degassed 30 wt% H_2SO_4 solution, replaced in the cell and anodically stripped. Methanol, formaldehyde and formic acid were studied under these conditions at 25°C.

    The data, as shown in Table A-17, indicate that formaldehyde and formic acid adsorb most strongly, and that adsorbed layers of these fuels give about twice as many coulombs as methanol on stripping. Thus methanol requires about 30 seconds to reach adsorption equilibrium while formaldehyde and formic acid reach equilibrium in 1 second or less. If we assume two electron oxidation of the respective fuels, then methanol would appear to occupy less sites on the electrode than either formaldehyde or formic acid.

CONSTANT CURRENT STRIPPING
OF ADSORBED FUEL LAYERS

$T = 25°C$. 30 wt.% H_2SO_4

Electrode Polarized to + 0.5 Volts Versus N.H.E. Before Adsorption		
Fuel	Adsorption Immersion Time, Sec	Millicoulombs in Film
CH_3OH (1 M)	1	4
	5	10
	15	12
	30	14
	60	14
	300	14
HCHO (1 M)	1	28
	5	32
	15	32
	30	34
	60	38
	300	32
	1800	32
HCOOH (1 M)	1	30
	5	26
	15	32
	30	34
	60	32
	300	34

Oxidation of the adsorbed fuel layer began only at potentials near those at which oxidation of the platinum surface was observed. A variation in fuel did not have a large effect on the observed oxidation potential. Typical stripping transients are shown in Figure A-5.

Figure A-5

Typical Anodic Stripping Transients

25°C.   30 wt.% H_2SO_4
i = 80 ma/cm^2
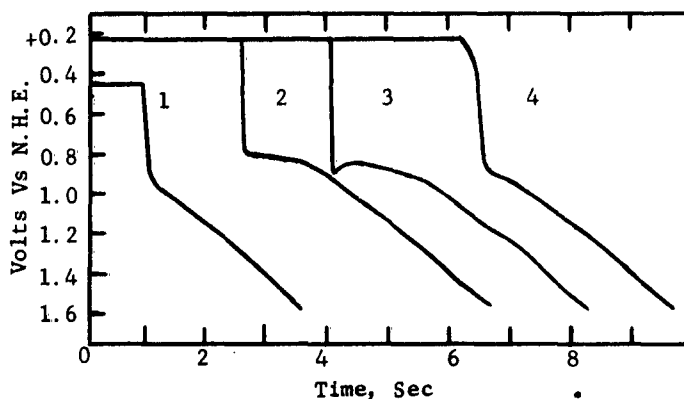
(1) Standard (30 wt.% acid) No fuel
(2) Formic Acid
(3) Formaldehyde
(4) Methanol

In experiments carried out with methanol alone, preconditioning of the electrode at certain potentials before adsorption affected the number of coulombs obtained in subsequent stripping. The layers adsorbed on surfaces preconditioned near +0.4 and +0.9 volts showed the least amount of oxidizable substance in subsequent stripping. The electrodes prepared at these levels also showed the best potentials after reimmersion in the cell. These results are shown in Table A-18.

TABLE A-18

Stripping Characteristics Of Adsorbed Methanol

1 M CH_3OH 25°C.   30 wt.% H_2SO_4

Potential Vs N.H.E. Of Pretreat	Potential Vs N.H.E. 5 Min. After Re-immersion	Millicoulombs Stripped (Excess Over Oxide)
+0.2	+0.40	32
0.3	0.24	24
0.4	0.21	18
0.5	0.24	24
0.6	0.32	32
0.7	0.25	26
0.8	0.215	24
0.9	0.23	20
1.0	0.29	30
1.1	0.32	26
1.2	0.305	29

Observations indicate that all three fuels under certain conditions exhibit open circuit polarizations 0.2 - 0.3 volts lower than those at which significant current can be drawn. These low polarization levels have often been ascribed to impurities in the system, notably hydrogen gas present from purification of solutions by electrolysis. Since these studies using adsorbed methanol layers and preconditioned electrodes were carried out in pre-electrolyzed and degassed acid, these low polarization conditions should not be due to an impurity in the system.

4.2 Task B, Air Electrode

The air electrode being developed for the methanol-air fuel cell is a unique redox system based on the electrochemical reduction at the cathode of a small quantity (1 wt.%) of HNO_3 dissolved in the H_2SO_4 electrolyte. Air is used indirectly in the cell for chemically regenerating HNO_3 from its reduction products. The advantage of this redox electrode over electrodes which reduce oxygen directly lies in its prospects for low polarization and long life. However, to use this system in a practical cell, the regeneration of HNO_3 must be highly efficient and HNO_3 and its reduction products must be prevented from interfering with the electrochemical oxidation of methanol.

Phase 1 - Mechanism of HNO_3 Redox Electrode

Part a - Experimental Technique

In earlier studies it was discovered that the performance of the O_2 electrode was considerably enhanced through the use of a mixed H_2SO_4 - HNO_3 electrolyte. While the system showed considerable promise, problems were encountered in obtaining good regeneration efficiency and maintaining compatibility with conventional fuel electrodes. Therefore, it was decided that the most fruitful approach would be to study thoroughly the mechanism of the HNO_3 reaction so as to determine which reactions are limiting and then use this information to find ways of circumventing the problems.

The study was carried out using chronopotentiometry on platinum and proprietary metal microelectrodes in the H_2SO_4-HNO_3 system. Chronopotentiometry involves the measurement of potential-time transients at the electrodes during constant current pulses. The transients obtained indicate the potentials at which species in solution are oxidized or reduced and can be related quantitatively to the concentration of a given species. Thus observations on the nitric acid reaction under a variety of conditions could provide information on the intermediates and products of the reaction and on the reaction steps involved.

A representative curve of the time dependency of potential is shown in Figure B-5.

For such a typical product wave where the potential-time transient is governed by diffusion of a species to the electrode:

$$\frac{i \, \tau^{1/2}}{c_R^o} = \frac{\pi^{1/2} \, n \, F \, D^{1/2}}{2}$$

where,

i = current, amperes / cm^2
τ = wave transition time, sec
c_R^o = concentration, moles/cc
n = number of electrons in reaction
F = Faraday constant, 96,500 coul./equiv.
D = diffusion coefficient of species, cm^2/sec

Simplifying the equation results in the expression

$$i\ \tau^{1/2}\ =\ K'c_R^o$$

K' = a combined constant.

Therefore, the concentration of a reacting species is calculable from the measurements of current and the transition time.

The experiments were carried out in 29 wt% H_2SO_4-1 wt% HNO_3 at 82°C., except where otherwise indicated. The test electrode, either platinum or proprietary metal, was pulsed with a constant current supplied by a 200 volt D.C. source. Transients, measured against a standard reference electrode in the system, were displayed on an oscilloscope and photographed. A diagram of the experimental arrangement is shown in Appendix Figure B-1.

Part b - The HNO_3 Reduction Process

The initial experiments showed that HNO_3 was not directly reduced electrochemically. The electrode voltage, expected to produce a diffusion controlled transient with transition time in excess of 100 seconds under the conditions employed, changed by more than 0.8 volts in times much less than 1 second. During the transition, the cathodic operating potential of the normal HNO_3 redox electrode (0.9 - 1.0 V. versus Normal Hydrogen Electrode) was passed with no indication of reaction. Typical transients are shown in Figures B-1 and B-2.

Figure B-1

Cathodic Transients On Smooth Platinum

System: 29 wt.% H_2SO_4 - 1% HNO_3 82°C.
          O_2 Saturated Solution

Time, Sec

29
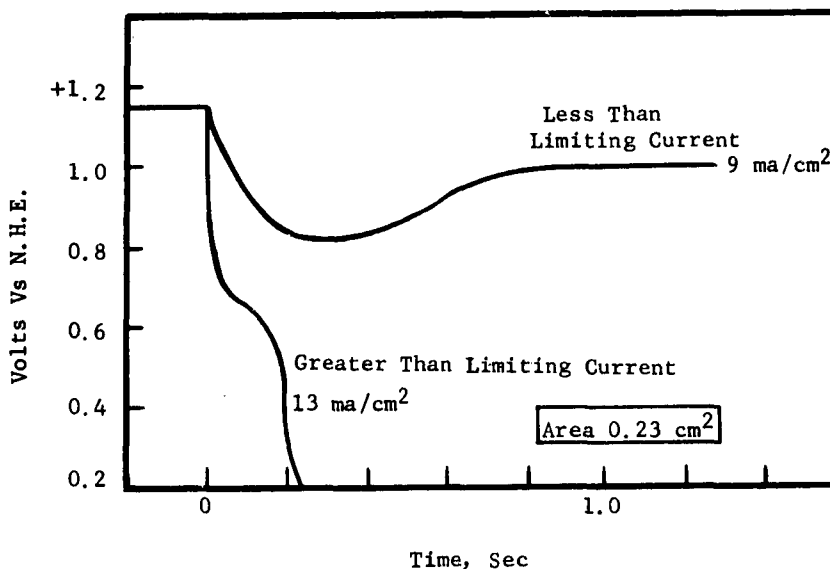
Cathodic Transients On The Proprietary Electrode

System: 29 wt.% H_2SO_4 - 1% HNO_3 82°C.
           O_2 Saturated Solution
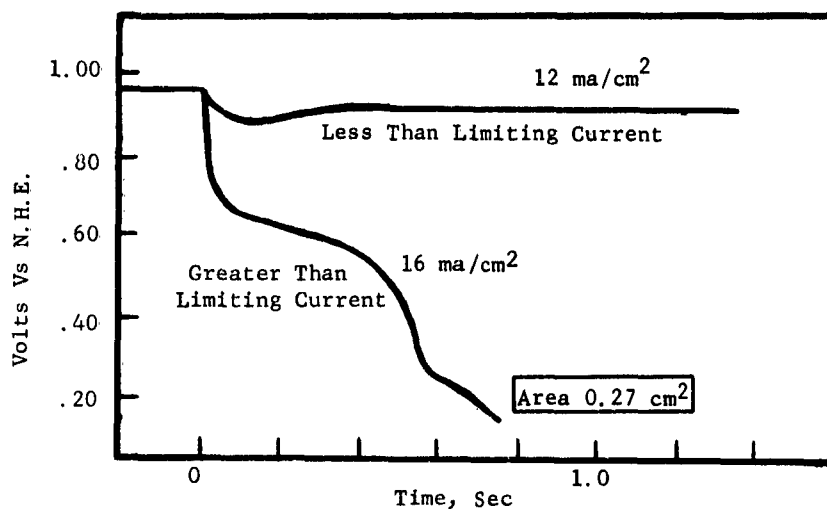
The electrochemical reaction on both catalysts was shown to be auto-catalyzed. Under loads less than the limiting current, the electrode polarized several tenths of a volt and then, still at constant current, recovered to a normal polarization. Apparently the electrochemical reaction product was able to chemically react to produce more reactant. Thus the absence of the diffusion controlled voltage transient previously mentioned was due to the fact that the reaction is controlled by a chemical step preceding the electrochemical one. This also explains other results showing that the limiting current decreases with stirring, since removal of local product by agitation decreases the rate of the auto-catalytic step. Typical transients are shown in Figures B-3 and B-4.

Figure B-3

Autocatalytic Nature Of HNO_3
Cathode Reaction-Single Pulse Behavior

System: 29wt.% H_2SO_4 - 1% HNO_3 82°C.
           Proprietary Electrode, Area = 0.27 cm^2
           O_2 Saturated Solution
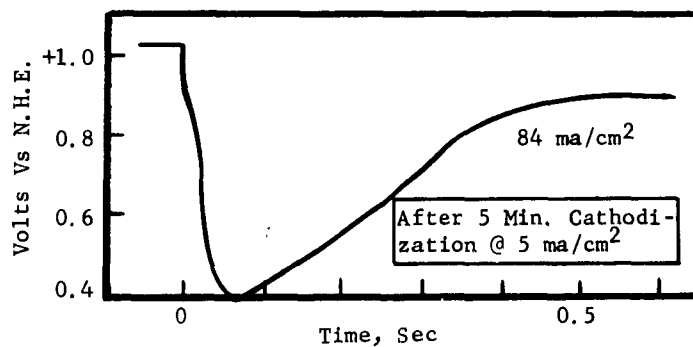
Figure B-4

Autocatalytic Nature Of HNO_3
Cathode Reaction-Repetitive Pulse Behavior
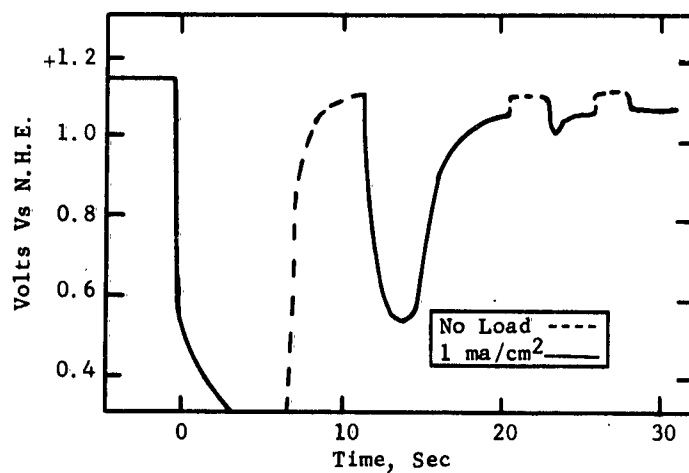
Using anodic current pulses, observations were made of the products of HNO_3 reaction. By producing the product at an auxiliary electrode (cathode) and observing its oxidation at the microelectrode it was possible to follow the appearance and disappearance of product under atmospheres of nitrogen and oxygen. It was found that the main product was a volatile compound which reacted with oxygen. Thus, although the product was displaced from solution by both oxygen and nitrogen, removal by oxygen was faster, indicating probable reaction. On this basis, the most probable product was nitric oxide (NO). These product transients and concentration-time curves are shown in Figures B-5 and B-6.

31

Figure B-5

Typical Product Wave

System: 29 wt.% H_2SO_4 - 1% HNO_3 82°C.
Proprietary Metal Electrode - 0.27 cm^2
Carbon Auxiliary Electrode
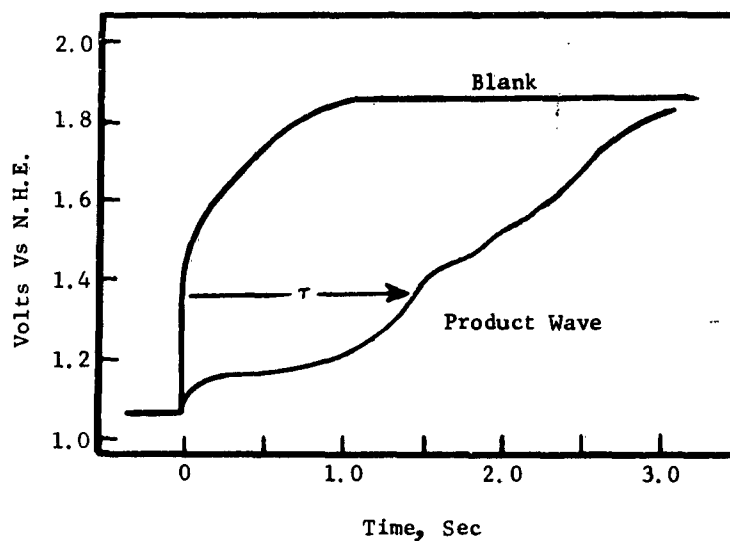
Figure B-6

Analysis Of The Product Transient

32
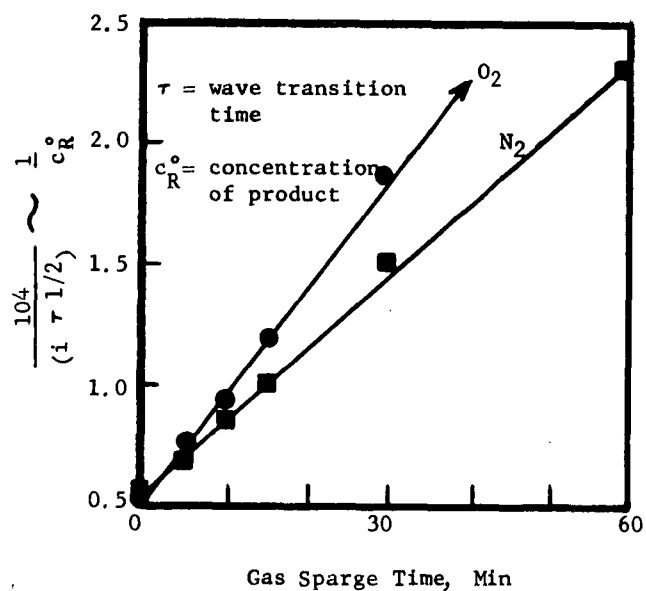
The confirmation of NO as the reaction product was obtained by experiments in solutions saturated with NO by means of a sparger. Anodic chronopotentiograms obtained on the proprietary metal electrode in 30 wt.% H_2SO_4 saturated with NO were identified as those produced by the reaction products. Furthermore, saturation of 29 wt.% H_2SO_4 - 1 wt.% HNO_3 solution with NO eliminated the autocatalytic behavior observed previously on proprietary metals. The overall HNO_3 reaction was shown to give a linear dependence of limiting current on HNO_3 concentration as shown in Figure B-7. (See also Task B, Phase 3.)

Figure B-7

Relationship Of Limiting Current And HNO₃ Concentration

System: 29 wt.% H_2SO_4 Variable HNO_3 82°C.
Proprietary Metal Electrode - Area 0.27 cm^2

Limiting Current, ma
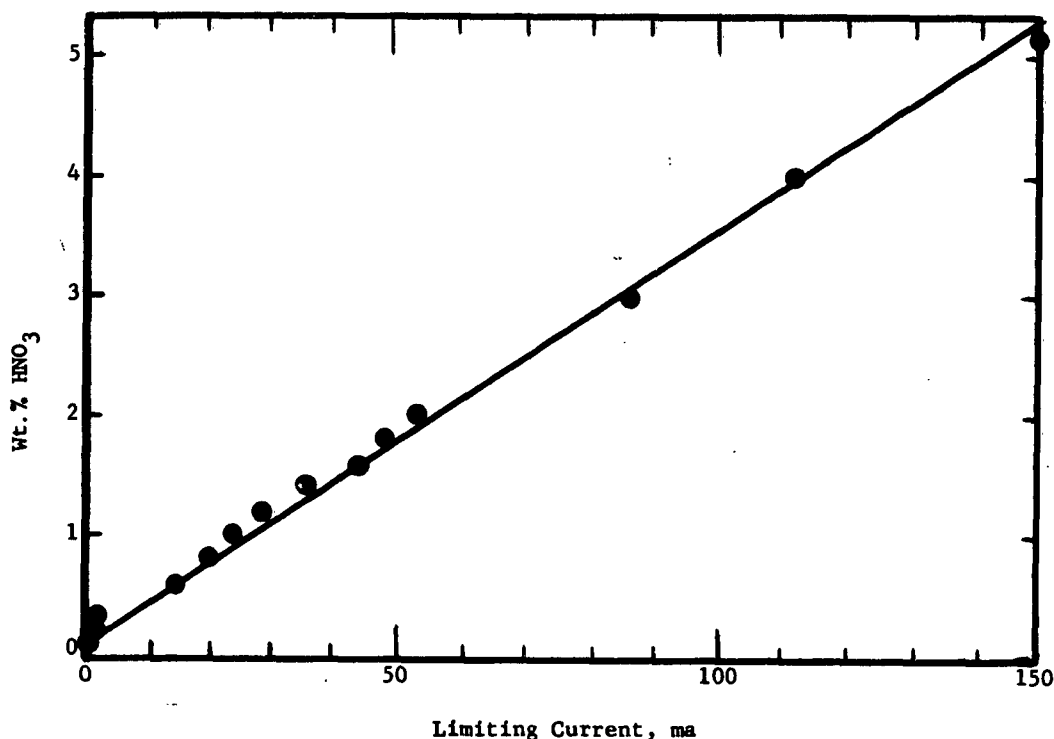
Part c - The Proposed Mechanism

The linear relation between limiting current and HNO_3 concentration, in conjunction with the autocatalytic nature of the reaction and the knowledge that the reaction product was NO, indicated the electrochemical reactant to be HNO_2. The following reaction mechanism is proposed:

Initiation: $HNO_3 \xrightarrow{\text{heat}} HNO_2$ (trace) + $1/2\ O_2$

Electrochemical: $HNO_2 + H^+ + e \longrightarrow NO + H_2O$

Chemical: $2NO + HNO_3 + H_2O \longrightarrow 3\ HNO_2$
(limiting)

33
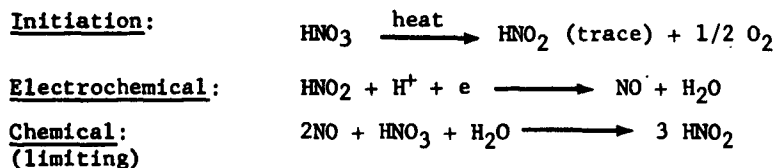
Previous data have also shown the limiting rate of the overall reaction to be dependent on H_2SO_4 concentration. Thus, the HNO_3 must enter the chemical reaction as the undissociated species, its concentration being controlled by the overall proton activity of the solution.

This mechanism satisfies all observations on the system to date. Since the reaction product is NO, regeneration must take place by NO reacting with O_2 to form NO_2 and the subsequent reaction of NO_2 with H_2O to form HNO_3.

Phase 2 - Air Electrode Performance

Studies were made of the effects of the major operating variables on the performance of the HNO_3 redox air electrode. The results are needed in the selection of the optimum conditions for operating the complete fuel cell. The parameters examined included electrolyte, temperature, HNO_3 concentration, electrode structure, gas flow rate, and gas type.

Part a - Experimental Technique

The influence of these variables was evaluated in terms of their effect on electrode performance. All runs were carried out in a concentric cell with a driven 5 cm x 7.6 cm platinum basket anode. Smooth Pt, platinum black, carbon, and several proprietary electrodes were employed. The electrolyte generally was a mixture of 29 wt.% H_2SO_4 and 1 wt.% HNO_3. When the effect of HNO_3 concentration was studied, a range of 0.2 to 2.0 wt.% HNO_3 was used. The temperature, normally maintained at 82°C., was varied from 30° to 106°C. during the temperature study. Oxygen, N_2, and NO were sparged into the solution through a glass frit. The experimental equipment, similar to that used in the regeneration studies, is shown in Appendix Figure B-2.

Part b - Electrolyte Selection

Previous work has shown that both H_2SO_4 and H_3PO_4 are suitable electrolytes for use with CH_3OH fuel electrodes. Sulfuric acid offers the advantage of higher electrolytic conductivity while H_3PO_4 is less corrosive. The electrolytes tested consisted of 1 wt.% HNO_3 mixed with either H_2SO_4 or H_3PO_4. The concentrations of these acids were varied from 5 to 50 wt.% H_2SO_4 and from 10 to 60 wt.% H_3PO_4. In addition, tests were made with 30 wt.% H_2SO_4 in which the HNO_3 concentration was varied between 0.1 and 2 wt.%.

It was found that O_2 electrode performance improved with increasing acid concentration in all cases. With 1 wt.% HNO_3, increasing the H_2SO_4 concentration from 5 to 50 wt.% decreased the polarization at open circuit from 0.07 volts to 0.01 volts and at 30 ma/cm^2 from 0.45 volts to 0.14 volts. Performance in H_3PO_4 was poorer. However, increasing its concentration from 10 to 60 wt.% resulted in polarization decreases from 0.12 to 0.03 volts at open circuit and from 0.06 to 0.20 volts at 30 ma/cm^2, as shown in Figure B-8. These responses of performance to acid concentration generally passed through a plateau. The reason for this is that the HNO_3-O_2 electrode reaction is limited by both H^+ activity and the concentration of NO_3^- so that the direct reduction of O_2 on the electrode controls at the lower acid concentrations. As indicated in Appendix B-1, the current densities at which this occurs depend upon the composition of the electrolyte.

Figure B-8

**The Effect Of Acid
Concentration On Oxygen Electrode Performance**

Oxygen   Electrode Polarization, Volts
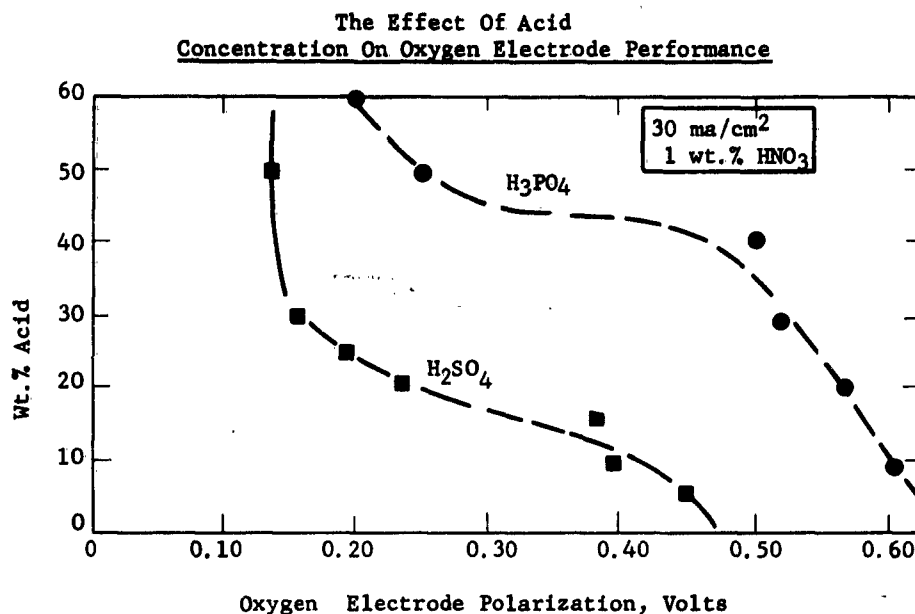
Part c - **Effect of Temperature**

Measurements were made of the limiting current at several different temperatures. These data are needed to establish the maximum performance obtainable. They also can be used to determine the energy of activation and hence the nature of the limiting step.

Performance was measured using electrolyte saturated with either O_2, N_2, or NO for two hours before each run. It was found that the limiting current increased exponentially with the reciprocal of temperature, as shown in Figure B-9. The activation energy amounted to 10 kcal/mole above about 60°C., with either N_2 or O_2, and 50°C. with NO, and 15 kcal/mole below these temperatures. Apparently there is a change in the limiting step at a specific temperature range depending on whether the solution is saturated with NO or contains only as much as is made at the cathode. The increase in limiting current at the higher temperatures corresponds to about 5% per °C.

Figure B-9

Effect Of Temperature On Limiting Current Of Oxygen Electrode
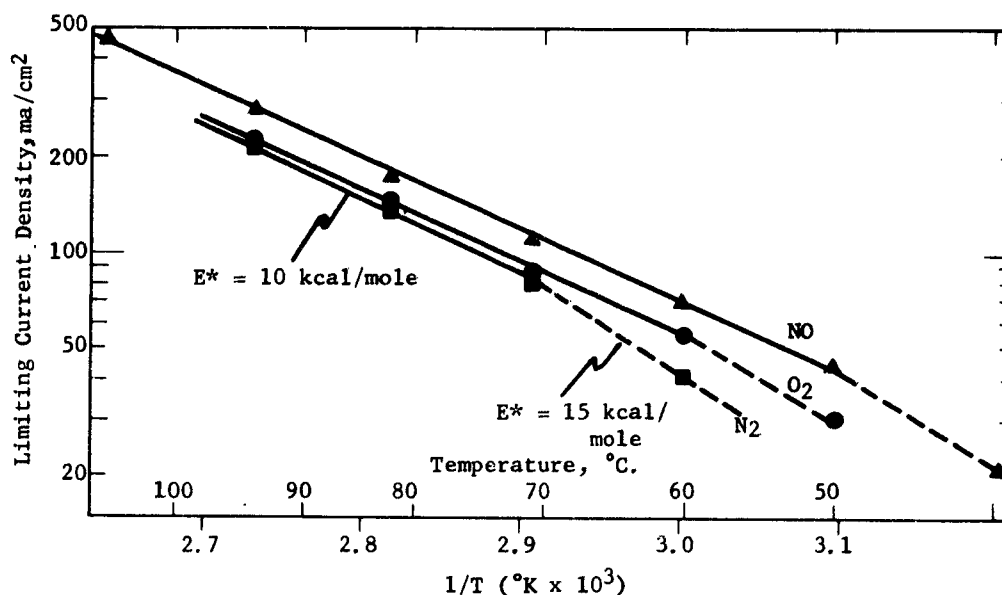
The absolute rates were comparable for N_2 and O_2 but were 25% greater with NO. This current increase with NO appears to be the result of a higher concentration of HNO_2 formed by the reaction $2NO + HNO_3 + H_2O \longrightarrow 3HNO_2$.

Part d - Effects of HNO_3 Concentration and Electrode Structure

Since the HNO_3 redox electrode performance is limited by a slow chemical reaction in the electrolyte rather than an electrochemical step, performance should be the same for different electrode structures, providing active catalysts are used. This was checked with a number of different electrode structures at HNO_3 concentraticns up to 2.0 wt.%. Three types of electrodes were employed: smooth metal electrodes, electrodes coated with finely divided metals, and a variety of porous and nonporous carbon electrodes.

Several catalysts were tested,including Pt, W, Pb, and Ta. In addition, a proprietary metal catalyst was also used. As expected, the three smooth metal electrodes which were catalytically active (Pt, W, and the proprietary catalyst) and the four carbon structures give the same performance. Figure B-10 shows that a straight line plot of limiting current versus wt.% HNO_3 is obtained for these materials above about 0.2 wt.%. The limiting current density measured at 1 wt.% HNO_3 was 80 ± 5 ma/cm^2. Lead with a PbO_2 coating, and a Ta electrode were inactive. The platinized Pt electrode (6 mg Pt/cm^2) and the proprietary electrode show a much greater slope in Figure B-10. Below about 0.2 to 0.4 wt.%, a constant current density of approximately 2 ma/cm^2 is obtained. In this region, O_2 is directly reduced on the catalyst.

Figure B-10

Effect Of HNO₃ Concentration And
Electrode Structure On Limiting Current

(Plot: Limiting Current Density, ma/cm^2 (y-axis, 0 to 250) vs. Wt.% HNO₃ (x-axis, 0 to 2))

Symbol	Electrode Type
●	Smooth Metals
■	Porous Carbons
▲	Finely Divided Metals
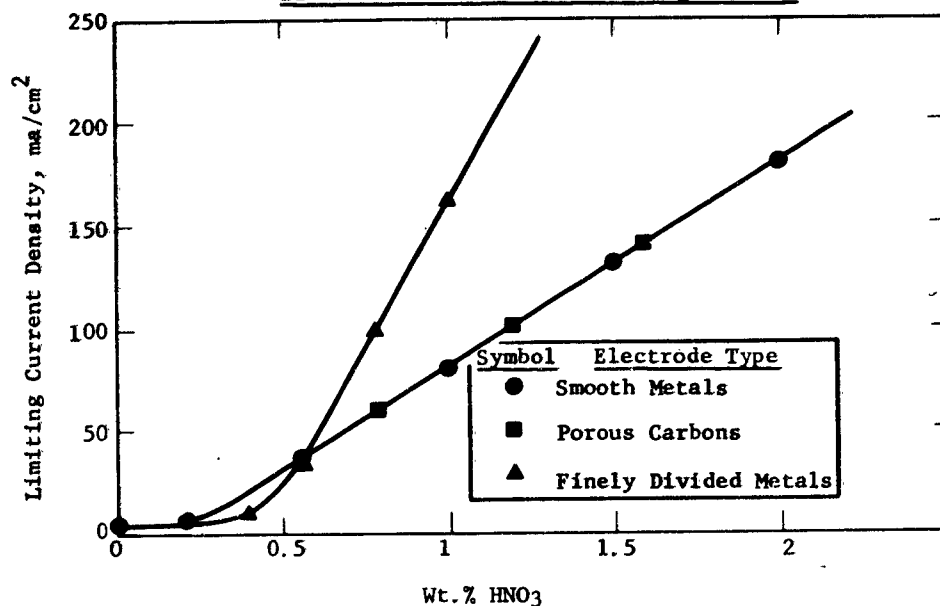
An additional acid resistant material was also tested as an air electrode. This was a graphite cloth clad with a stainless steel current collector. The tests were made at 82°C. in 30 wt.% H2SO4 - 1 wt.% HNO3. The graphite cloth exhibited good catalyst activity. This electrode was polarized 0.11 volts at open circuit and 0.26 volts at 10 ma/cm^2. However, its limiting current, as expected, amounted to only about 70 ma/cm^2. The stainless steel current collector is not a catalyst for the reaction and would not contribute to this performance.

Part e - Effect of Gas
        Flow Rate

A program was carried out to study the effects of O_2, N_2, and NO flow rate on performance. Gas flows ranging from 0 to 100 cc/min were used. The results, as given in Figure B-11, show that the limiting current decreases with greater O_2 and N_2 flow rate and improves with NO flow rate. The loss in limiting current is larger for N_2 than O_2. For example, the current density decreased from 150 ma/cm^2 at no flow to 115 ma/cm2 and 85 ma/cm^2 at 60 cc/min using O_2 and N_2, respectively. NO, on the other hand, improved the limiting current to 175 ma/cm^2 at 60cc/min. Appendix Figure B̄-2 shows these results in detail.

At a polarization of 0.21 volts, as shown in Figure B-12, O_2 reached a maximum current density of 82 ma/cm^2 at 20 cc/min and then decayed back to 75 ma/cm^2 at 100 cc/min. Nitrogen reached 73 ma/cm2 at 10 cc/min followed by a decay to 60 ma/cm^2 at 50 cc/min. Above this flow rate no further change in current density occurred. Nitric oxide caused a steady improvement in current density with flow rate, reaching 95 ma/cm^2 at 20 cc/min and 98 ma/cm^2 at 100 cc/min. These results are also given in Appendix Figure B̄-3.

37

Figure B-11

Effect Of Flow Rate On Limiting Current

82°C.
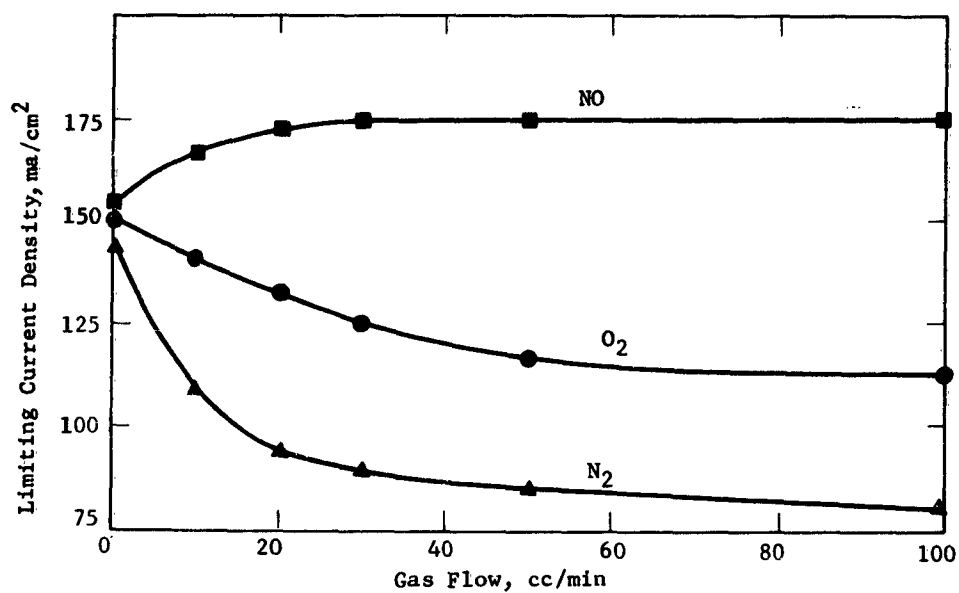
Figure B-12

Effect Of Flow Rate On Current Density At Constant Polarization

82°C.

38
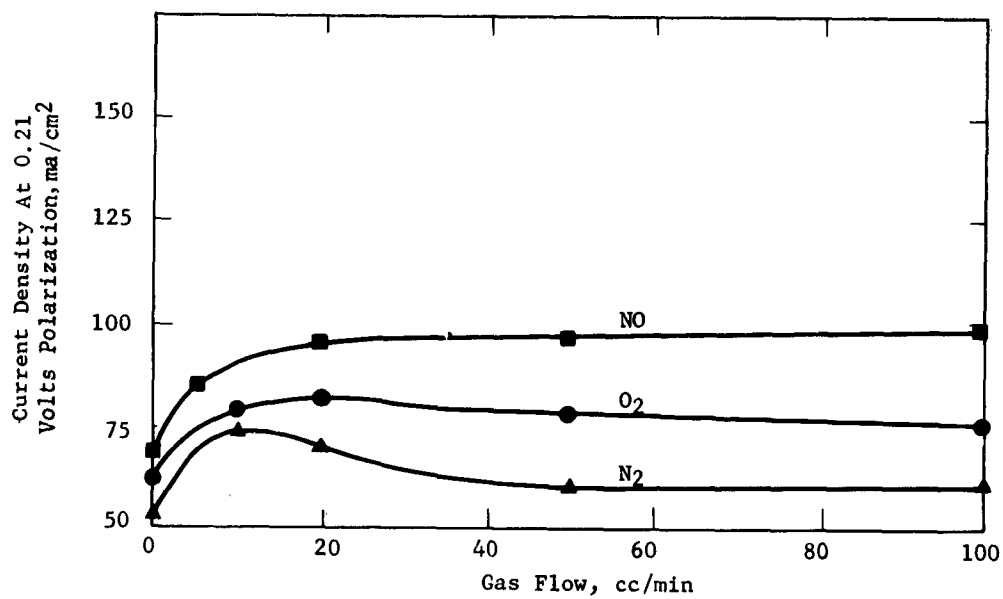
Phase 3 - HNO3 Regeneration

Because of the nature of the reactions and limitations on the size of the fuel cell, it is neither practical nor desirable to completely regenerate all the HNO_3. The extent of regeneration, therefore, is a compromise between the amount and cost of HNO_3 that must be added to the cell and the cell volume required for regeneration. The most important factor would be the quantity required since HNO_3 would in effect be a fuel.

The preliminary target is 5 regenerations. By this we mean that 5 coulombs of electricity must be produced per coulomb obtainable if HNO_3 were consumed and not regenerated. At this efficiency, approximately 1 lb of HNO_3 will be required per hour to operate a 1 KW unit at a cost of 10¢/KWH. This would represent a total consumption, including CH_3OH, of 2.5 lbs/hr and would be approximately the same total fuel requirement as a gasoline engine. Further increases in efficiency would reduce these requirements. For logistical reasons a low HNO_3 demand would be desirable and further research will aim at higher targets than the 5 regenerations adopted as an initial goal.

Table B-1 shows the fuel requirements in lb/hr of HNO_3 and HNO_3 + CH_3OH in a 1 KW unit for various numbers of regenerations.

TABLE B-1

The Effect Of Regeneration On Fuel Requirements

Coulombs Coulomb Equiv. of HNO3	Fuel Requirement, Lb/Hr For 1 KW Unit	
	HNO3	HNO3 + CH3OH
1	5.0	6.5
5	1.0	2.5
10	0.5	2.0
20	0.3	1.8

The successful development of the HNO_3 redox air electrode also requires that the HNO_3 be regenerated efficiently in a small volume. Therefore experiments were carried out to both determine which steps are limiting regeneration and to evaluate the effects of the major operating variables and electrode design on the efficiency of this process.

The main variables tested included gas type, gas flow rate, current density, HNO_3 concentration, the type of electrode structure, and the effect of added surface area. The experiments were made under standardized conditions to compare results on a relative basis. Briefly, the runs were made using the same equipment used to measure electrode performance (See Appendix B-4). Air and O_2 were both used as oxidants in an electrolyte of 30 wt.% pre-electrolyzed H_2SO_4 and 1 to 1.6 wt.% HNO_3. The gas flow rate was normally 30 cc/min, a value at least several fold in excess of the amount required for complete regeneration. The temperature was maintained at 82°C. and the constant current applied was approximately 30 ma/cm^2. The polarization of the air electrode decreased with HNO_3 concentration and varied between 0.2 and 0.4 volts.

Part a - Limiting Step of
HNO3 Regeneration

Previous work has shown that HNO_3 is regenerated by the reaction of NO with O_2 and the subsequent hydrolysis of NO_2. Further studies were made to determine which of these steps limits the efficiency of HNO_3 regeneration. Reaction rates were measured at 82°C. with 100cc of 30wt.% H_2SO_4 equilibrated with N_2. The reaction of NO_2 with water was studied by sparging the gas into the electrolyte at a constant rate. In similar studies of the reaction between NO and O_2, the gases were introduced separately into the electrolyte. The rate of HNO_3 production was determined by measuring its concentration at various time intervals.

These experiments indicated that the reaction of NO with O_2 is the slow step in regeneration. The rate of HNO_3 production from NO_2 was 3 moles/hour per liter of electrolyte. This was three times the rate obtained when NO and O_2 were added. These data are shown in Appendix Figure B-3.

Part b - Effects of Gas
Flow Rate

Experiments were carried out using O_2 and air to determine the effect of gas flow rate on the efficiency of regeneration. It was found that the efficiency of regeneration was only slightly affected by variation in gas flow rate. Increasing the O_2 flow rate from 4.3 to 13 times the stoichiometric O_2 rate (10 to 30 cc/min) increased the regeneration efficiency from 3.1 to 4.2 coulombs/coulomb equivalent to HNO_3 consumed. At a comparable air rate (30 cc/min), which is 2.6 times the stoichiometric amount of O_2, the efficiency decreased to 2.1. With a 17-fold excess of air blown into solution (200 cc air/min), there was no regeneration, and the regeneration efficiency amounted to only 1.1 coulombs/coulomb equivalent to HNO_3 consumed. Table B-2 illustrates these results.

TABLE B-2

Effect Of Flow Rate On Regeneration

Electrode	Gas	Gas Flow Rate cc/min	Excess Over Stoichiometric	Regeneration Efficiency Coulombs Measured / Coulomb Equivalent to HNO_3 Consumed
Plat. Pt	O_2	10	4.3	3.1
Porous Carbon	O_2	10	4.3	2.5
Plat. Pt	O_2	30	13	4.2
Porous Carbon	O_2	30	13	4.0
Plat. Pt	Air	30	2.6	2.1
Plat. Pt	Air	200	17	1.1

Part c - Effect of Current Density
and HNO3 Concentration

Several runs were made at 12.5 and 16 ma/cm^2 and compared with the previous experiments that were performed at 30 ma/cm^2 to find the effect of current density on regeneration efficiency. No significant differences were observed.

One experiment was performed starting with 1.6 wt.% rather than 1 wt.% HNO$_3$, but no improvement was observed at the higher initial HNO$_3$ concentration. Table B-3 illustrates these findings on platinized Pt and porous carbon electrodes.

TABLE B-3

Effect Of Current Density And
HNO$_3$ Concentration On Regeneration

4.3 Fold Excess O$_2$ Over Stoichiometric   29 wt.% H$_2$SO$_4$ 82°C.

Electrode	HNO$_3$ wt.%	ma/cm^2	Coulombs Coulomb Equiv. to HNO$_3$ consumed
Platinized Pt	1.0	32	4.2
Platinized Pt	1.0	12.5	5.3
Platinized Pt	1.0	12.5	4.0
Porous Carbon	1.6	26	4.6

Part d - Effect of Electrode Structure

The most efficient regeneration was obtained using a wetproofed, uncatalyzed, porous carbon electrode. This results from the intimate contacting obtainable when O$_2$ is forced through the large pores of the electrode. The regeneration efficiency amounted to 18.2 coulombs/coulomb equivalent to HNO$_3$ consumed. This is substantially higher than the 4 coulombs/coulomb equivalent to HNO$_3$ consumed achieved with metal electrodes or 2.7 with porous carbon electrodes which received O$_2$ by bubbling the gas around the electrode. However, the efficiency with air amounted to only 1.9 coulombs/coulomb equivalent to HNO$_3$ consumed. Table B-4 summarizes these results.

TABLE B-4

Effect Of Electrode Structure On Regeneration

Electrode	Gas	Coulombs/ Coulomb Equivalent to HNO$_3$ Consumed
Porous Carbon	O$_2$	2.7
Platinized Pt	O$_2$	4.2
Porous Diffusional	O$_2$	18.2
Carbon	Air	1.9

Part e - Effect of Surfactants

Studies were carried out to test whether foaming agents can be used to improve contacting and permit longer residence times with bubbles of foam and thus improve regeneration. The foam furnishes electrolyte in the walls of the bubbles, thus supplying a path for returning HNO$_3$ to the bulk electrolyte.

41

The experiments were run under conditions used for all regeneration experiments. In this way results can be compared on a relative basis. The surfactant was added in concentrations ranging between 0.02 to 2 wt.%, either directly into the solution or via the sparger.

A large number of surfactants were tested, with many significantly improving the regeneration efficiency. Platinized Pt electrodes were used with O₂ as the oxidizing agent. These results are tabulated in Appendix B-5. Two surfactants, sodium dodecylated oxydibenzene disulfonate (Benax 2A1 of Dow Chem. Co.) and a monophosphate ester of tridecyl alcohol-ethylene oxide adduct in a mol ratio of 1:10 (General Aniline's GAFAC RS 710) gave the highest increase in regeneration efficiency and were relatively stable in the electrolyte. With 1 wt.% Benax 2A1 added directly to the solution and O₂ flow, regeneration improved from 4.2 without the added surfactant to 10.2 coulombs/coulomb equivalent to HNO₃ consumed. This was improved further to 24 coulombs/coulomb equivalent to HNO₃ consumed by sparging the O₂ downward from an injector placed above the electrode. With 1 wt.% GAFAC RS 710 as well as with its related tridecyl alcohol-ethylene oxide adduct, TD-90, 10.5 coulombs/coulomb equivalent to HNO₃ consumed were measured.

Other surfactants tested included fluorocarbon surfactants that gave large amounts of foam at low surfactant concentration, but drained too rapidly and were not chemically stable. Kelzan, a polysaccharide, was used alone and in combination with GAFAC RS 710 to increase the viscosity of foam and electrolyte. Kelzan alone gave 7.6 coulombs/coulomb equivalent to HNO₃ consumed while 14.0 regenerations were obtained with the mixture of both compounds. Table B-5 summarizes these results.

TABLE B-5

Effect Of Surfactant On Regeneration Using Oxygen

82°C.   30 ma/cm^2 29 wt.% H₂SO₄ - 1 wt.% HNO₃

Surfactant	Electrode	Coulombs Measured/ Coulomb Equivalent to HNO₃ Lost
None	Platinized Pt	4.2
Benax 2A1, 1 wt.%	Platinized Pt	10.2
Benax 2A1, 1 wt.%	Platinized Pt*	24.0
GAFAC RS 710, 1 wt.%	Platinized Pt	10.5
TD 90, 1 wt.%	Proprietary Carbon	10.5
Kelzan, 0.5 wt.%	Platinized Pt	7.6
Kelzan + 710, 0.5 and 1 wt.%	Platinized Pt	14.0

*Downward sparging

The substitution of O₂ by air leads to an overall reduction in regeneration efficiency, but the same surfactants still give the best results. With Benax 2A1, over 5.5 regenerations were measured, with GAFAC RS 710, 4.2 regenerations, and with TD 90, 7.1 regenerations, as compared with 2.1 regenerations without foam. Table B-6 shows these results. Other nonionic, anionic, and cationic surfactants were tried, but all either failed a preliminary foaming test in the hot electrolyte or gave no significant improvement.

TABLE B-6

Effect Of Substituting Air For O₂ On Regeneration

82°C.　30 ma/cm² 　29 wt.% H₂SO₄-1 wt.% HNO₃　 Plat. Pt

Surfactant	Regeneration Efficiency Coulombs Measured	
	Coulomb	Equiv. to HNO₃ Lost
None		2.1
Benax 2A1, 0.5 wt.%		3.9
Benax 2A1, 1 wt.%*		5.5
GAFAC RS 710, 1 wt.%		4.2
TD-90, 1 wt.%		7.1

*Downward sparging

Part f - Effect of Increased Surface Area

Tests were also carried out on the use of high surface area materials for catalyzing the oxidation of NO to NO₂. These experiments were carried out by covering the electrolyte surface above the electrode with glass wool. A considerable increase in regeneration was achieved with both O₂ and air. Efficiency increased from 4.2 to 7.3 and from 2.1 to 4.4 coulombs/coulomb equivalent to HNO₃ consumed for O₂ and air, respectively. These results are shown in Table B-7.

TABLE B-7

Effect Of Glass Wool On Regeneration

82°C. 　　30 ma/cm² 　　29 wt.% H₂SO₄ - 1 wt.% HNO₃
Platinized Pt

Gas	Glass Wool	Coulombs Measured	
		Coulomb	Equivalent to HNO₃ Consumed
O₂	No		4.2
O₂	Yes		7.3
Air	No		2.1
Air	Yes		4.4

Part g - Effect of Nitrate Salts on Regeneration

Sodium nitrate and ammonium nitrate were tested as possible inexpensive and easily storable substitutes for HNO₃. Both salts were used in 0.2 M concentrations, equivalent to 1 wt.% HNO₃. As expected, electrode performance was comparable to HNO₃. The regeneration efficiency was 3.1 coulombs/coulomb equivalent to HNO₃ consumed for NaNO₃ but only 1.7 for NH₄NO₃. Thus NaNO₃ is somewhat lower than HNO₃ alone while NH₄NO₃ is not suitable as a substitute. The very low regeneration efficiency of NH₄NO₃ is due to its reaction with HNO₂ in acidic solution, liberating N₂. Table B-8 shows these results compared with HNO₃.

43

TABLE B-8

Effect Of Nitrate Salts On Regeneration

82°C.   30 ma/cm^2 29 wt.% H_2SO_4 Platinized Pt

Nitrate Source	Coulombs
	Coulomb Equivalent To HNO_3 Consumed
HNO_3	4.2
$NaNO_3$	3.1
NH_4NO_3	1.7

4.3 Task C, The Total Cell

The ultimate objective of this research is the development of a soluble carbonaceous fuel-air fuel cell as a compact power unit. The important consideration in accomplishing this objective is that various substances added to or produced in the cell can affect the performance or efficiency of the complete cell. Of particular importance is the migration of CH_3OH to the cathode and HNO_3 or its reduction products to the anode. Therefore a complete cell was designed taking these factors into account. This cell has been constructed and tests are now under way to determine the extent of the problems.

Phase 1 - Compatibility of Cell Components

Part a - The Effects of HNO_3 on CH_3OH Performance

To assess the effects of HNO_3 and its reaction products on the CH_3OH fuel electrode two series of experiments were run in which HNO_3 was added in 0.2 wt.% increments to the electrolyte. In one case, a porous carbon cathode was exposed to the HNO_3, thus reducing the HNO_3. In the other series of runs, a Pt cathode was isolated from HNO_3, preventing formation of HNO_3 reduction products. In both cases, 0.25 and 0.5 M CH_3OH were used in 30 wt.% H_2SO_4 at 82°C. Details of the apparatus used are given in Appendix Figure B-2.

It was found, as shown in Figure C-1, that HNO_3 could be tolerated in concentrations as high as 1.8 wt.% when its reduction products are absent, but that in the presence of these products electrode failure occurs at 0.8 wt.%. In previous experiments, with a somewhat different mode of operation, electrode failure had occurred below 0.5 wt.% in the presence of reduction products. It was also observed that carbon catalyzed the reaction between a HNO_3 reaction intermediate, presumably HNO_2, and CH_3OH to form NO and CO_2. Appendix C-1 gives the experimental results in detail.

Figure C-1

Effect Of HNO_3 On CH_3OH Performance

Legend:
- ■ No HNO_3 Reduction Products
- ● HNO_3 Reduction Products Present

X-axis: Wt.% HNO_3
Y-axis: Polarization At 6.5 ma/cm^2, V
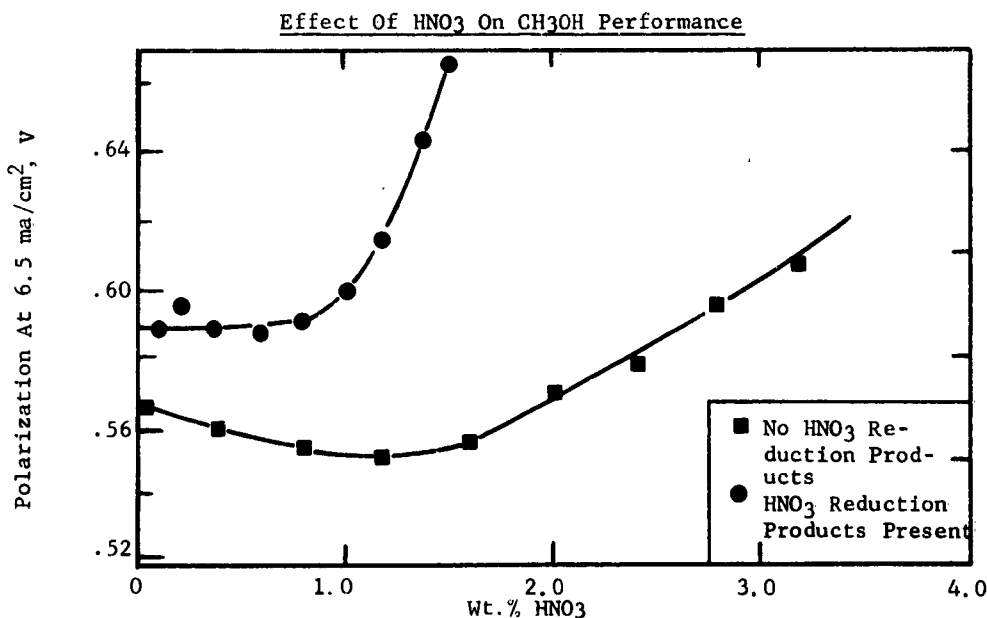
Part b – The Effects of HNO_3 on
Ethylene Glycol Performance

In addition to the tests with CH_3OH, HNO_3 was also added to the electrolyte while using ethylene glycol as fuel. The cathode was isolated from HNO_3 so that reduction products were not formed. Nitric acid concentrations of up to 1.0 wt.% were used in 30 wt.% H_2SO_4 and 1 M ethylene glycol at 82°C. Appendix Figure B-2 gives the experimental setup.

As shown in Figure C-2 it was found that HNO_3 could be tolerated in concentrations up to about 0.2 wt.%. For example, at 10 ma/cm^2, the fuel electrode polarization was 0.58 volts with no HNO_3, 0.59 volts at 0.2 wt.%, and increased to 0.64 volts at 0.6 wt.%.

Figure C-2

Effect Of HNO_3 On Ethylene Glycol
Performance In Absence Of Reduction Products
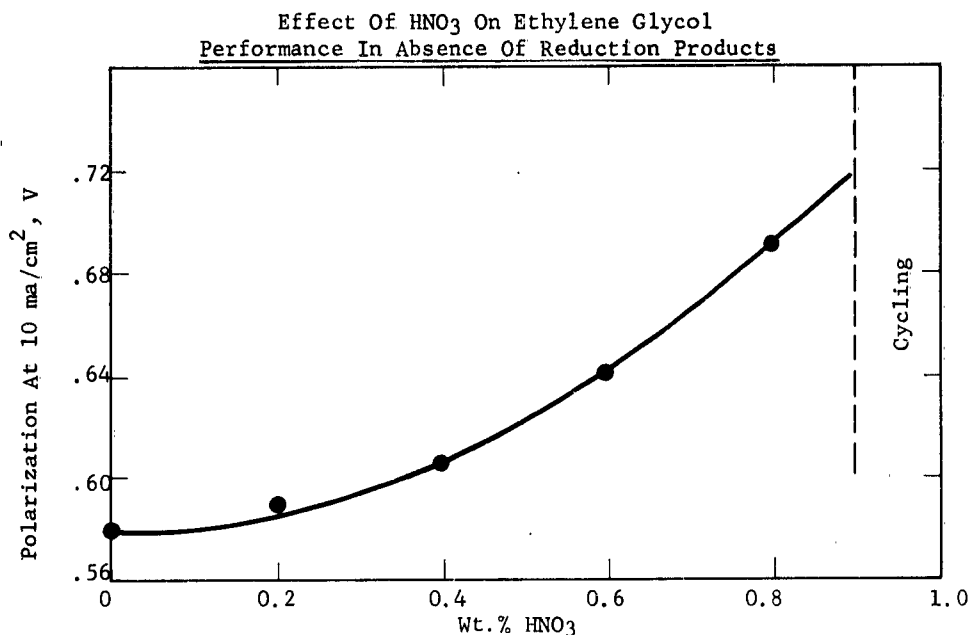
Part c – Separation of HNO_2
From Fuel Electrodes

Two methods were tested to prevent HNO_2 from reaching the fuel electrode. In one case, a graphite cloth barrier was placed between electrodes as a catalyst for the chemical reduction of HNO_2 by CH_3OH. The other method consisted of passing O_2 near the anode to oxidize HNO_2 to HNO_3. These tests were carried out at 82°C. in 30 wt.% H_2SO_4 - 1 wt.% HNO_3 electrolyte.

Neither technique performed satisfactorily. Despite the graphite shield, enough HNO_2 reached the fuel electrode to cause it to fail in 30 minutes of operation. Oxygen addition to the anolyte permitted operation of the fuel electrode, but resulted in periodic potential oscillations of over 0.5 volts.

Part d - Effect of CH3OH on Cathode Performance

Experiments were carried out to determine the effect of CH_3OH on the performance of the HNO_3 redox air electrode. The tests were performed using up to 1 M CH_3OH in 30 wt.% H_2SO_4 and 1 wt.% HNO_3 at 82°C. The experimental apparatus is described in Appendix Figure B-2.

The tests showed that the air electrode polarization increased appreciably with CH_3OH concentrations greater than about 0.1 M. For example, at 30 ma/cm², the polarization with no added CH_3OH was 0.18 volts but increased to 0.30 volts at 0.2 M and 0.78 at 0.5 M. These results are shown in Figure C-3.

Figure C-3

Effect Of CH_3OH On HNO_3-Air
Electrode Performance
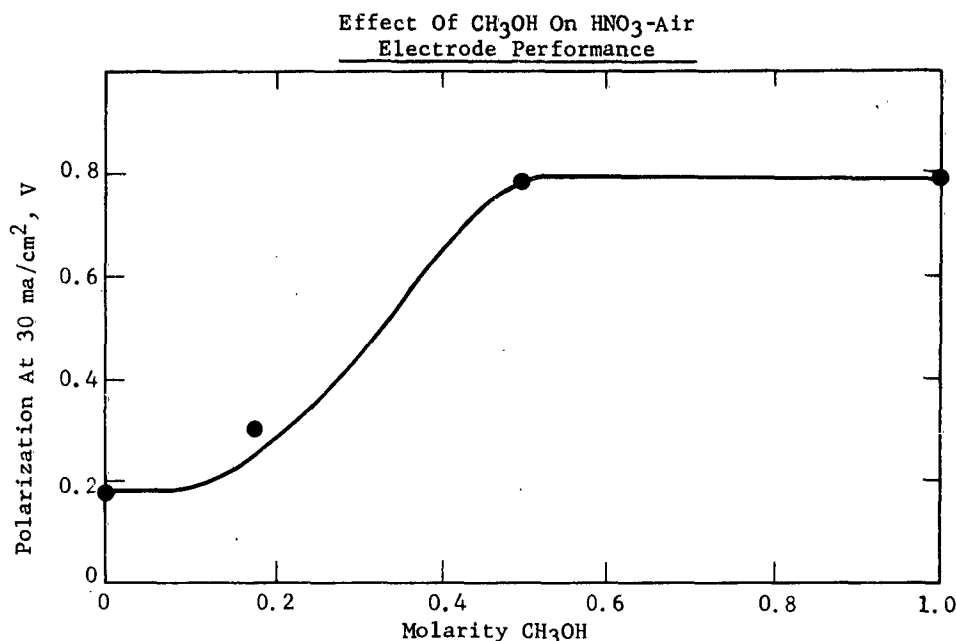
Phase 2 - Total Cell Design

Part a - Fuel Electrode Design

The fuel electrode can be operated with CH_3OH concentrations as low as 1 vol.% without decreasing performance. However, it would be desirable to reduce the concentration further at the cathode. This can be accomplished by designing the cell for CH_3OH addition to the anode face on the opposite side from the cathode. In this manner CH_3OH would react on the walls of the pores in the electrode before it can diffuse through to the electrolyte and thence to the cathode. This is shown in Figure C-4.

47

Figure C-4

Schematic Representation Of Effect
Of Electrochemical Reaction On Methanol Concentration

Fuel Electrode
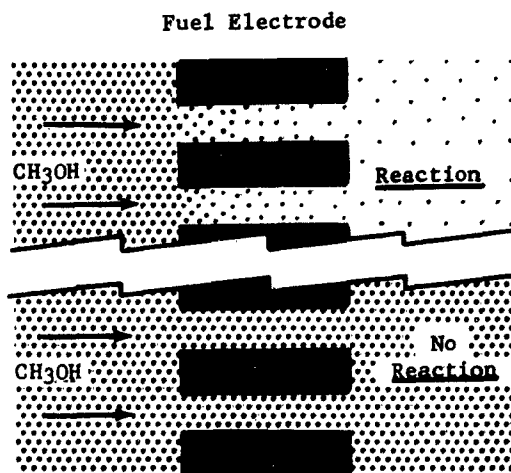
With this as a basis an analysis was made to determine the extent of reduction possible. The analysis was primarily mathematical because experimental evaluations of various possible structures would require over one hundred hours for each test. The mathematics, however, was verified in a limited number of experiments.

The mathematical model is described in detail in Appendix C-2 . In essence, the model assumes that CH_3OH is fed into a chamber in back of the fuel electrode. It then diffuses into a series of parallel pores and reacts on their walls. Calculations were made of the concentration gradients of CH_3OH within these pores. The effect of CO_2 flow longitudinally from within the structure was neglected. Calculations were made for transient conditions as well as steady state.

The analysis of transient conditions was made to compare the mathematics with experimental data obtained at various current densities. In these experiments, the electrodes consisted of 80 mesh platinum-rhodium screen having a 3 mil wire diameter and platinized with 8 gms of platinum black/ft^2. The pores of the final structure were ...easured microscopically and averaged 8 mils in diameter. A membrane, AMFion C313, was included as part of the anode structure to prevent bulk mixing of the liquids due to CO_2 evolution on either side of the screens. Methanol was fed into a fuel chamber where its concentration was maintained at 4 vol.%. It then diffused through the anode structure into a stirred sampling chamber. The sampling chamber was separated from the driven cathode by a second membrane. The equipment is shown, schematically, in Figure C-5.

48

Figure C-5

Equipment Used For
Evaluating Anode Design
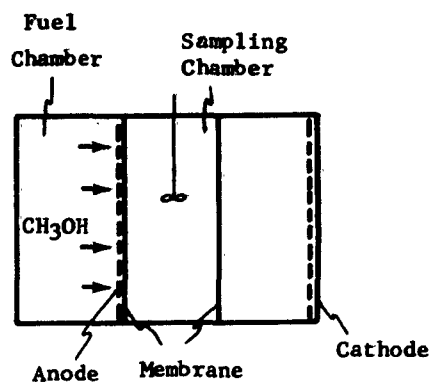
Figure C-6

The Effect Of Electrode
Reaction On CH₃OH Concentration
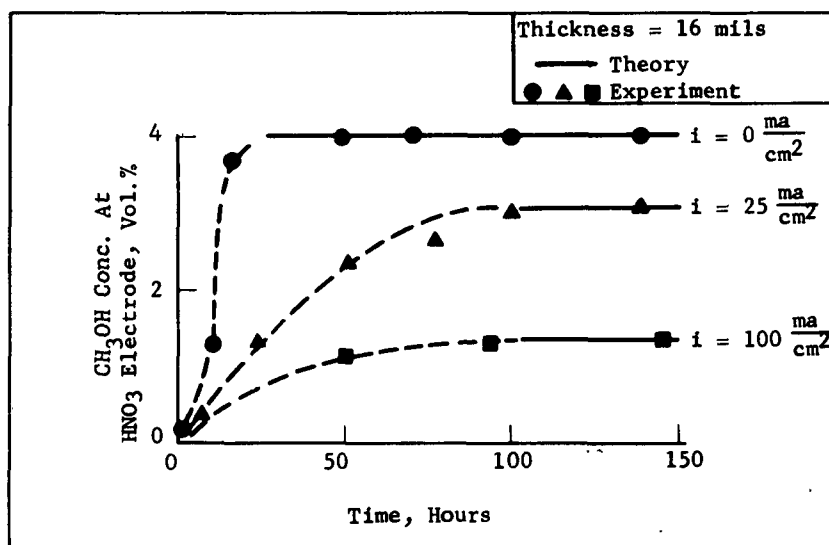
Figure C-7

The Effect Of Electrode
Reaction On CH₃OH Concentration
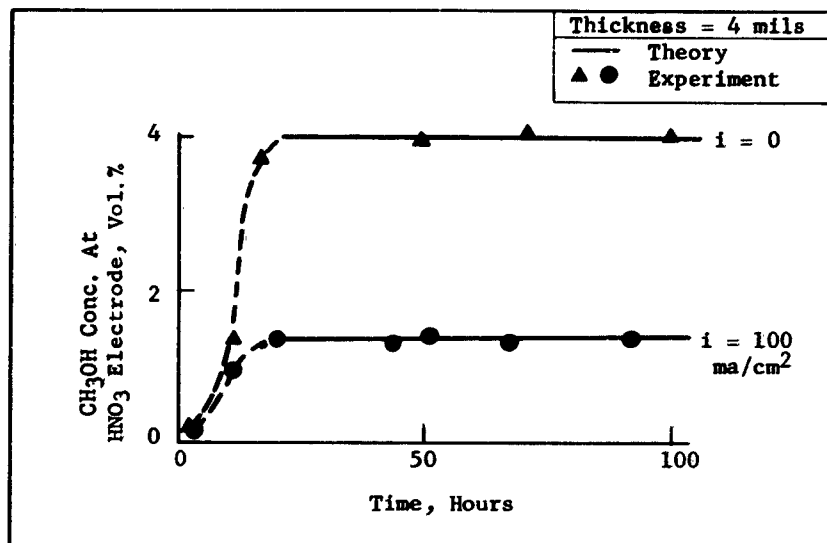
Samples were taken from the sampling chamber at various times and analyzed for CH₃OH. The accumulation of CH₃OH thus represents the amount of CH₃OH diffusing to the air side of the unit cell. The measurements were made in 30 wt.% H_2SO_4 at 32°C. and 1 atmosphere.

The results of the mathematical analysis and experimental measurements are in agreement. They verified the hypothesis that the CH₃OH diffusion can be restricted by feeding the fuel on one side of the electrode. The mathematics showed and it was confirmed experimentally that the interposing of a 16 mil thick electrode results in the CH₃OH concentration being reduced 25% at 25 ma/cm² and 67% at 100 ma/cm². These results are shown in Figure C-6 in which the calculations are compared with experiments. Electrode thickness does not appear to be important since comparable steady state values were obtained for electrodes only 4 mils thick (see Figure C-7).

50

Phase 3 - Fuel Cell Operation

A complete fuel cell was assembled to evaluate the operability of the CH_3OH fuel electrode in the presence of the air-HNO_3 redox system, especially with respect to the electrical performance capabilities of the working cell.

Briefly, the cell consists of 10 cm diameter electrodes separated by an electrolyte chamber contained between two membranes to prevent bulk mixing of fuel and oxidant. Each electrode is approximately 12 mils thick. Electrolyte chambers, 62 and 250 mils thick were used. In more recent experiments, the chamber was eliminated so that only a 5 mil membrane separated the two electrodes. The electrodes of platinum screen were coated with electrodeposited platinum black. Fuel was continuously fed through the fuel chamber as 0.6 to 2 vol.% CH_3OH in 30 wt.% H_2SO_4. The oxidant was 1 wt.% HNO_3 in 30 wt.% H_2SO_4 recycled through an air sparged regeneration section as shown in Figure C-8.

Figure C-8

Research Fuel Cell

Membrane Clad
Electrodes

51
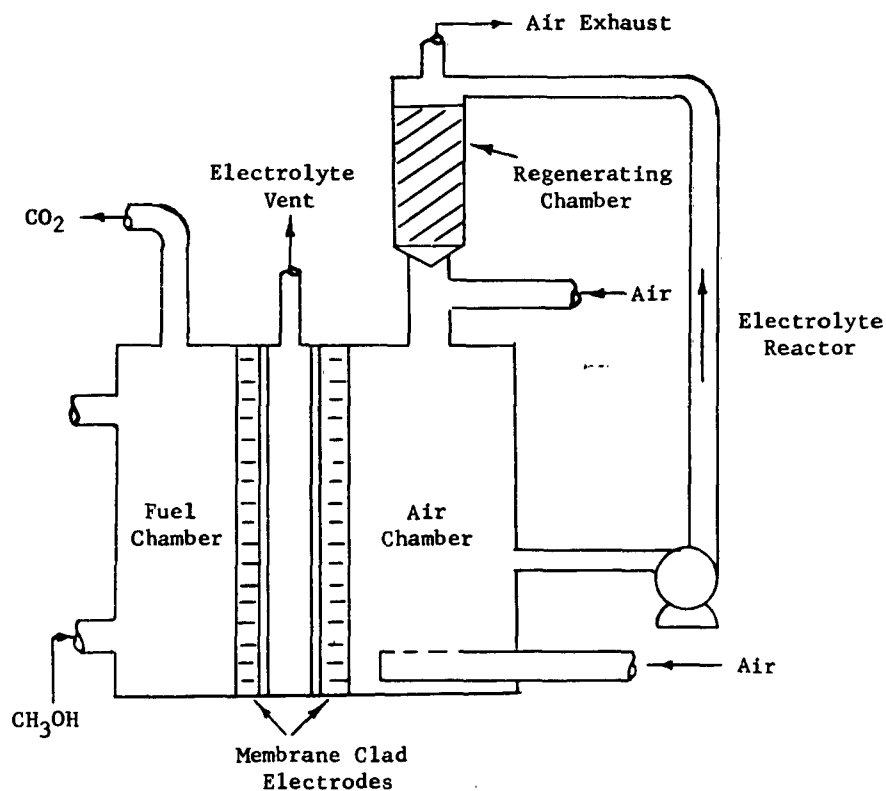
Part a - <u>Electrical Performance</u>

   The initial tests were carried out mainly to demonstrate the performance of the CH_3OH electrode in the presence of the air-HNO_3 redox system. The electrical performance of the total cell was measured in experiments ranging in duration from 3 to 55 hours at current densities up to 79 ma/cm². Good agreement was found when the results were compared with data obtained on half cell studies.

   The polarizations obtained at both the CH3OH and air-HNO3 electrodes in the total unit cell were in agreement with the polarizations previously obtained in the half cell studies of the individual electrodes. Thus the total cell voltage, neglecting IR losses in the electrolyte, agrees with previous half cell studies. This is illustrated in Figure C-9 . The data from these tests are summarized more completely in Appendix C-3.

<div align="center">

Figure C-9

Total Cell Performance Versus Half Cell Prediction

</div>
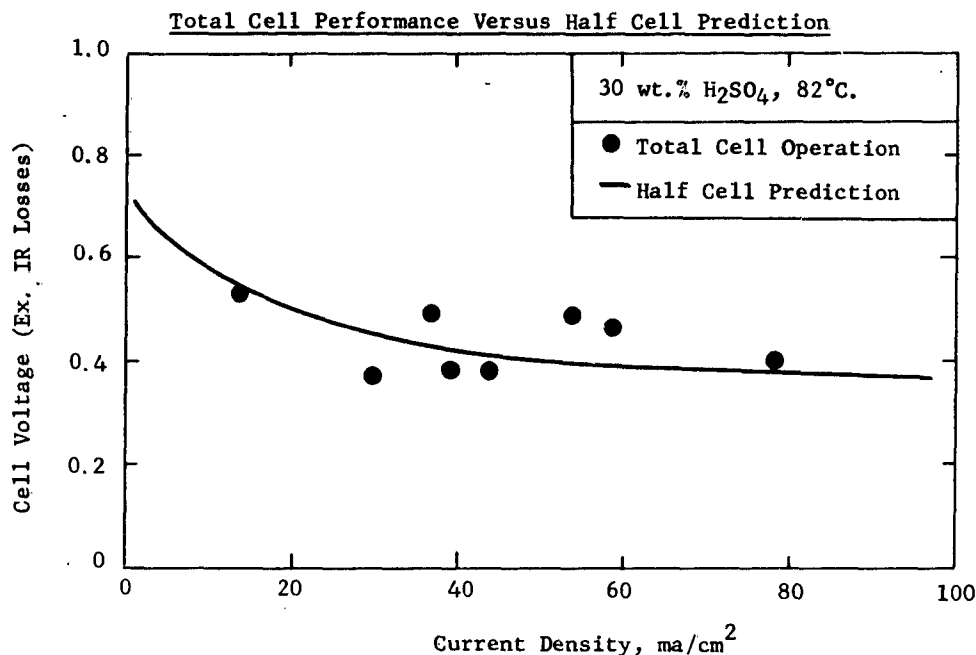
Part b - <u>Efficiency of CH3OH Utilization</u>

   One important criterion in the development of the fuel cell is the need to limit CH3OH diffusion to the air electrode. The CH3OH reaching the air electrode reduces efficiency by increasing air electrode polarization and by reacting chemically with the HNO3. As previously indicated, the problem is minimized by feeding CH3OH at the lowest possible concentration to the side of the fuel electrode opposite to the air electrode. Therefore an evaluation of the extent of this problem was made by measuring the amount of CH3OH reacting chemically at the air-HNO3 cathode during operation of the fuel cell.

   Both 52 and 80 mesh platinum black electrodes were used. During the test periods, CH3OH was fed at 82°C. to the cell at concentrations of 0.8, 1.0 and

2.0 vol.% in 30 wt.% H2SO4. The actual concentration within the fuel chamber was less because of the electrochemical reaction. The extent of reaction varied between 9 and 63% of the CH3OH converted, depending on the flow rates employed.

Data obtained in these fuel cell tests show that the CH3OH oxidation loss at the cathode is related to the resulting CH3OH concentration in the fuel chamber. It was found that as high as one quarter of the CH3OH reacted was lost through chemical oxidation when the fuel chamber contained 1.8 vol.% CH3OH. However, operating with 0.5 vol.% CH3OH reduced the loss to about 12%. Finally with 0.35 vol.% CH3OH, the chemical loss was only 4% of the methanol reacting. This effect is shown in Figure C-10.

<p style="text-align:center"><u>Figure C-10</u></p>

<p style="text-align:center">Effect Of CH3OH Concentration
On Chemical Loss At The Cathode</p>

CH3OH At Anode, Vol.% (After Conversion)
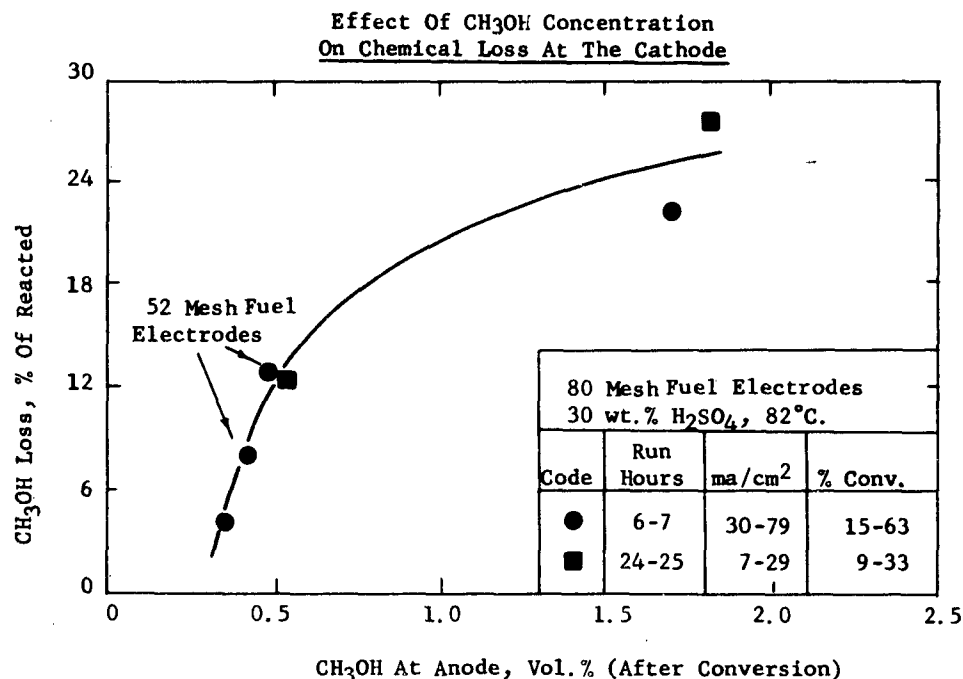
Part c - <u>HNO3 Regeneration With Air</u>

There was no special attempt made to study the operation of the air electrode. However, measurements were also made of the efficiency of HNO3 regeneration and air utilization. In these tests the 1 wt.% HNO3 in 30 wt.% H2SO4 electrolyte was continuously recirculated through the cell to simulate somewhat the contacting necessary for both the NO (produced by the HNO3 reduction) with the air and the NO2 with H2O. This HNO3 reduction is the result of both the desirable electrochemical redox process and by the undesirable chemical oxidation of CH3OH. The lower the chemical oxidation of CH3OH, the less oxygen needed for NO oxidation, and therefore air requirements are lowered and the CH3OH utilization is improved.

This is evident in the tests so far. Some regeneration of HNO3 was obtained in the tests. As much as 2.0 to 2.9 coulombs of electrical energy were measured per coulomb equivalent of HNO3 consumed, for oxygen consumptions from 51 to 125% of the stoichiometric amounts for the electrochemical process.

The data, however, cannot be used for analyzing regeneration efficiency quantitatively, because in tests where higher than stoichiometric oxygen was used, the CH_3OH oxidation at the cathode was excessive, and when lower than stoichiometric amounts were used, air supplied to the cell was insufficient. The data are summarized in Table C-1 and given in more detail in Appendix C-3.

TABLE C-1

HNO_3 Regeneration And Air Utilization

HNO_3 Regeneration, Coulombs Meas. Per Coulomb Equiv. Of HNO_3 Used	2.0	2.5	2.9	2.9	2.9
O_2 Consumed, % Of Stoichiometric % Of O_2 In Air That Reacted % Of O_2 Reacted Used For HNO_3 Regeneration	51 87 100	60 40 100	65 71 100	76 51 85	125 69 80
CH_3OH Loss, % Of CH_3OH Reacted	4	8	3	13	22

In these tests, 40 to 87% of the oxygen in the air was consumed. The utilization for regeneration was only 80 to 85% when the CH_3OH loss was 13 to 22%. At lower CH_3OH losses of 8% and less, the utilization was 100% but the air fed was not sufficient to meet stoichiometric requirements.

Part d - Electrolyte Conductance Losses

One of the problems in the tests of the complete cell was that the CO_2 produced at the anode in the electrochemical oxidation of CH_3OH could cause an increased IR loss in the electrolyte. This is a result of CO_2 gas bubbles blocking ionic flow in the pores of the electrode.

In tests with three 80 mesh screens as the electrode, an ohmic loss of as much as 0.2 volts was evident at 40 ma/cm^2. At current densities greater than 20 ma/cm^2 the current and fuel electrode voltage oscillated as the CO_2 was non-uniformly released from the electrode. Operating with a single screen as the electrode reduced the loss to 0.05 volts in the 20 to 30 ma/cm^2 range. However, at higher currents the ohmic loss was still severe for the single electrode. This effect is shown in Figure C-11.

54

Figure C-11

Voltage Loss Caused By CO_2 Evolution
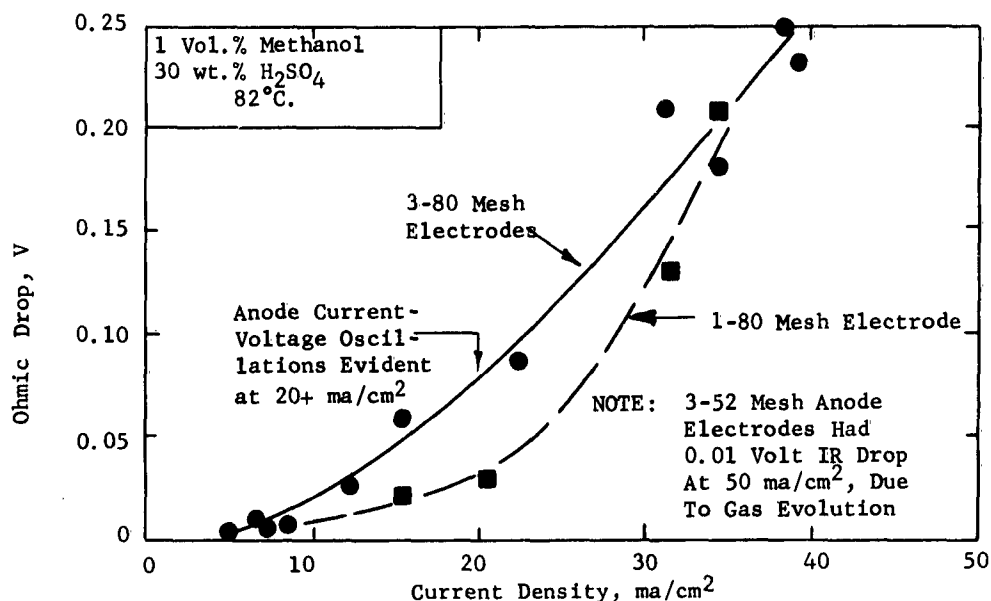
It is desirable that the electrode porosity be as small as possible to mimimize fuel loss. A solution of the gas evolution ohmic loss problem as well as the minimizing of the fuel loss seems to present no real difficulty. For example, it was also found that with a 52 mesh electrode, the IR loss at 50 ma/cm^2 amounts to only 0.01 volts. However, the higher mesh size is desirable for minimizing the loss of fuel. A compromise between these factors should be possible with proper choice of materials.

Part e - Fuel Electrode
            Catalyst Deactivation

During the operation of the cell, the fuel electrode slowly decreased in activity and eventually failed completely. However, electrode life could be pro-longed by returning the cell to open circuit for about 5 to 40 seconds each hour (See Appendix Figures C-11 and 12). Apparently, the adsorption characteristics of electrode poisons are potential dependent.

This effect was never present in any of the half-cell studies. Therefore, the materials used in the construction of the cell are likely sources of this poisoning. In this highly corrosive system, many of the materials used might degrade to form electrode poisons. Therefore, tests were made to determine the effect of the ma-terials used in cell construction on the CH$_3$OH electrode. All of the materials that contact electrolyte were checked.

In one group of tests, the materials were subjected to 0.25 M CH$_3$OH - 30 wt.% H$_2$SO$_4$ solution at 82°C. for 6 hrs. A second group of tests were performed under the same conditions, but 0.05 wt.% HNO$_3$ was also added. At this concentration, HNO$_3$ or its reduction products would not adversely affect CH$_3$OH performance. After these extractions, the CH$_3$OH-electrolyte solutions were tested in the half cell described

in Appendix A-8, using a platinum black electrode. The performance of the electrode was measured before and after each test with spectroquality CH_3OH to insure that any change in performance was caused by poisons.

The results of these tests, shown in Table C-2, indicate that three materials may be the source of the catalyst deactivation. These were Viton and Hypalon tubing used for circulating CH_3OH and HNO_3, and the membrane used between the electrodes.

TABLE C-2

Effect Of Cell Materials On Performance

| Material | Volts Increase In CH_3OH Polarization at 50 ma/cm^2 (82°C. and 1 atm.) | |
	0.25 M CH_3OH 30 wt.% H_2SO_4	0.25 M CH_3OH 30 wt.% H_2SO_4 + 0.05 wt.% HNO_3
Teflon	0	0
Silastic	0	0
Silicone Stopcock Grease	0	0
Viton	0.05	0.02
Hypalon	0.22	0.30
AMFion C313 Membrane	0	0.08

The deleterious effect of the AMFion C313 membrane was eliminated by subjecting it to a severe acid treatment before use. Several membranes were treated with a 30 wt.% H_2SO_4 - 28 wt.% HNO_3 solution at 82°C. for 6 hours and then equilibrated at 82°C. for 6 hours in a solution containing 0.25 M CH_3OH, 0.05 wt.% HNO_3 and 30 wt.% H_2SO_4. This solution gave no evidence of affecting electrode performance. Furthermore the membranes did not appear to be harmed by this process.

CONCLUSIONS

5.1 Task A, Fuel Electrode

Phases 1 and 2 - Catalysts Prepared By
Electrodeposition; New Catalyst
Techniques And Physical Properties

The codeposition of noble and base metals with platinum results in catalysts with improved activity. This incorporation with base metals, either by electrodeposition or reduction with $NaBH_4$, can produce catalysts resistant to H_2SO_4 attack. Their catalyst activity increases with increasing electropositivity of the base metal, the greatest effects being obtained so far with the most electropositive metals tested, Fe and Mo. However, the fact that these catalysts polarize more rapidly with increased current densities means that the improvements are small at practical current densities.

The improvements in the Pt-Fe catalyst were found to be independent of changes in the lattice structure or in the catalyst surface area. Thus the effects of co-metal deposition must be due to other causes, such as changes in the number of d band electrons, work function, or electrocapillary maximum (potential of zero surface charge). Alternatively, minute amounts of base metal leached from the electrode surface might increase the active area or alter the nature of the exposed platinum crystal planes.

The electrochemical reaction can produce CO_2 at small but nevertheless significant current densities with polarizations as low as 0.2 volts. This indicates that there is no inherent voltage limitation on performance and that the limitation is catalytic in nature.

Improvements can also be effected by the addition of Mo to the electrolyte. Its cause has not been determined. However, this improvement may be due to strong adsorption of the $MoO_4^=$ in the electrical double layer causing changes in the surface charge and consequently resulting in either more efficient methanol adsorption or charge transfer.

Based on the studies to date, improved fuel electrodes are still needed. However, both the work on developing new catalysts and the studies on the mechanism of the reactions indicate that lower polarizations should be possible with improved catalysts.

Phase 3 - Fuel Variable Study

Three partially oxygenated hydrocarbons were selected as most suitable for use in the fuel cell - methanol, ethylene glycol, and glycerin. Methanol proved to be the best overall because it gave the lowest polarization under long term operation.

Two possible disadvantages of methanol were found not to be critical. These were its low boiling point, which could result in appreciable vaporization losses at the temperatures required to remove the product water, and secondly, the fact that methanol can significantly decrease air electrode performance. The problems are not severe because the fuel electrode can be operated with sufficiently low concentrations of methanol without impairing performance. This minimum methanol

57

concentration as well as voltage efficiency is favored by low H_2SO_4 concentrations. Therefore selection of the optimum electrolyte concentration will depend on the extent to which air electrode performance and electrolyte resistance losses are affected by acid concentration.

Finally, since surfactants are harmful to fuel electrode performance, membranes would be required to prevent their migration from the air electrode should they prove necessary at the latter electrode.

Phase 4 - Mechanism Studies

Using platinum as the catalyst, the data on methanol, formaldehyde and formic acid present a complex reaction scheme. Its nature is dependent upon the current density and appears to fall into three distinct regions. The first occurs at extremely low current densities where methanol and its two reaction intermediates all oxidize at comparable potentials. The second region occurring at higher current densities is characterized by an oscillatory behavior on the part of all three fuels. The third region is the region of limiting current.

Studies employing the preadsorbed layers showed that in the first region all three fuels, despite differences in their theoretical oxidation potentials, oxidize at about the same voltage. This indicates a common limiting step. This limitation may be dependent on a change in the surface charge (from positive to negative) which has been reported to occur at these potentials. In regions of positive surface charge the partial protonation of oxygenated hydrocarbons could interfere with adsorption and thus be the governing factor.

The oscillations observed in the second region are not easily explained. The variation of adsorption with the pretreat potential suggests that the oscillations may be associated with a potential-dependent condition of the surface. Furthermore from the experiments using repeated pulses, it appears that outside the voltage boundaries of the oscillation, desorption of an oxidizable intermediate occurs. Thus, an intermediate produced or adsorbed at one polarization may be further oxidized at a lower polarization. However, the existence of oscillations with all three fuels makes difficult the assignment of such an intermediate.

In the third region, that of the limiting current, chronopotentiograms indicate diffusion control for the formaldehyde reaction but nondiffusional control for methanol. The data on formic acid is not sufficient to establish its limitation. Thus, as indicated by the anodic stripping experiments, the slow adsorption of methanol could be the ultimate limitation on its reaction.

Assuming there are no one-electron-dimer products such as glyoxal or glycolic acid, these same experiments indicate a two electron oxidation of formaldehyde as well as formic acid. Methanol, under the same assumptions, since it yields about half as many coulombs, must occupy fewer sites at equilibrium than the other two fuels.

These data point out the need for more information on the nature of the catalyst surface and its charge. They also indicate the need for a catalyst with surface properties different from those of platinum alone.

58

5.2 Task B, Air Electrode

Phases 1 and 2 - Mechanism; Air
Electrode Performance

The studies on the mechanism of the HNO_3 redox reaction showed that the electrochemical reaction is limited by the concentration of HNO_2 formed rather than HNO_3 itself. The linear dependence of the limiting current on HNO_3 concentration together with its large temperature dependency indicate that the air electrode should be operated at the highest possible temperature and HNO_3 concentration consistent with other requirements of the complete cell. Furthermore, since the reaction is limited chemically rather than by mass transport, improved performance may be attainable through catalysis. In addition, this limitation is favored by both greater catalyst surface area and high concentration of the product intermediates. Consequently, improved performance may be attainable by minimizing the air rate and by proper design of the electrode.

It was also found that H_2SO_4 was a better electrolyte than H_3PO_4. Comparable performance with H_3PO_4 was possible but at extremely high concentrations which are unfavorable to the fuel electrode. Furthermore, the marked improvement obtainable by increasing H_2SO_4 concentration more than compensates for the decrease in the methanol electrode performance up to about 30 wt.% H_2SO_4.

The HNO_3 redox electrode has been shown to operate at low polarizations with both air as well as O_2. In addition further improvements may still be possible, if desired.

Phase 3 - HNO_3 Regeneration

The extent of regeneration required should amount to at least 5 coulombs of HNO_3 produced per coulomb equivalent to the HNO_3 consumed. This target is attainable with O_2 using porous carbon electrodes through which the O_2 flows. However it is not reached using nonporous flow-through electrodes or when air is employed. This is the result of both inefficient contacting and the slow reaction of NO with air.

The efficiency of regeneration is only slightly affected by such operating variables as air flow rate, HNO_3 concentration, or current density over the ranges studied. However, improved efficiencies that meet the preliminary target are obtainable by the addition of foaming agents to improve the contacting of NO with O_2 in the small bubbles of foam. These surfactants are not completely stable. However, sodium dodecylated oxidibenzene sulfonate in 1% concentration has proved to be the most efficient, chemically stable additive tested. In addition, the regeneration efficiency can be increased twofold by accelerating NO oxidation by providing more surface for reaction. This is accomplished by placing a high surface area material such as glass wool over the electrode.

The HNO_3 does not necessarily have to be added directly. $NaNO_3$ can be substituted with little or no loss in performance or efficiency of regeneration; NH_4NO_3 does not permit efficient regeneration because it reacts chemically with HNO_2.

5.3 Task C, The Total Cell

Phase 1 - Compatibility of Cell Components

It was found that HNO_3 can be tolerated at the CH_3OH fuel electrode in concentrations up to 1.8 wt.% when its reduction products are absent. In the presence of reduction products however, only about 0.8 wt.% HNO_3 can cause electrode failure. In some cases, 0.5 wt.% or less produced complete failure. Ethylene glycol is more sensitive to HNO_3, with 0.2 wt.% being the tolerable limit. The effect of methanol on the HNO_3 redox air electrode is negligible up to about 0.1 M, at which point polarization begins to increase rapidly. These results indicate the necessity of proper cell design to minimize the mixing of fuel and HNO_3. Several possible ways of accomplishing this are discussed in the succeeding phases.

Phase 2 - Total Cell Design

The use of a flow-through fuel electrode, with methanol introduction at the side opposite to the air electrode, results in methanol concentration reductions of up to 67% at the air electrode. This is caused by reaction of the methanol on the fuel electrode pore walls as it diffuses through. Based on these data, a fuel electrode only 5 mils thick can be operated with virtually no impairment of air electrode performance due to methanol.

Phase 3 - Fuel Cell Operation

Combination of the methanol fuel electrode and HNO_3 air electrode gives identical performance to that obtained with half-cell tests. The only additional source of polarization is due to ohmic loss through the electrolyte. Chemical oxidation of methanol by HNO_3 is dependent on its concentration at the fuel electrode. By using 0.25 M methanol, chemical loss is only 4%.

Two problems which arose with full cell operation were a blanketing of the fuel electrode with CO_2 and a slow decline in its activity. The evolved CO_2 caused an increase in ohmic polarization by blocking ionic flow through the electrode pores. Both the decline activity and the increase in ohmic polarization can be eliminated through careful selection of construction materials and proper cell design.

SECTION 6

PROGRAM FOR NEXT INTERVAL

The work carried out in the first half of 1962 concentrated primarily on improving the performance of the fuel and air electrodes and on translating the results into compatible electrode-electrolyte systems. The research during the second half of 1962 will continue along similar lines, but with somewhat greater emphasis on the development of the fuel electrode and on studying problems associated with the operation of a compact unit cell.

The past and projected distribution of effort on each of these tasks are as follows. The exact division of emphasis of course will depend on the rates of progress in each area.

Task	Title	Effort Expended in 1962 Actual Jan-June	Projected July-Dec.
A	Fuel Electrode	40	55
B	Air Electrode	30	10
C	Total Cell	30	35

It is expected that the research will concentrate on the following aspects of the problem.

6.1 Task A, Fuel Electrode

Further efforts will continue to concentrate on finding cocatalyst systems more active than platinum and yet stable in H_2SO_4. Methanol will be used as the main fuel in most of these experiments. Studies on the mechanism of the reaction also will continue with particular emphasis on the kinetics on the Pt-base metal catalysts that exhibit low polarizations at significant current densities.

6.2 Task B, Air Electrode

Most of the work with the air electrode will involve its incorporation into the compact cell. However, some effort will be directed toward further improvments in performance and efficiency of regeneration.

6.3 Task C, Total Cell

A new cell will be constructed based upon the operating experiences in the initial model. Experiments will be carried out in this cell aimed at determining the influence on performance of such operating variables as electrolyte composition and air rate. The air electrode and air chamber will be designed for compact operation and tested to determine the electrical performance and HNO_3 regeneration efficiency obtainable.

61

SECTION 7

IDENTIFICATION OF PERSONNEL AND DISTRIBUTION OF HOURS

7.1 Background Of Personnel

<u>Carl E. Heath</u> (Ph.D., Chemical Engineering, University of Wisconsin) as section head is responsible for all fuel cell research activities within Esso Research. Dr. Heath has 6 years experience in such diverse fields as fuel cell, combustion, and radiochemical research. He has 7 patents and 10 publications in these fields in addition to having written a chapter on kinetics and catalysis for the forthcoming Academic Press publication on fuel cells.

<u>Barry L. Tarmy</u> (Ph.D., Chemical Engineering, Columbia University) is the project leader directly supervising the research on the soluble carbonaceous fuel-air fuel cell. Dr. Tarmy's previous experience has been in the fields of combustion, radiochemistry, and heat and mass transfer. In addition to 9 patents, he has 8 publications in these areas.

<u>Eugene L. Holt</u> (Ph.D., Physical Chemistry, Yale University) joined Esso Research and its fuel cell activities in 1960. At Yale, Dr. Holt investigated ion-molecule interactions during mass transport using differential conductance measurements of diffusion coefficients of weak electrolytes. He is currently engaged in the development of improved fuel electrode catalysts.

<u>Duane G. Levine</u> (M.S., Chemical Engineering, Johns Hopkins University) has worked since 1959 at Esso Research on a variety of basic engineering research studies in the fields of combustion and fuel cells, and has 3 publications in these fields. His projects included fundamental studies of surface ignition, flame propagation, and electrode development. He presently is working on the development of practical electrodes.

<u>Andreas W. Moerikofer</u> (Ph.D., Physical Organic Chemistry, Swiss Federal Institute of Technology) came to Esso Research in 1961 after having been a postdoctoral associate at Purdue University. At Purdue he worked with Professor H. C. Brown on the kinetics of the hydroboration of olefins and the structural chemistry of the products. Dr. Moerikofer has 7 publications in this and other areas of physical organic chemistry. His present area of research is the HNO3 redox air electrode.

<u>Joseph A. Shropshire</u> (Ph.D., Physical Chemistry, Yale University) has been at Esso Research since 1957 working in the fields of fuel cells and corrosion. Dr. Shropshire's doctoral dissertation was also on electrochemistry. He is the author of six publications largely in the above fields. His present assignment has been the elucidation of the mechanisms of the fuel and air electrode processes.

<u>James A. Wilson</u> is an engineering associate with 25 years experience at Esso Research in the development of spectrographic, electronic analytical equipment, and control systems. Prior to that time he served three years in the U.S. Army Signal Corps. In recent years he has been responsible for special projects in the areas of automotive research, combustion, and automation. In addition, he has designed the special control and monitoring equipment used in fuel cell operations.

63

Charles H. Worsham (M.S., Chemical Engineering, Virginia Polytechnical Institute) has been at Esso for 24 years with the exception of 4 years as a petroleum supply officer in the United States Army. During this time he has worked in such widely differing fields as uranium extraction, ram-jet development, and hydrocarbon synthesis as well as having 4 years experience with fuel cells. He holds 3 patents and has written 4 articles in these fields. His present assignment is the construction and operation of a complete fuel cell.

7.2 Distribution Of Hours

The following are the technical personnel who have contributed to the work covered by this report and the approximate number of hours of work performed by each:

Carl E. Heath	443
Barry L. Tarmy	861
Eugene L. Holt	982
Duane G. Levine	864
Andreas W. Moerikofer	961
Joseph A. Shropshire	922
James A. Wilson	20
Charles H. Worsham	858
Total	5911

TECHNIQUE OF ELECTRICAL CODEPOSITION

Electrodepositions were carried out from solutions of $H_2PtCl_6 \cdot 6H_2O$ and a salt of the other metal or metals. To determine proper plating conditions, polarographic curves of the various solutions were obtained to find the deposition potentials and limiting currents of each species. Where H_2 evolution interfered with deposition of the more electropositive elements, the pH was increased by addition of NaOH.

The following is a typical curve obtained from a solution of 1.5 wt.% each of $H_2PtCl_6 \cdot 6H_2O$ and $NiCl_2 \cdot 6H_2O$ with 0.04 wt.% $Pb(Ac)_2$ added. The pH was adjusted to 7 to retard H_2 evolution. Pt deposition began at +0.2 V. versus the std. H_2 potential. A limiting current was reached at 8-11 ma/cm^2, where the potential increased rapidly until Ni deposition commenced at -0.40 V. When a potential of -0.70 V. was reached H_2 evolution occurred. Appendix A-4 describes the deposition of Pt and Pt-Fe in the absence of added $Pb(Ac)_2$.

Figure A-1

Typical Deposition Curve Of Pt And Ni
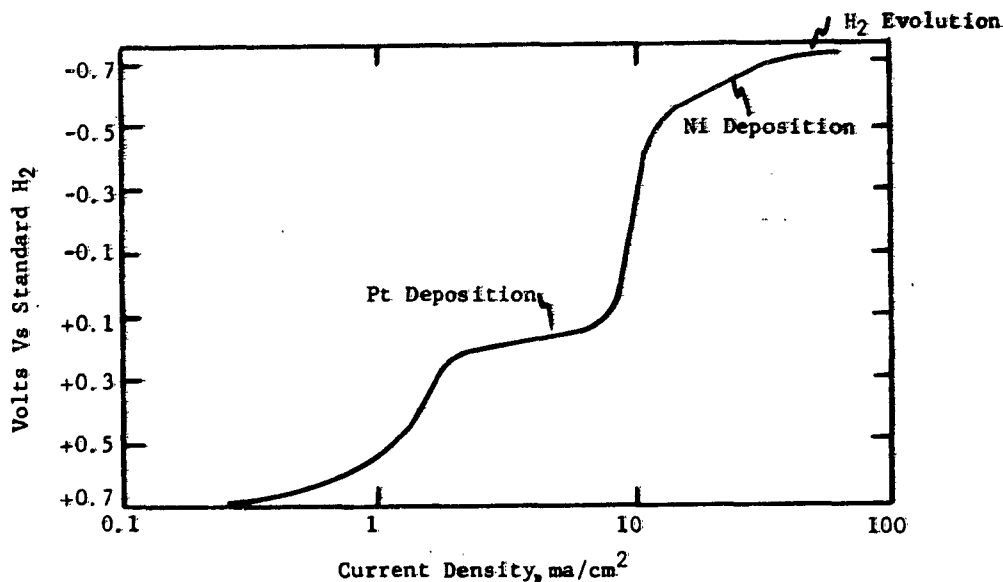
Not all metals tried could be codeposited. Some, such as Sn and Mo, formed precipitates in the presence of $PtCl_6$ or when the pH was raised. Others, such as Ir, Ru, and W could not even be plated from their pure solutions and Cr prevented a uniform black Pt coat from forming. The salts used successfully with $H_2PtCl_6 \cdot 6H_2O$ were $FeCl_3$, $CoCl_2 \cdot 6H_2O$, $NiCl_2 \cdot 6H_2O$, $CuCl_2$, $Pb(NO_3)_2$, $RhCl_3$, $AuCl_3$ and $PdCl_2$.

EQUIPMENT USED IN CATALYST PREPARATION AND TESTING

All voltage and current measurements were made with Keithley Model 600A or 610A Electrometers. Reference electrodes were saturated Ag/AgCl connected to the fuel electrode through a Luggin capillary filled with 30 wt.% H_2SO_4. Long term performances were taken with Esterline-Angus Style 90 M recorders. The counter-electrode was driven from either a 6-12 V. ATR Rectifier Power Supply or a 10 V. Electro-Analysis Power Unit. Temperature was controlled to $\pm1°C$. by Variac Auto-transformers.

For the surface area measurements, a Tektronix Type 345A Oscilloscope with a Type D plug-in unit was employed. Voltage-time traces were recorded photo-graphically. Two Eveready W-365 45 V. batteries connected in parallel served as the power supply. Gas chromatographic analyses of the gaseous product obtained from a Pt-Mo electrode were performed with a Perkin-Elmer Model 154 vapor fractometer on a Type S (silica gel stabilized with di-2-ethylhexyl sebacate) 1/4" column.

APPENDIX A-3

PREPARATION AND
PERFORMANCE OF ELECTRODEPOSITED CATALYSTS

Electrode No. And Composition	Deposition Conditions ma/cm²	V. vs H2	Time	Deposition Solution	Volts Polarized Versus CH3OH at ma/cm² 0	1	10	50	100	200	Tafel slope(b)	-Log Io
27 Pt	10	+0.08 to +0.12	10' 0"	3% H2PtCl6·6H2O	0.41	0.51	0.56	0.61	0.63	0.67	0.065	7.7
39 Pt	22	-0.04 to -0.09	10' 0"	3% H2PtCl6·6H2O	.33	.47	.53	.57	.62	.66	.068	6.9
55 Pt	19	-0.02 to -0.05	10' 38"	3% H2PtCl6·6H2O	--	.47	.53	.57	.60	.65	.062	7.5
56 Pt	18	-0.03 to -0.06	11' 0"	3% H2PtCl6·6H2O	--	.47	.54	.59	.61	.65	.068	7.0
57 Pt	17	-0.03 to -0.07	11' 46"	3% H2PtCl6·6H2O	--	.49	.55	.60	.62	.66	.064	7.6
67 Pt	22	-0.05 to -0.08	8' 34"	3% H2PtCl6·6H2O	--	.48	.56	.61	.64	.67	.074	6.5
68 Pt	10	+0.12	18' 53"	3% H2PtCl6·6H2O	--	.50	.57	.62	.65	.69	.071	7.0
72 Pt	12-13	-0.05	9' 44"	3% H2PtCl6·6H2O	.45	.50	.56	.62	.65	.71	.051	9.9
74 Pt	9	-0.76	13' 25"	3% H2PtCl6·6H2O + 0.18% ZnSO4	.38	.53	.59	.65	.69	.74	.062	8.6
75 Pt	12	-0.05	10' 42"	3% H2PtCl6·6H2O	.38	.51	.56	.62	.65	--	.053	9.5
77 Pt	6	-0.04	21' 04"	3% H2PtCl6·6H2O @ 0°C.	.36	.51	.55	.61	.64	--	.061	8.2
78 Pt	114	+0.05 to -0.06	1' 08"	3% H2PtCl6·6H2O @ 70°C.	.37	.50	.55	.61	.65	--	.053	9.4
80 Pt	12	-0.05	10' 50"	3% H2PtCl6·6H2O	Used For Surface Area Measurements Only							
82 Pt	10	-0.05	13' 0"	3% H2PtCl6·6H2O	Used For Surface Area Measurements Only							
84 Pt	12	-0.05	11' 06"	3% H2PtCl6·6H2O	Used For Surface Area Measurements Only							
85 Pt	13	-0.04	10' 30"	3% H2PtCl6·6H2O	Used For Surface Area Measurements Only							
3 Rh	300	-0.25 to -0.36	3' 0"	3% H3RhCl6	--	.51	.57	.60	.63	.69	.045	12.2
5 Rh	450	--	2' 0"	3% H3RhCl6	--	.50	.54	.57	.63	--	.040	12.9
16 Pt-Rh	450	-0.19	1' 0"	0.6% H2PtCl6 + 2.4% H2RhCl6	.39	.51	.53	.57	.60	.63	.057	8.3
20 Pt-Rh	--	Polarographic Trace	--	3% H2PtCl6 + 3% H3RhCl6	.36	.46	.52	.56	.58	.62	.059	7.8
21 Pt-Rh	10	+0.40 to -0.31	19' 45"	3% H2PtCl5 + 3% H3RhCl6	.42	.51	.58	.63	.68	.76	.066	7.8
22 Pt-Rh	20	+0.25	12' 0"	3% H2PtCl6 + 3% H3RhCl6	.40	.49	.54	.58	.60	.64	.050	9.8
23 Pt-Rh	30	+0.21 to +0.18	8' 24"	3% H2PtCl6 + 3% H3RhCl6	--	.42	.50	.55	.58	.62	.071	6.0
24 Pt-Rh	50	+0.06 to +0.02	5' 40"	3% H2PtCl6 + 3% H3RhCl6	.36	.48	.54	.59	.61	.65	.065	7.7
25 Pt-Rh	70	-0.01 to -0.08	5' 40"	3% H2PtCl6 + 3% H3RhCl6	.25	.47	.52	.56	.58	.61	.060	7.6
30 Pt-Rh	20	-0.12 to -0.03	10' 0"	2.4% H2PtCl6 + 0.6% H3RhCl6	.34	.45	.52	.56	.59	.64	.063	7.2
31 Pt-Rh	30	-0.05 to -0.18	10' 0"	1.5% H2PtCl6 + 1.5% H3RhCl6	.36	.46	.53	.58	.61	.65	.071	6.5
32 Pt-Rh	45	+0.04 to -0.04	10' 0"	0.6% H2PtCl6 + 2.4% H3RhCl6	.33	.41	.49	.56	.58	.62	.089	4.6
33 Pt-Rh	45	-0.02 to -0.05	10' 0"	0.3% H2PtCl6 + 2.7% H3RhCl6	.43	.51	.55	.58	.60	.64	.042	12.1
34 Pt-Rh	45	-0.05	10' 0"	0.1% H2PtCl6 + 2.9% H3RhCl6	.40	.49	.54	.57	.59	.63	.050	9.7
35 Pt-Rh	45	-0.04	10' 0"	1.0% H2PtCl6 + 2.0% H3RhCl6	.34	.46	.52	.57	.59	.63	.066	6.9
36 Pt-Rh	45	-0.02 to -0.06	10' 0"	0.5% H2PtCl6 + 2.5% H3RhCl6	.41	.48	.55	.59	.61	.65	.052	9.5
9 Pt-Pd	54-80	-0.16	1' 40"	2.7% H2PtCl6 + 0.3% H2PdCl4	.50	.57	.61	.64	.68	.75	.033	21
18 Pt-Au	75	-0.10	3' 0"	2.7% H2PtCl6 + 0.3% HAuCl4·3H2O	--	.51	.57	.62	.65	.69	.058	8.8
8 Rh-Pd	190-280	-0.21	1' 0"	2.7% H2PdCl4 + 0.3% H3RhCl6	--	.55	.59	.65	--	--	.060	9.0
26 Pt-Cu	10	+0.10	10' 0"	2.94% H2PtCl6·6H2O + 0.06% CuCl2	--	.45	.52	.57	.61	.67	.063	7.2
28 Pt-Cu	10	-0.01 to -0.09	10' 0"	2.7% H2PtCl6·6H2O + 0.3% CuCl2	.42	.51	.60	.63	.70	.73	.068	7.7
40 Pt-Cu	16	-0.03	18' 10"	2.94% H2PtCl6·6H2O + 0.06% CuCl2	.39	.49	.53	.59	.62	.67	.047	10.3
37 Pt-Pb	4.5	-0.39 to -0.50	10' 0"	1.5% H2PtCl6·6H2O + 1.5% Pb(NO3)2	.39	.50	.56	.61	.64	.68	.065	7.6
38 Pt-Pb	15	-0.79	10' 0"	1.5% H2PtCl6·6H2O + 1.5% Pb(NO3)2	.34	.48	.56	.63	.67	.72	.10	4.4

Electrode No. And Composition	ma/cm²	V. vs H2	Time	Deposition Solution	Volts Polarized Versus CH3OH at ma/cm² 0	1	10	50	100	200	Tafel Slope(b)	-Log I_0
46 Pt-Ni	------	Polarographic Trace		1.5% H2PtCl6·6H2O + 1.5% NiCl2	.31	.42	.51	.57	.62	.67	.088	4.8
47 Pt-Ni	------	Polarographic Trace		1.5% H2PtCl6·6H2O + 1.5% NiCl2	.32	.45	.54	.57	.63	.67	.10	4.5
48 Pt-Ni	9	0.26 to 1.10	22' 8"	1.35% H2PtCl6·6H2O + 0.15% NiCl2	--	--	--	.58	.62	.68	.14	3.5
49 Pt-Co	------	Polarographic Trace		1.5% H2PtCl6·6H2O + 1.5% CoCl2	--	.45	.54	.59	.63	.66	--	--
50 Pt-Co	10	0.12 to 0.76	30' 0'	1.35% H2PtCl6·6H2O + 0.15% CoCl2	--	--	--	.62	.64	.68	.084	5.6
41 Pt-Fe	------	Polarographic Trace		1.5% H2PtCl6·6H2O + 1.5% FeCl3	.23	.41	.50	.57	.61	.66	.095	4.3
42 Pt-Fe	24	0.07	10' 0"	1.5% H2PtCl6·6H2O + 1.5% FeCl3	.20	.39	.51	.60	.64	.70	.12	3.3
43 Pt-Fe	16	0.41 to 0.50	14' 30"	2.7% H2PtCl6·6H2O + 0.3% FeCl3	.21	.40	.50	.56	.59	.63	--	--
44 Pt-Fe	10	0.16 to 0.60	24' 0"	2.94% H2PtCl6·6H2O + 0.06% FeCl3	.32	.45	.54	.60	.63	.68	.090	5.0
45 Pt-Fe	16	0.17 to 0.21	15' 57"	2.82% H2PtCl6·6H2O + 0.18% FeCl3	.18	.36	.46	.54	.57	.63	.11	3.4
53 Pt-Fe	11	0.20 to 0.76	22' 0'	2.82% H2PtCl6·6H2O + 0.18% FeCl3	--	.39	.49	.58	.61	.65	.11	3.4
54 Pt-Fe	9-15	0.38 to 1.0	21' 0'	2.82% H2PtCl6·6H2O + 0.18% FeCl3	--	.46	.55	.62	.65	.68	.10	4.5
58 Pt-Fe	11-17	0.10 to 0.26	17' 30"	2.82% H2PtCl6·6H2O + 0.18% FeCl3	--	.43	.53	.59	.62	.65	.10	4.4
59 Pt-Fe	11-17	0.08 to 0.24	17' 30"	2.82% H2PtCl6·6H2O + 0.18% FeCl3	--	.43	.53	.60	.64	.68	--	--
60 Pt-Fe	--	--	--	2.82% H2PtCl6·6H2O + 0.18% FeCl3	.26	.42	.52	.60	.63	.68	.097	4.4
61 Pt-Fe	11-15	0.19 to 0.26	18' 30'	2.82% H2PtCl6·6H2O + 0.18% FeCl3	.26	.41	.52	.60	.63	.66	.11	3.9
62 Pt-Fe	9-11	0.48 to 0.50	24' 30"	2.82% H2PtCl6·6H2O + 0.18% FeCl3	.25	.41	.51	.58	.62	.65	.11	3.9
66 Pt-Fe	22	0.05 to 0.08	11' 34'	2.82% H2PtCl6·6H2O + 0.18% FeCl3	--	.46	.55	.61	.63	.67	.088	5.2
69 Pt-Fe	5	0.06 to 0.72	25' 36"	2.82% H2PtCl6·6H2O + 0.18% FeCl3								
70 Pt-Fe	5-8	0.01 to 0.22	15' 0'	2.82% H2PtCl6·6H2O + 0.18% FeCl3	------- Not Tested Due to Poisoning -------							
71 Pt-Fe	--	Polarographic Trace		2.82% H2PtCl6·6H2O + 0.18% FeCl3								
73 Pt-Fe	5-8	0.48	16' 56"	2.82% H2PtCl6·6H2O + 0.18% FeCl3	.26	.46	.54	.60	.63	.67	.109	4.2
76 Pt-Fe	5-6	0.53 to 0.63	22' 40"	2.82% H2PtCl6·6H2O + 0.18% FeCl3	.24	.44	.54	.60	.63	--	.091	4.9
81 Pt-Fe	6-8	0.35 to 0.62	18' 40'	2.82% H2PtCl6·6H2O + 0.18% FeCl3	----- Used For Surface Area Measurements Only -----							
83 Pt-Fe	6	0.66 to 0.86	21' 30'	2.82% H2PtCl6·6H2O + 0.18% FeCl3	.37	.51	.56	.61	.64	--	.065	7.7
86 Pt-Fe	6	0.28 to 0.56	11' 0'	2.82% H2PtCl6·6H2O + 0.18% FeCl3	----- Used For Surface Area Measurements Only -----							
63 Pt-Rh-Fe	10	0.06	22' 49"	{ 0.75% H2PtCl6·6H2O +	.28	.42	.50	.56	.58	.62	.082	5.1
64 Pt-Rh-Fe	12	0.08	10' 0'	0.75% H3RhCl6 + 0.1% FeCl3	.31	.44	.52	.57	.60	.65	.079	5.5
65 Pt-Rh-Fe	11-13	0.10 to 0.13	19' 30"	0.75% H PtCl6·6H2O + 0.75% H3RhCl6 + 1.5% FeCl3 }	.32	.45	.53	.58	.61	.65	.081	5.5
79 Pt-Pb-PbO2	13-17	0.36 to 0.68	22' 0'	2.4% H2PtCl6·6H2O + 0.6% Pb(NO3)2 Anodic and Cathodic Deposition	.38	.50	.56	--	--	--	.053	9.5

Figure A-2

Comparison Of Electrode Performances

30 Wt.% H_2SO_4 1 M CH_3OH 60°C.
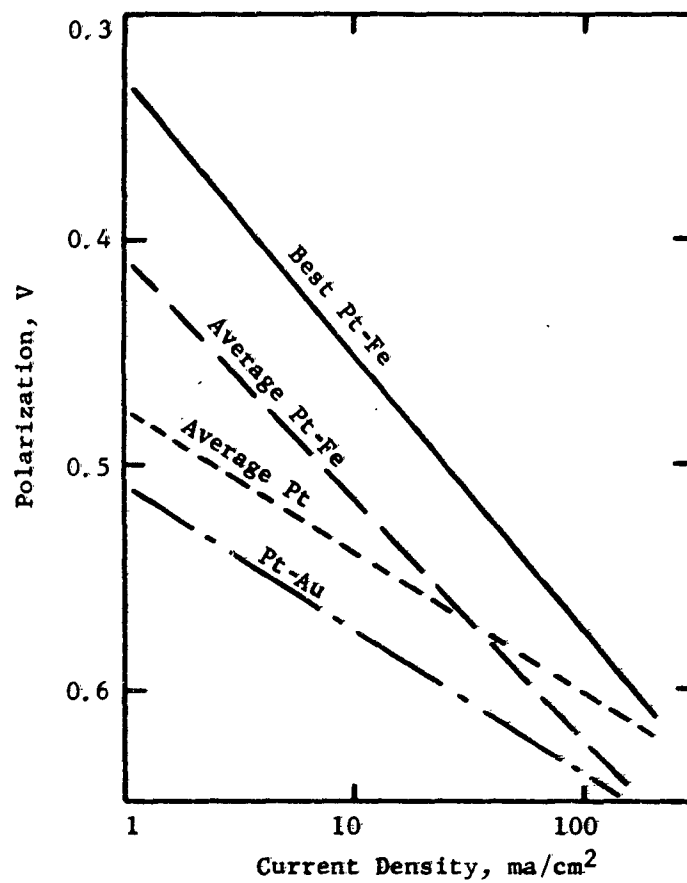
ELECTRODEPOSITION OF Pt AND Pt-Fe
CATALYSTS WITHOUT ADDED Pb(Ac)₂

A Pt and a Pt-Fe electrode were electrodeposited from solutions free of Pb(Ac)$_2$. This compound is normally added in small amounts to increase the deposit fineness. Since black deposits could not be obtained starting with bright Pt surfaces using solutions containing no Pb(Ac)$_2$, normal Pb containing coats were used as bases. The additional Pt or Pt-Fe was electrodeposited from Pb(Ac)$_2$ free solutions. These catalysts were screened in 1 M CH$_3$OH in 30 wt.% H$_2$SO$_4$ solutions at 60°C.

In the case of both Pt and Pt-Fe, activities of the Pb free preparations were poorer than their Pb containing counterparts. For example, Pb free Pt-Fe was polarized 0.46 V. versus the theoretical methanol potential while Pb containing Pt-Fe was polarized 0.41 V. at 1 ma/cm^2. At 50 ma/cm^2 the polarizations were 0.61 and 0.57 V., respectively. Pb free Pt was polarized 0.50 V. at 1 ma/cm^2 and normal Pt 0.47 V. The values at 50 ma/cm^2 were 0.61 and 0.57 V., respectively. Table A-1 shows these results.

TABLE A-1

Effect Of Pb(Ac)₂ Deletion

Catalyst	Polar. @ Indicated ma/cm^2		
	1	10	50
Pt-Fe, Pb Free	0.46	0.55	0.61
Normal Pt-Fe	0.41	0.50	0.57
Pt, Pb Free	0.50	0.56	0.61
Normal Pt	0.47	0.54	0.59

TECHNIQUE FOR PREPARATION OF
CATALYSTS BY NaBH4 REDUCTION

The preparation of Pt-Mo catalysts illustrates the general method used. half a ml each of 0.5 M aqueous solutions of Na_2PtCl_6 and $(NH_4)_6 Mo_7O_{24} \cdot 4H_2O$ are added dropwise and simultaneously to 45 ml of a 2 wt.% aqueous $NaBH_4$ solution. The reaction mixture is allowed to stand at room temperature until H_2 evolution has ceased, which requires about 10 minutes. The resulting precipitate is washed several times with 30 wt.% H_2SO_4. The final wash is with H_2O. Following this, the precipitate is suspended in a small quantity of H_2O and applied to a carefully cleaned and roughened Pt surface. The electrode is then dried at 65°C. for 10 minutes. Two or three such applications give a smooth, uniform and adherent deposit. These electrodes are then handled and tested in the same manner as electrodeposited electrodes.

Another method of preparation, found to be less satisfactory than the one just described, consists of applying the reacting solutions directly to the electrode surface. This can be done by evaporating a solution of the desired metal salts on the electrode and then adding $NaBH_4$ solution, or else adding the two solutions simultaneously to the electrode surface. The former approach was used with electrodes C-87 and C-89 and the latter with C-90 and C-93. The deposits obtained were of poorer quality than those resulting from the technique described in the previous paragraph.

71

PERFORMANCE OF NaBH₄ REDUCED CATALYSTS

Electrode	Reaction Solution	Drying Conditions	Polarization At Indicated ma/cm²					Limiting Current ma/cm²	Tafel Slope	-Log Io
			0	1	10	50	100			
C-87 Pt	Adsorbed H₂PtCl₆·6H₂O + 2 wt% NaBH₄	--	--	--	.58	.62	.65	--	.064	8.3
C-87a Pt-Co	Adsorbed CoCl₂ + 2 wt% NaBH₄	--	.41	.53	.58	.62	.66	--	.058	9.4
C-88 Pt	Electrodeposited Pt Black + 2 wt% NaBH₄	--								
C-88a Pt-Ni	Adsorbed NiCl₂ + 2 wt% NaBH₄	--	--	.52	.57	.62	.65	--	.066	8.0
C-89 Pt	2 Drops 1 M Na₂PtCl₆ + 2 Drops 2 wt% NaBH₄ (Repeated 6 times)		.44	.52	.59	.63	.68	--	.060	9.1
C-90 Pt-Fe	1 Drop 1 M Na₂PtCl₆ + 1 Drop 1 M FeSO₄ + 2 Drops 2 wt% NaBH₄ (Repeated 6 Times)	10 Min. @ 120°C.	.45	.53	.57	.61	.63		.047	11.2
C-93 Pt-Mo	1 Drop 0.1 M Na₂PtCl₆ + 1 Drop 0.05 M (NH₄)₆ Mo₇O₂₄ + 2 Drops 2 wt% NaBH₄ (5 times)	10 Min. @ 120°C.	.36	.47	.54	.60	.62	--	.073	6.5
C-94 Pt-Mo	0.5 ml Each 1 M H₂PtCl₆·6H₂O + 0.5 M (NH₄)₆ Mo₇O₂₄ in 45 ml 2 wt% NaBH₄ (2 times)	15 Min. @ 120°C.	.46	.53	.60	.67	.70	--	--	--
C-95 Pt-Mo	0.5 ml Each 1 M H₂PtCl₆·6H₂O + 0.5 M (NH₄)₆ Mo₇O₂₄ in 45 ml 2 wt% NaBH₄ (2 times)	1 Hour @ 65°C.	.32	.48	.54	.58	.61	--	--	--
C-96 Pt-Mo	0.5 ml Each 1 M H₂PtCl₆·6H₂O + 0.5 M (NH₄)₆ Mo₇O₂₄ in 45 ml 2 wt% NaBH₄ (2 times)	1 Hour @ 65°C.	.20	.47	.53	.57	.60	>500	--	--
C-97 Ir	1 ml 1 M H₂IrCl₃ + 45 ml 2 wt% NaBH₄	1 Hour @ 65°C.	.15	.37	.52	.57	.59	>750	--	--
C-99 Pt-Mo	0.5 ml 0.5 M Na₂PtCl₆ + 0.5 ml 0.5 (NH₄)₆ Mo₇O₂₄ in 45 ml 2 wt% NaBH₄	1 Hour @ 65°C.	.40	.53	.58	.62	.66	--	.053	9.9
C-100 Pt-Mo	0.5 ml 0.5 M Na₂PtCl₆ + 0.5 ml 0.5 (NH₄)₆ Mo₇O₂₄ in 45 ml 2 wt% NaBH₄	10 Min. @ 65°C.	.16	.28	--	--	--	--	--	--
C-101 Pt-Mo	0.5 ml 0.5 M Na₂PtCl₆ + 0.5 ml 0.5 (NH₄)₆ Mo₇O₂₄ in 45 ml 2 wt% NaBH₄	10 Min. @ 65°C.	.12	.22	--	--	--	--	--	--
	2 wt% NaBH₄	10 Min. @ 65°C.	.16	.49	--	--	--	--	--	--

72

Electrode	Reaction Solution	Drying Conditions	Polarization At Indicated ma/cm^2					Limiting Current ma/cm^2	Tafel Slope	-Log I_o
			0	1	10	50	100			
C-102 Pt-Mo	0.5 ml 0.5 M Na2PtCl6 + 0.5 ml 0.5 M (NH4)6Mo7O24 in 45 ml 2 wt% NaBH4	10 Min. @ 65°C.	.13	.46	--	--	--	--	--	--
C-103 Pt-Mo	0.5 ml 0.5 M Na2PtCl6 + 0.5 ml 0.5 M (NH4)6 Mo7O24 in 45 ml 2 wt% NaBH4	10 Min. @ 65°C.	.12	.25	--	--	--	--	--	--
C-104 Pt-Mo	0.5 ml 0.5 M Na2PtCl6 + 0.5 ml 0.5 M (NH4)6 Mo7O24 in 45 ml 2 wt% NaBH4	10 Min. @ 65°C.	.15	.32	--	--	--	--	--	--
C-105 Pt-Mo	1 ml 0.5 M (NH4)6 Mo7O24 - Otherwise Same As C-104	10 Min. @ 65°C.	--	.44	--	--	--	--	--	--
C-106 Pt-Mo	0.25 ml 0.5 M (NH4)6 Mo7O24 - Otherwise Same As C-104	10 Min. @ 65°C.	.15	.36	--	--	--	--	--	--

73

SURVEY OF SOLUBLE CARBONACEOUS FUELS FOR FUEL CELLS

Oxygenated Hydrocarbon	Formula	Boiling Point °C.	Solubility Gms @ 20°C. Per 100 ml H_2O	Cost ¢/lb[1]	Elec. Power KWH/lb[5]	Power Cost ¢/KWH	Maximum ma/cm^2[6]	% Selec. To CO_2[6]
n-Alcohols								
Methyl	CH_3OH	64.6	∞	4.5	1.94	2.32	300+	97-99
Ethyl	CH_3CH_2OH	78.5	∞	7.9	2.54	3.11	300+	3
n-Propyl	$C_2H_5CH_2OH$	97.2	∞	13	2.89	4.49	--	~2-4
n-Butyl	$C_3H_7CH_2OH$	117.7	7.9	19	3.10	6.12	100+	1
Sec-Alcohols								
Sec-Propyl	$CH_3CHOHCH_3$	82.3	∞	6.4	2.86	2.23	300+	0.1
Sec-Butyl	$C_2H_5CHOHCH_3$	99.7	12.5	12.5	3.10	4.03	300+	2-10
Sec-Amyl	$C_3H_7CHOHCH_3$	119.3	5.3	28	3.25	8.60	100+	8
Sec-Hexyl	$C_4H_9CHOHCH_3$	140	v.sl.s.	--	--	--	--	--
Isobutyl	$(CH_3)_2CHCH_2OH$	108.4	9.5	13.0	3.10	4.19	--	--
Tert-Butyl	$(CH_3)_3COH$	82.8	∞	13.5	3.10	4.35	--	--
Aldehydes								
Formaldehyde	$HCHO$	-21	60	10.8	1.52	7.12	200+	100(7)
Acetaldehyde	CH_3CHO	21	∞	10.0	2.26	4.42	100+(3)	6.5
Propionaldehyde	C_2H_5CHO	48.8	20	17(2)	2.68	6.35	--	--
Butyraldehyde	C_3H_7CHO	75.7	3.7	19.5	2.92	6.67	--	--
Ketones								
Acetone	CH_3COCH_3	56.5	∞	7.0	2.63	2.66	$10^{(3)}$	--
Methyl Ethyl	$CH_3COC_2H_5$	79.6	35.3	12.5	2.90	4.31	--	--
Methyl Propyl	$CH_3COC_3H_7$	101.7	v.sl.s.	28(2)	3.06	9.15	--	--
Acids								
Formic	$HCOOH$	100.7	∞	17	0.55	31.1	200+	100
Acetic	CH_3COOH	118.1	∞	10	1.28	7.82	--	--
Propionic	C_2H_5COOH	141.1	∞	22	1.80	12.2	--	--
Butyric	C_3H_7COOH	163.5	5.6	22(2)	2.20	10.0	1	--
Glycols and Glycerols								
Ethylene Glycol	CH_2OHCH_2OH	197	∞	13.5	1.68	8.03	300+	100(4)
Propylene Glycol	$CH_2OHCHOHCH_3$	189	∞	16	2.2u	7.26	230+	Low
α - Butylene Glycol	$CH_2OHCHOHC_2H_5$	192	sl.s.	--	--	--	--	--
Tetraethylene Glycol	$CH_2OHCH_2CH_2CH_2OH$	230	∞	29	2.56	11.3	--	--
Glycerin	$CH_2OHCHOHCH_2OH$	290	∞	23.7	1.55	15.3	300+	100(4)
Erythritol	$(CH_2OHCHOH)_2$	331	61.5	--	--	--	--	--

(1) Chem. & Engr. News Quarterly Report on Current Prices, October 30, 1961.
(2) Estimated.
(3) Estimated from relative activities.
(4) Intermediates produced but react 100% to CO_2 at 40-50% conversion.

(5) Assuming 70% voltage efficiency and complete oxidation to CO_2 and H_2O.
(6) % carbon in feed reacted converted to CO_2 when tested in H_2SO_4 electrolyte using Pt-Black catalyst.
(7) 100% CO_2 produced at 40% conversion (formic acid intermediate).

APPENDIX A-8

EQUIPMENT FOR PERFORMANCE VARIABLES STUDY

1. Model AW 1 ma Voltage Recorder, Esterline Angus Co.
2. Model AW 0.15 amp, Amp Recorder, Esterline Angus Co.
3. 0.15 to 50 amp shunts, Esterline Angus Co.
4. Rectifier, Model 620C-Elit, Art Mfg. Co.
5. Type WIDMT3, Variac Autotransformer, General Radio Co.
6. Calomel Reference Electrode, Beckman Instruments, Inc.
7. Model 610A Electrometer, Keithley Instruments
8. 210 Watt, 110 Volt Heater For Cell, Glass (Not Shown)

1 → Anode Voltage Recorder

2 → Current Recorder

7 →

3

5

CO_2

6

DC — 4

Fuel Plus
H_2SO_4

5 mm I.D.

Anode 0.025 mm
Pt Sheet Plus
8 mg/cm^2 of
Platinum Black

Cathode 0.025 mm
Pt Sheet

1.9 cm Length
10.2 cm I.D.
0.6 cm Wall
Thickness Pyrex
Tubing
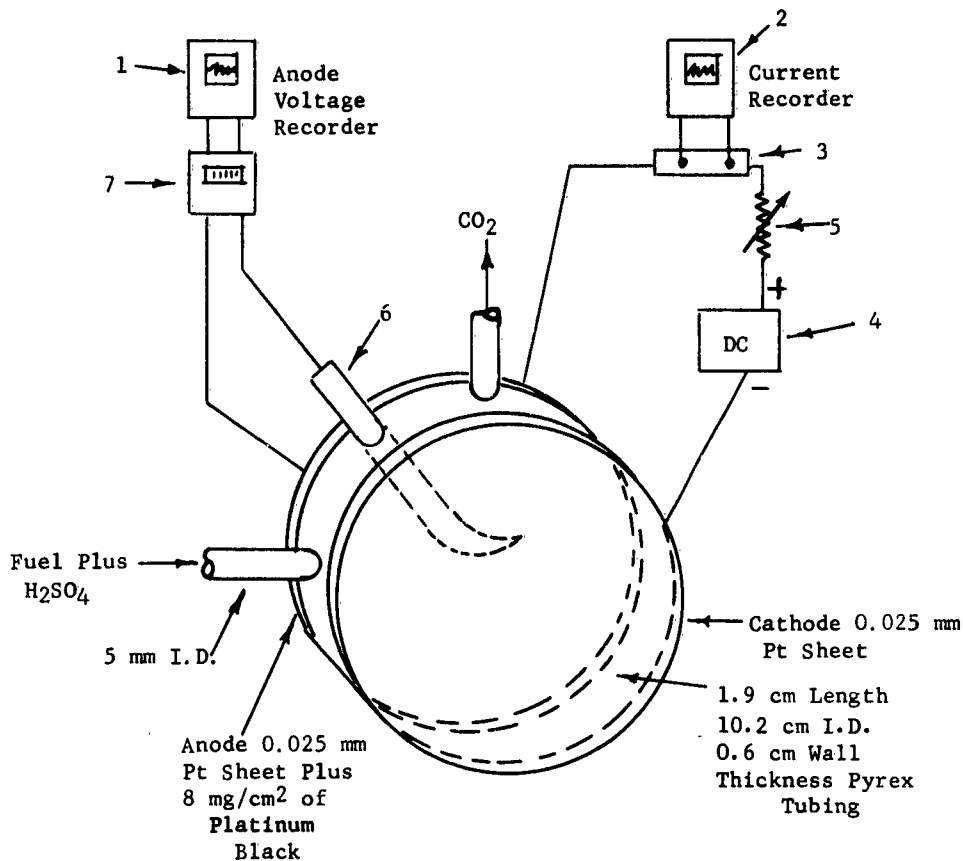
PERFORMANCE TESTS WITH CH₃OH AND INTERMEDIATES IN H₂SO₄

Run Number	3579-34	3579-46	3579-48	3579-50	3579-52	3579-54	3579-60	3579-68	3579-69	3579-70	3579-71	3579-73	3579-74	3579-76	3579-80	3579-81	3617-13
Electrolyte																	
Fuel	CH₃OH(2)	CH₃OH	CH₃OH	CH₃OH	CH₃OH	None	CH₃OH	CH₃OH	CH₃OH	CH₃OH	CH₃OH	CH₃OH	CH₃OH	CH₃OH	CH₃OH	CH₃OH	CH₃OH
Fuel M/L	1.0	1.0	0.5	0.25	0.5	0.0	0.5	0.5	0.5	0.5	0.5	0.5	0.5	3.0	0.5	1.0	0.50
H₂SO₄ wt.%	4.0	24	24	24	12	24	12	12	30	40	56	4	72	30	30	30	30
Anode				─── Pt-Black Deposited On Pt Sheet ───					─ Pt Sheet DC Driven ─ (1)						Pt & Rh Black		Pt Black on Pt Sheet
mg/cm² Pt-Black	8.0	8.0	8.0	8.0	8.0	8.0	8.0	8.0	8.0	8.0	8.0	8.0	8.0	8.0	6.0	6.0	8.0
Cathode																	
Temp. °C.	82	82	82	82	82	82	82	82	82	82	82	82	82	82	82	60	82
Press. Atm. Abs.	1.0	1.0	1.0	1.0	1.0	1.0	1.0	1.0	1.0	1.0	1.0	1.0	1.0	1.0	1.0	1.0	1.0
Electrical Performance																	
Polariz. Volts at: (3)																	
0.0 ma/cm²	0.10	0.31	0.33	0.36	0.28	0.22	0.29	0.14	0.13	0.09	0.13	0.09	0.20	0.13	0.12	0.08	0.06
1.0 ma/cm²	0.44	0.46	0.45	0.45	0.48	0.48	0.47	0.46	0.48	0.47	0.50	0.46	0.52	0.50	0.48	0.51	0.40
10 ma/cm²	0.50	0.50	0.51	0.51	0.52	--	0.51	0.51	0.53	0.54	0.57	0.51	0.58	0.55	0.53	0.55	0.48
50 ma/cm²	0.53	0.54	0.55	0.55	0.54	--	0.54	0.53	0.57	0.58	0.62	0.53	0.65	0.57	0.57	0.58	0.54
100 ma/cm²	0.55	0.55	0.57	0.58	0.56	--	0.56	0.55	0.59	0.60	0.64	0.54	0.73	0.58	0.59	0.60	0.58
300 ma/cm²	--	0.58	0.60	0.63	0.57	--	0.57	0.56	0.61	0.61	--	0.55	--	0.61	0.61	0.62	0.64
ma/cm² @ Polar. of:																	
0.4 volts(3)	0.25	0.08	0.08	0.06	0.05	0.11	0.05	0.08	0.09	0.10	0.06	0.33	0.05	0.10	0.16	0.12	1.0
0.5 volts(3)	5.7	2.5	3.1	3.4	1.0	1.0	1.7	2.8	1.0	1.1	0.5	6.1	0.52	1.0	1.7	0.69	17.2
0.6 volts(3)	170	300	132	100	390	1.9	400	400+	69	64	15	368+	9.7	115	172	115	161
0.7 volts(3)	180	390+	390+	390+	400+	2.2(5)	400+	--	400+	400+	184	--	80	400+	380	400+	400+
Max. ma/cm²	280+(4)	390+	390+	390+	400+	2.2	400+	400+	400+	400+	253	368+	160	400+	380	400+	400+
% of Current Due to CO₂ at 50 ma/cm²	--	--	--	--	98.8	--	98.8	--	--	--	--	--	--	--	--	--	--

(1) 10.2 cm Dia. electrodes, 1.9 cm part (78.6 cm² superficial surface)
(2) Spectroquality
(3) Vs CH₃OH→CO₂ in acid media. Indicated E° for CH₃OH→CO₂ = 0.016 vs H₂ @ 25°C. and unit activities.
(4) Plus indicates measurement was limited by capacity of DC source.
(5) Current possibly due to residual methanol since electrodes were washed only once after run 3579-52.

CONVERSION OF METHANOL TO CO_2

Run Number	Temp. °C.	H_2SO_4 wt. %	Initial Methanol Vol. %	Current Density ma/cm^2	Fuel Reacted, %	% of Current Due to CO_2
3617-14	82	30	2.0	50	5.5	100.0
	82	30	2.0	50	11.0	97.0
	82	30	2.0	50	22.0	97.4
	82	30	2.0	50	27.5	97.8
	82	30	2.0	50	38.5	97.6
	82	30	2.0	50	49.5	97.5
3617-19	82	30	0.6	50	39.9	100.0
	82	30	0.6	50	57.4	97.8
3617-20	93	30	0.6	50	20.1	94.5
	93	30	0.6	50	40.1	104.5
	93	30	0.6	50	59.5	104.0
3617-22	82	30	0.6	30	36.0	97.5
	82	30	0.6	30	48.0	99.0
	82	30	0.6	30	59.9	97.5
3617-26	82	30	0.6	10	42.2	97.6
	82	30	0.6	10	63.3	96.7
3617-31	82	20	0.6	50	66.2	95.2
3617-35	82	20	0.6	30	75.4	96.8
3617-33	82	40	0.6	50	54.0	92.5
3617-37	82	40	0.6	30	49.0	94.0

TESTS WITH ETHYLENE GLYCOL IN H_2SO_4 ELECTROLYTE

Run Number	3513-73	3513-102 & 3579-36	3513-126	3579-1	3579-2	3579-9	3579-10
Electrolyte							
Fuel M/L	1.0	3.0	3.0	3.0	3.0	1.0	6.0
H_2SO_4 wt.%	4.0	4.0	4.0	24.0	24.0	4.0	24.0
Anode[1]	------------------ Pt Black Electrodeposited On Pt ------------------						
mg/cm^2 Pt-Black	8.0	8.0	8.0	8.0	8.0	8.0	8.0
Cathode[1]	----------------------- Pt Sheet DC Driven -----------------------						
Cell Code	(1)	(1)	(1)	(1)	(1)	(1)	(1)
Temp. °C.	82	82	51	49	82	107	82
Press. Atm. Abs.	1.0	1.0	1.0	1.0	1.0	1.0	1.0
Electrical Performance							
Polarization Volts at:[2]							
0.0 ma/cm^2	0.16	0.12	0.18	0.16	0.16	0.11	0.14
1.0 ma/cm^2	0.48	0.48	0.52	0.56	0.57	0.47	0.57
10 ma/cm^2	0.57	0.55	0.61	0.72	0.63	0.54	0.61
50 ma/cm^2	0.67	0.61	0.66	0.88	0.71	0.61	0.67
100 ma/cm^2	0.74	0.63	0.68	0.97	0.78	0.66	0.72
300 ma/cm^2	0.95	0.66	0.76	1.14	0.92	0.75	0.83
ma/cm^2 @ Polarization Of							
0.4 Volts	0.16	1.5	--	--	--	0.09	0.02
0.6 Volts	17	46	9.0	1.7	4.6	42	3.5
0.8 Volts	142	--	330	25.3	276	--	230
Max. ma/cm^2	415	333	370	395	390	345+	400+
CO_2 Production							
Meas. @ ma/cm^2 Of	22-40	115	115	--	57.5	115	115
% of Current Due to CO_2 at Coulombic Conv. Of:							
10%	40	26	57	--	22.6(3)	40.7	6.2(3)
25%	40	44	60	--	--	--	--
50%	98	--	70	--	--	--	--
75%	197	--	--	--	--	--	--
% Electrical Conversion End of Run	77.0	43.3	66.5	0.6	6.0	11.0	5.7
% Distribution of Carbon from Reacted Glycol As:							
Glycolic Acid	33.4	56.1	46.8	--	--	--	--
Formic Acid	1.4	1.1	2.2	--	--	--	--
CO_2	65.2	42.8	51.0	--	--	--	--
% of Fuel Reacted to Products	87.6	50.5	80.0	--	--	--	--
Coulombic Balance % of Current Attributed To:							
Glycolic Acid (4e⁻/molecule)	15.1	25.7	24.1	--	--	--	--
Formic Acid (3e⁻/molecule)	1.0	0.7	1.8	--	--	--	--
CO_2 (5e⁻/molecule)	75.0	51.8	68.8	--	22.6	40.7	6.2
% of Meas. Coulombs Accounted For	91.1	78.2	94.7	--	--	--	--
% Conversion, for Current to Equal CO_2	50.5	40.0	65.0	--	--	--	--
Soln. Color end of run	Yellow	Dk. Brown	Clear	Clear	Brown	Sl. Yellow	Brown

(1) 10.2 cm dia. electrodes, 1.9 cm apart (78.6 cm^2 superficial surface).
(2) Theory, ethylene glycol → CO_2 = +0.006 volts vs. Std. H_2 (unit activities @ 25°C.).
(3) At less than 10% conversion.

TESTS WITH ETHYLENE GLYCOL AND GLYCOLIC ACID IN H_2SO_4 ELECTROLYTE

Run Number	3617-1	3617-2	3617-3	3517-4	3617-7	3617-6	3617-9	3617-10
Fuel	------------------------ Ethylene Glycol ----------------------------							Glycolic Acid
Electrolyte								
Fuel M/L	0.25	0.5	1.0	2.0	0.5	0.5	0.5	0.5
H_2SO_4 wt.%	30	30	30	30	30	30	30	30
Anode	---------------------- Pt Black Electrodeposited on Pt ---------------------------							
mg/cm^2 Pt-Black	8	8	8	8	8	8	8	8
Cathode	---------------------------- Pt Sheet DC Driven --							
Cell Code	(1)	(1)	(1)	(1)	(1)	(1)	(1)	(1)
Temp. °C.	82	82	82	82	49	65	93	81
Press. Atm. Abs.	1.0	1.0	1.0	1.0	1.0	1.0	1.0	1.0
Electrical Performance								
Polarization at:[2]								
0.0 ma/cm^2	0.09	0.09	0.09	0.09	0.06	0.08	0.09	0.29
1.0 ma/cm^2	0.53	0.53	0.54	0.53	0.58	0.56	0.56	--
10 ma/cm^2	0.59	0.60	0.58	0.58	0.69	0.63	0.60	--
50 ma/cm^2	0.64	0.64	0.63	0.63	0.83	0.68	0.62	--
100 ma/cm^2	0.68	0.66	0.65	0.64	--	0.73	0.63	--
300 ma/cm^2	--	0.72	0.70	0.69	--	--	0.66	--
ma/cm^2 at Polarization of:								
0.4 volts	0.24	0.23	0.15	0.30	0.21	0.20	0.40	0.02
0.6 volts	16	10	14	17	15	16	10.0	0.1
0.8 volts	210	400+	400+	400+	40	180	400+	0.25
Max. ma/cm^2	220	400+	400+	400+	90	230+	400+	0.25
Product Solution Color	Clear	Clear	Clear	Clear	Clear	Clear	Sl. Yellow	--

(1) 10.2 cm dia. electrodes, 1.9 cm apart (78.6 cm^2 superficial surface.)
(2) Theory, ethylene glycol $\longrightarrow CO_2$ =+0.006 volts vs H_2 @ unit activities and 25°C.

APPENDIX A-13

TESTS WITH GLYCOLS AND GLYCERIN IN H_2SO_4 ELECTROLYTE

Run Number	1379-15	1379-16	1379-17	1379-18	1379-19	3574-12	3579-24	3579-22 & 38	3579-42	3579-32
Electrolyte										
Fuel	Ethylene Glycol							Glycerin	Glycerin	Propylene Glycol
Fuel M/L	0.5	0.5	0.5	0.5	1.0	12.8	6	1.0	3.0	1.0
H_2SO_4 wt.%	4.0	4.0	24.0	24.0	24.0	24.0	4.0	4.0	24.0	4.0
Anode										
mg/cm^2 Pt-Black	8.0	8.0	8.0	8.0	8.0	8.0	8.0	8.0	8.0	8.0
Cathode	Pt Sheet DC Driven									
Cell Code	(1)	(1)	(1)	(1)	(1)	(1)	(1)	(1)	(1)	(1)
Temp., °C.	65	82	65	82	82	118	82	82	82	82
Press. Atm. Abs.	1.0	1.0	1.0	1.0	1.0	1.0	1.0	1.0	1.0	1.0
Electrical Performance Polarization Volts At:(2)										
At 0.0 ma/cm^2	0.11	0.04	0.11	0.13	0.12	0.24	0.08	0.10	0.11	0.05
1.0 ma/cm^2	0.61	0.53	0.61	0.58	0.57	0.59	0.50	0.48	0.48	0.51
10 ma/cm^2	0.72	0.59	0.70	0.65	0.68	0.64	0.56	0.56	0.55	0.57
50 ma/cm^2	--	1.15	0.76	0.71	0.73	0.69	0.59	0.61	0.59	0.61
100 ma/cm^2	--	--	0.81	0.73	0.76	0.72	0.63	0.63	0.60	0.64
300 ma/cm^2	--	--	--	--	1.04	0.81	0.82	0.65	0.61	--
ma/cm^2 @ Polarization of:										
0.4 Volts	--	0.05	0.09	0.03	0.06	0.02	0.03	0.09	0.09	0.06
0.6 Volts	0.9	11.5	0.8	1.6	2.4	1.7	68	35	115	40
0.8 Volts	16	37	89	172	153	276	268	--	--	230
Max. ma/cm^2	26	50	160+	230+	288+	330+	320+	300+	300+	230+
CO_2 Production										
Meas. @ ma/cm^2	--	--	--	--	34.2	--	--	46	--	57.5
% of Current Due to CO_2	--	--	--	--	51.4(3)	--	--	--	--	(4)
At Coulombic Conv. of:										
10%	--	--	--	--	--	--	--	27	--	--
25%	--	--	--	--	--	--	--	82	--	--
50%	--	--	--	--	--	--	--	--	--	--
75%	--	--	--	--	--	--	--	--	--	--
% Electrical Conversion End of Run	--	--	--	--	8.1	--	--	28.9	--	24
% Conversion for Current to Equal CO_2	--	--	--	--	--	--	--	29	--	--
Soln. Color End of Run	Clear	Clear	Clear	Clear	Clear	Black	Clear	Sl. Yellow	Clear	Clear
% of Current Attributed to:										
CO_2	--	--	--	--	--	--	--	48.7	--	--
Glyceric Acid	--	--	--	--	--	--	--	34.0	--	--
HCOOH	--	--	--	--	--	--	--	7.1	--	--

(1) 10.2 cm. dia. circular electrodes spaced 1.9 cm apart (78.6 cm^2 superficial surface).
(2) Theory, Glycerol $\rightarrow CO_2$ = 0.000 volts vs Std. H_2 (unit activities at 25°C.). Theory, Ethylene Glycol $\rightarrow CO_2$ = +0.006 volts vs Std. H_2 (unit activities at 25°C.).
(3) At less than 10% conversion.
(4) Product odor showed presence of intermediates. CO_2 low but measurement not quantitative.

INFLUENCE OF CONVERSION OF ETHYLENE GLYCOL ON PERFORMANCE & CO_2 PRODUCTION

H_2SO_4 = 30 wt.%
Initial Ethylene Glycol Concentration = 0.25 and 0.5 molar
Current Density = 50 ma/cm^2 constant during run
Temperature = 82°C.

Run Length Minutes	CO_2 Gms Collected During Time Interval	% of Current Attributed To CO_2 During Time Interval	Cumulative % Coulombic Conversion	Volts Polarization at Fuel Electrode	Calculated Molar Conc. Ethylene Glycol In Anolyte
0.5M					
0	None	--	--	0.64	0.50
30	0.2645	37.0	10.5	0.64	0.45
60	0.5073	71.0	21.0	0.68	0.40
90	0.5375	75.5	31.5	0.72	0.34
120	0.5475	76.7	42.0	0.74	0.29
182	1.0031	70.4	64.0	0.76-1.34	0.18
0.25M					
0	None	--	--	0.59	0.25
30	0.3827	53.5	20.4	0.60	0.20
58	0.5463	82.0	39.5	0.60-1.0	0.15

DIAGRAM OF EQUIPMENT USED FOR CONSTANT CURRENT PULSING
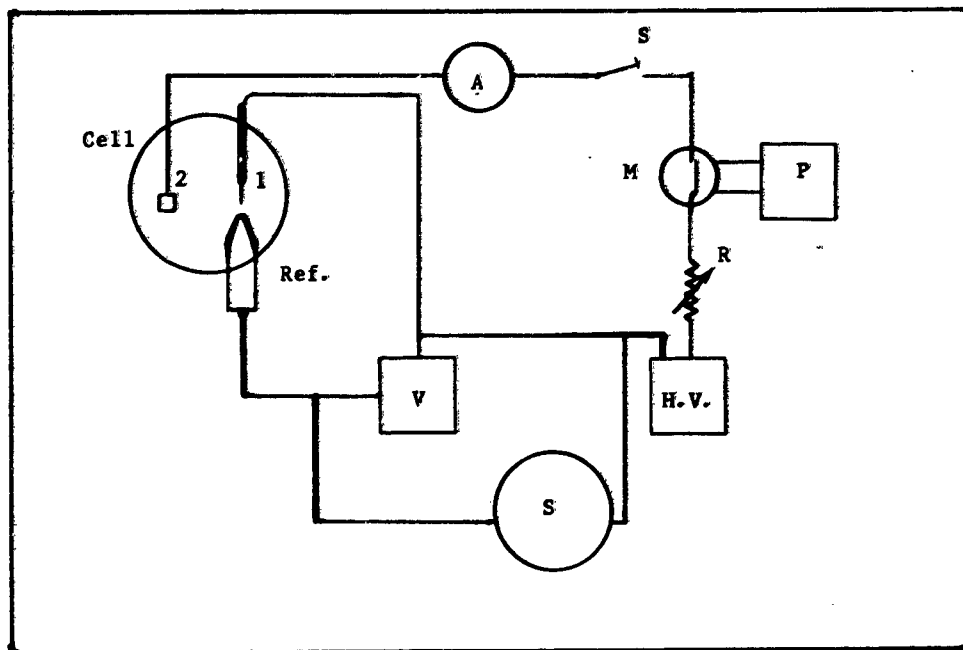
1   - Metal Microelectrode-Anode
2   - Cathode
A   - Keithley Model 600A Electrometer
S   - Microswitch for Manual Pulse
M   - Mercury Relay
P   - Tektronix Models 161 and 162 Variable
          Frequency Pulse Generator
R   - High Resistance
H.V. - New Jersey Electric Co. Model S-300 or
          Home-Made High Voltage Source
V   - Keithley Model 610 Electrometer
S   - Tektronix Model 545A Oscilloscope
          with Camera
Ref. - Saturated Calomel Reference Electrode

Figure A-3

Natural Voltage Oscillations With Methanol
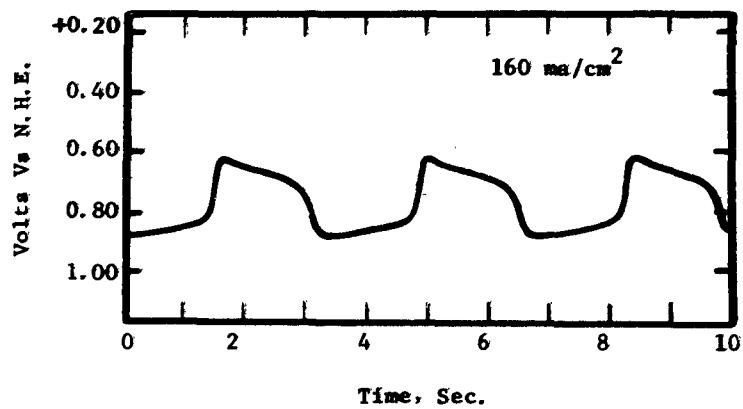
25°C.   1 M/L CH$_3$OH   30 wt.% H$_2$SO$_4$

160 ma/cm^2

(Volts Vs N.H.E. vs Time, Sec.)

Figure A-4

Natural Voltage Oscillations With Formaldehyde

25°C.   1 M/L H$_2$CO   30 wt.% H$_2$SO$_4$

61 ma/cm^2

(Volts Vs N.H.E. vs Time, Sec.)
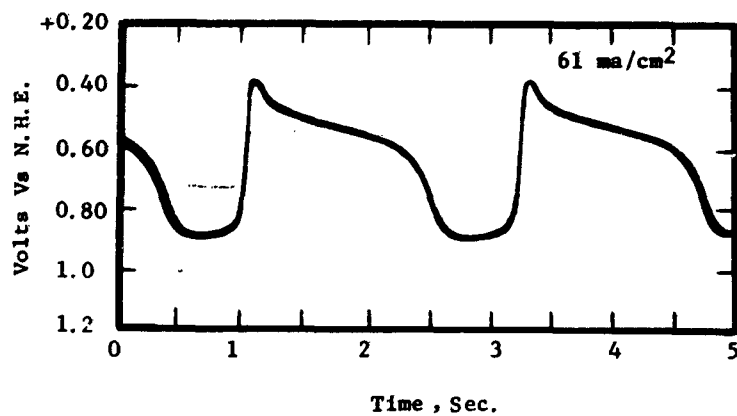
83

Figure Ā-5

Natural Voltage Oscillations With Formic Acid

25°C.   1 M/L HCOOH   30 wt.% H_2SO_4
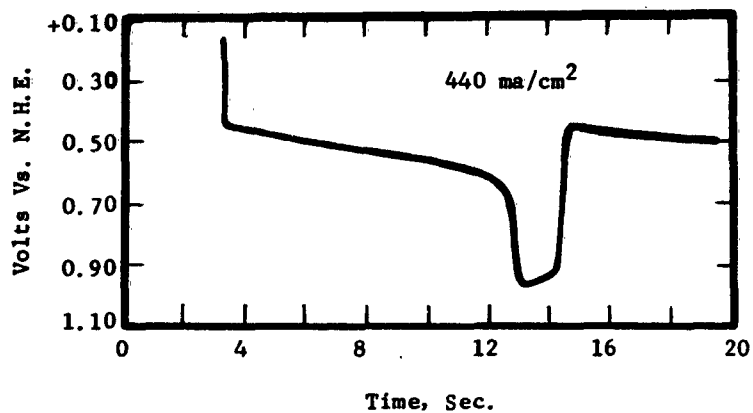
Figure Ā-6

Consecutive Current Pulses-Methanol

25°C.   1 M/L CH_3OH 30 wt.% H_2SO_4

480 ma/cm^2

84
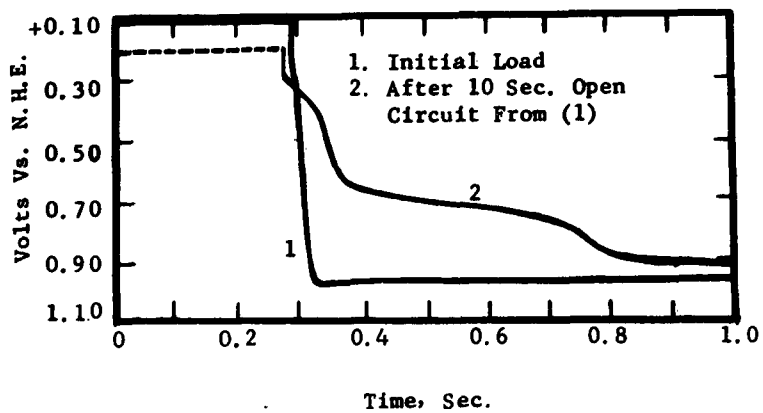
Figure Ā-7

Response To Pulsed Load-Formaldehyde

Return To +0.4 V Vs N.H.E. Allowed
80 ma/cm^2
25°C.   1 M/L H$_2$CO   30 wt.% H$_2$SO$_4$

Figure Ā-7 caption — Response To Pulsed Load-Formaldehyde
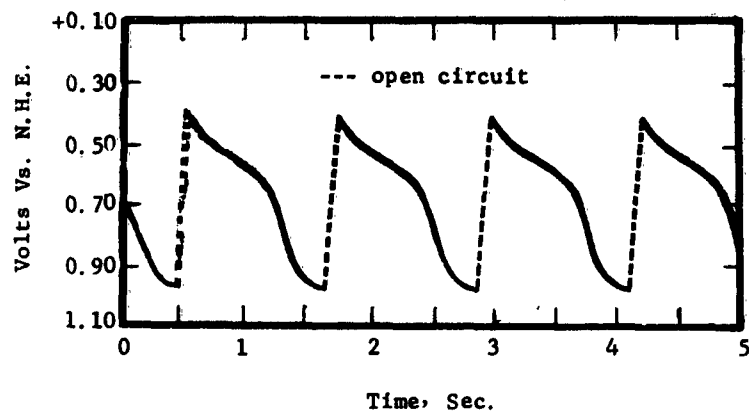
Figure Ā-8

Response To Pulsed Load-Formaldehyde

Return to + 0.3 V Vs. N.H.E. Allowed
80 ma/cm^2
25°C. 1 M/L H$_2$CO   30 wt.% H$_2$SO$_4$

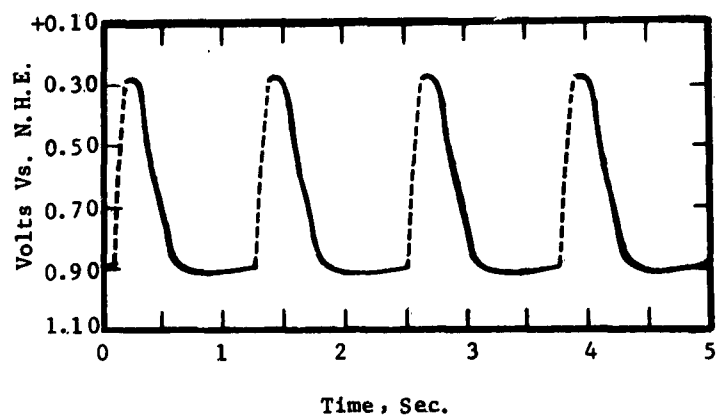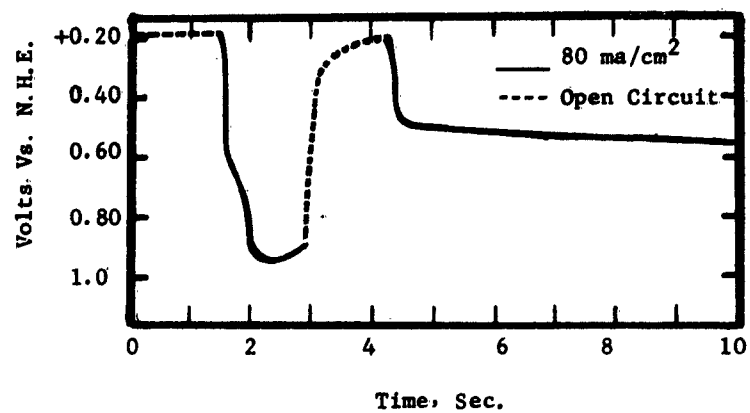Figure Ā-8 caption — Response To Pulsed Load-Formaldehyde

Figure A-9

Formic Acid-Consecutive Current Pulses

25°C. 1 M/L HCOOH 30 wt.% H_2SO_4

POTENTIAL-TIME DEPENDENCE FOR
AN IRREVERSIBLE ELECTRODE REACTION

Making no assumptions concerning the kinetics of the electrode reaction, Delahay et al (1) have derived the potential-time dependence for a totally irreversible process.

Thus:

$$E = \frac{RT}{\alpha\, n_a F} \ln \frac{n F c_B^0 k^0}{i} + \frac{RT}{\alpha\, n_a F} \ln \left[1 - (t/\tau)^{1/2}\right]$$

where:

E = potential
R = gas constant
T = absolute temperature
F = Faraday's constant
α = charge transfer coefficient
n_a = no. of electrons in limiting step
n = no. of electrons in overall process
c_B^0 = bulk concentration of species involved
k^0 = specific rate constant
i = current amps/cm^2 (constant)
t = time (sec)
τ = transition time = $\dfrac{\pi n^2 F^2 c_B^{0\,2} D}{4\, i^2}$

D = diffusion coefficient of species.

Thus a plot of E vs $\log \left[1 - (t/\tau)^{1/2}\right]$ should have a slope $\dfrac{2.303\ RT}{\alpha\, n_a F}$, permitting calculation of the product αn_a.

(1) Delahay, P., "New Instrumental Methods In Electrochemistry", p. 187, Interscience 1954.

CURRENT-TIME DEPENDENCE FOR
DIFFUSION CONTROLLED REACTION

For the electrode process, $R \longrightarrow O + ne$, where the quantity of R at a planar electrode surface is governed by diffusion to the plane, application of a current pulse in excess of the available diffusional flux will produce a voltage time transient as in Appendix Figure A- 10 where τ, the transition time, is related to the current:

$$\tau^{1/2} = \frac{\pi^{1/2} \; nF \; D^{1/2} c_R^o}{2 \; i}$$
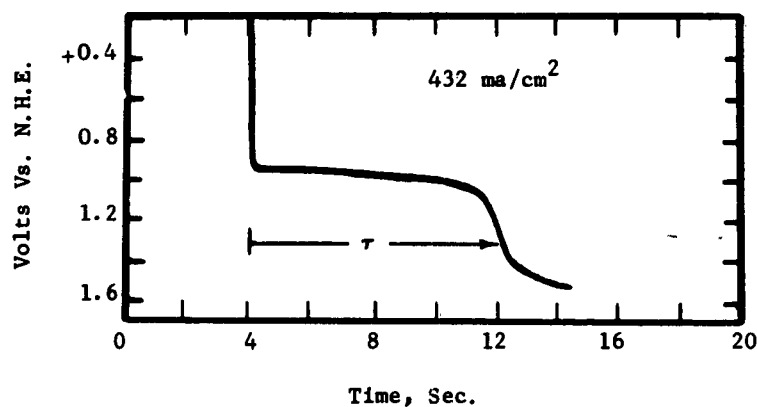
where:

τ = transition time

n = no. of electrons in overall process

F = Faraday's constant

i = current density

D = diffusion coefficient of R

c_R^o = bulk concentration of R

Figure A-10

Typical Trace For Obtaining Transition Time

1 M/L CH_3OH 25°C. 30 wt.% H_2SO_4

Time, Sec.

THE EFFECT OF ACID COMPOSITION ON
OXYGEN ELECTRODE PERFORMANCE

Proprietary Carbon Electrode   82°C.

Acid Conc. wt.%	wt.% HNO_3	O_2 Electrode Polar. From Theory @ ma/cm^2			Limiting Current, ma/cm^2
		0	10	30	
H_3PO_4					
10	1	0.12	0.39	0.61	3
20	1	0.10	0.36	0.57	9
30	1	0.09	0.29	0.52	13
40	1	0.08	0.18	0.50	25
50	1	0.05	0.15	0.25	43
60	1	0.03	0.12	0.20	62
H_2SO_4					
5	1	0.07	0.24	0.45	14
10	1	0.07	0.15	0.39	19
15	1	0.06	0.13	0.38	28
20	1	0.05	0.13	0.23	38
25	1	0.06	0.12	0.19	57
30	1	0.05	0.11	0.16	79
50	1	0.01	0.08	0.14	>90
30	0	0.08	0.38	0.53	--
30	0.10	0.10	0.28	0.51	12
30	0.20	0.10	0.20	0.53	15
30	0.40	0.07	0.15	0.35	28
30	0.50	0.07	0.14	0.31	30
30	0.65	0.08	0.13	0.19	57
30	0.80	0.07	0.13	0.20	--
30	0.90	0.08	0.13	0.19	69
30	1.0	0.06	0.11	0.18	84
30	2.0	0.06	0.11	0.17	--

EFFECT OF FLOW RATE
AND TEMPERATURE ON LIMITING CURRENT

| | NO | | | | | O_2 | | | | | N_2 | | | | |
| | Flow Rate, cc/min | | | | | Flow Rate, cc/min | | | | | Flow Rate, cc/min | | | | |
T, °C.	0	10	30	50	100	0	10	30	50	100	0	10	30	50	100
60	70*	70	70	70	70	50	3	3	3	3	40	125	75	50	50
71	110	111	111	111	111	94	78	60	51	39	98	38	28	25	21
82	16	17	18	18	18	150	135	121	115	106	138	108	85	83	80
93	-	-	-	-	-	229	241	240	241	236	195	193	190	185	178

* ma/cm^2

EFFECT OF FLOW RATE
AND TEMPERATURE ON CURRENT DENSITY AT 0.21 VOLTS POLARIZATION

| | NO | | | | | O_2 | | | | | N_2 | | | | |
| | Flow Rate, cc/min | | | | | Flow Rate, cc/min | | | | | Flow Rate, cc/min | | | | |
T, °C.	0	10	30	50	100	0	10	30	50	100	0	10	30	50	100
60	23*	30	30	30	30	6	0	0	0	0	13	4	3	3	3
71	40	56	56	56	56	43	43	35	31	25	49	18	13	13	11
82	53	88	93	95	98	63	80	75	80	74	58	75	65	63	58
93	90	145	150	151	153	98	133	148	238	235	78	115	84	113	113

* ma/cm^2

APPENDIX B-4

EXPERIMENTAL DETAILS OF AIR ELECTRODE
PERFORMANCE AND REGENERATION VARIABLE STUDIES

Performance studies were carried out in glass cells containing, usually, a platinized Pt wire O_2 electrode (6 mg/cm^2 of Pt) within a circular Pt basket counter-electrode. Of course during the electrode structure work, a variety of O_2 electrodes, as already described, were used in addition to the Pt wire. For regeneration experiments, the O_2 electrode was contained in an alundum thimble wrapped with two layers of cationic membrane, usually types C103, C110 or C313 of the American Machine and Foundry Company. The thimble was sealed to the inner glass sleeve of the cell head with Teflon tape, preventing gas contact between the two compartments. The membranes were held in place with a Viton gasket and a glass cup at the bottom of the thimble. Fresh membranes were used for each run.

Temperatures were controlled to $\pm 0.5°C$. with a Therm-O-Watch regulator or to $\pm 2°C$. with a Variac Autotransformer. Gases were introduced through glass spargers of 10-15 or 170 $-$ 200 micron pore sizes. Comparable results were obtained with both.

All electrical measurements were made with Keithley Model 600A or 610A electrometers. Long term performances were taken with Esterline-Angus Style 90-M recorders or with previously developed robot program recorders. Saturated Ag/AgCl electrodes, connected to the working electrode through a Luggin capillary filled with 30 wt.% H_2SO_4, served as reference electrodes. The driven electrode was operated with a 6 volt ATR Rectifier or Electro-analysis 10 volt power supply. For constant potential measurements a Duffers Model 600 potentiostat was used with a Model 620 8 volt power supply and a Hewlett Packard Model 428A ammeter.

Gas flows were measured with Fisher and Porter rotameters. A Fisher governor pressure regulator was also used with diffusion electrodes.
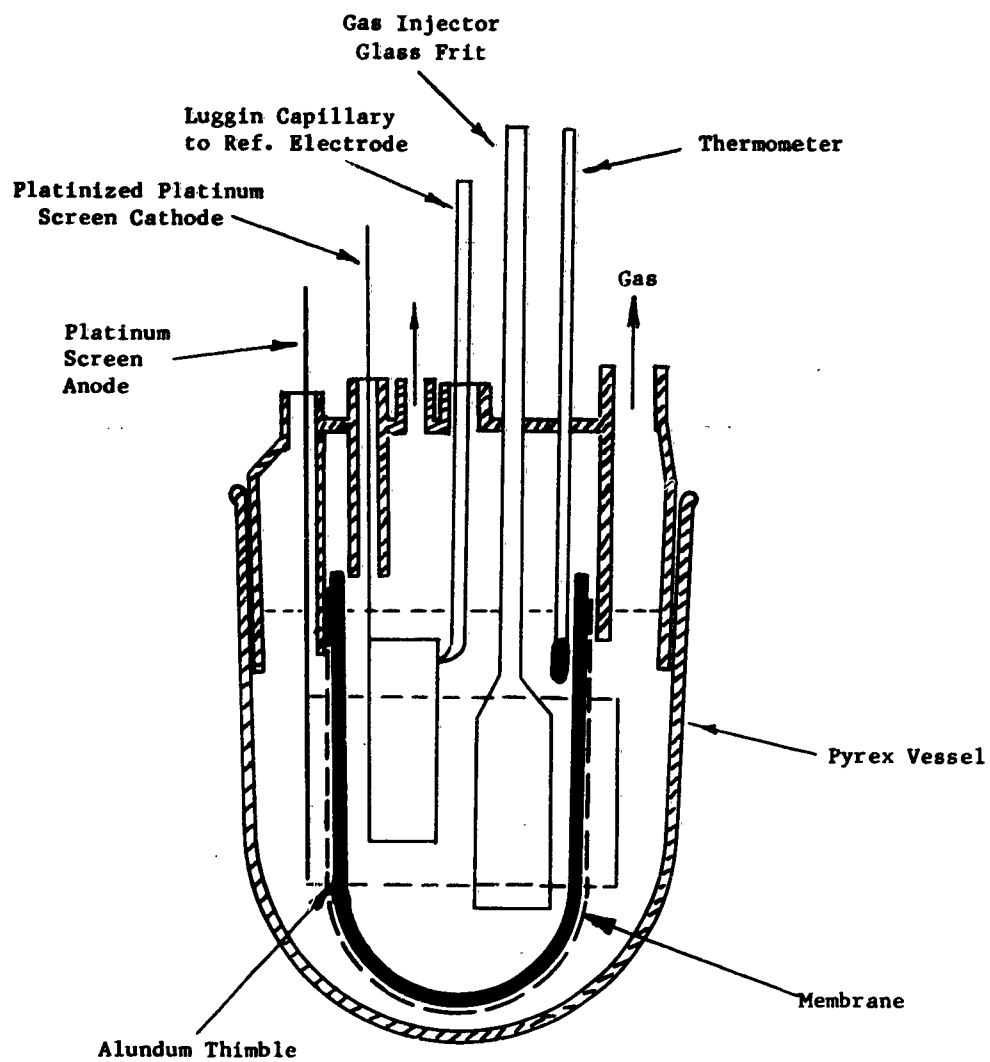
91

Figure B-1

Equipment Used For Recording Chronopotentiograms
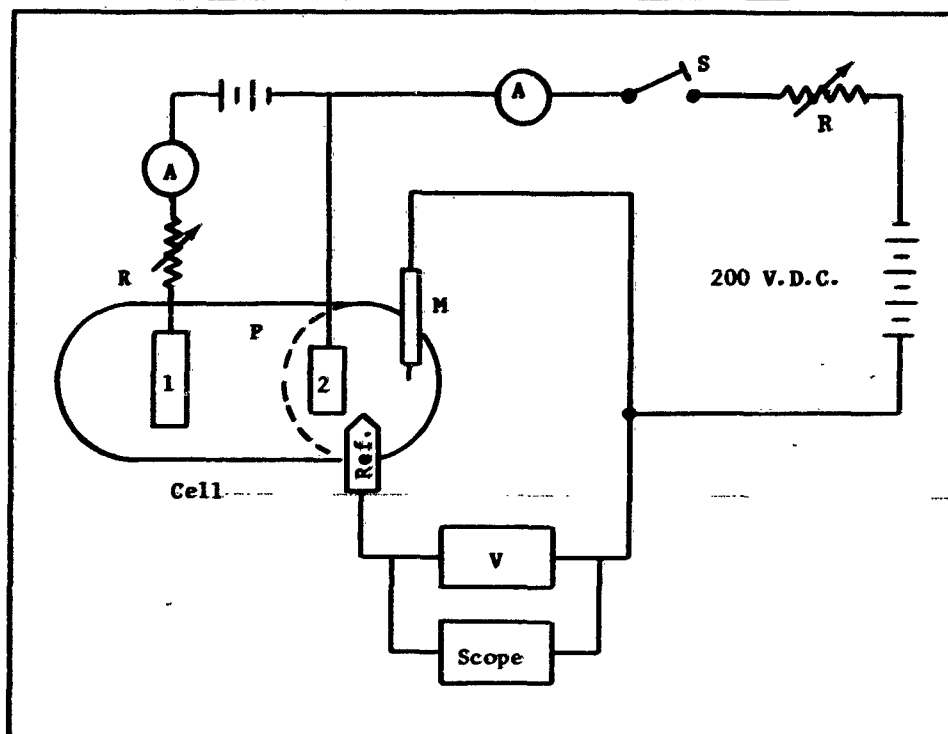
A	-	Ammeters
M	-	Metal Microelectrode
Ref.	-	Saturated Calomel Reference
V	-	Keithley 600A Electrometer
S	-	Switch
R	-	Variable Resistance Box
1,2	-	Auxiliary Electrodes
P	-	Porous Alundum Thimble
Scope	-	Tektronix With Polaroid Camera

HNO₃ Regeneration Test Cell

Gas Injector
Glass Frit

Luggin Capillary
to Ref. Electrode

Thermometer

Platinized Platinum
Screen Cathode

Gas

Platinum
Screen
Anode

Pyrex Vessel

Membrane

Alundum Thimble

Figure B-3

Production Of HNO_3 From Reaction
Of Reduced Gases With 30 wt.% H_2SO_4

94
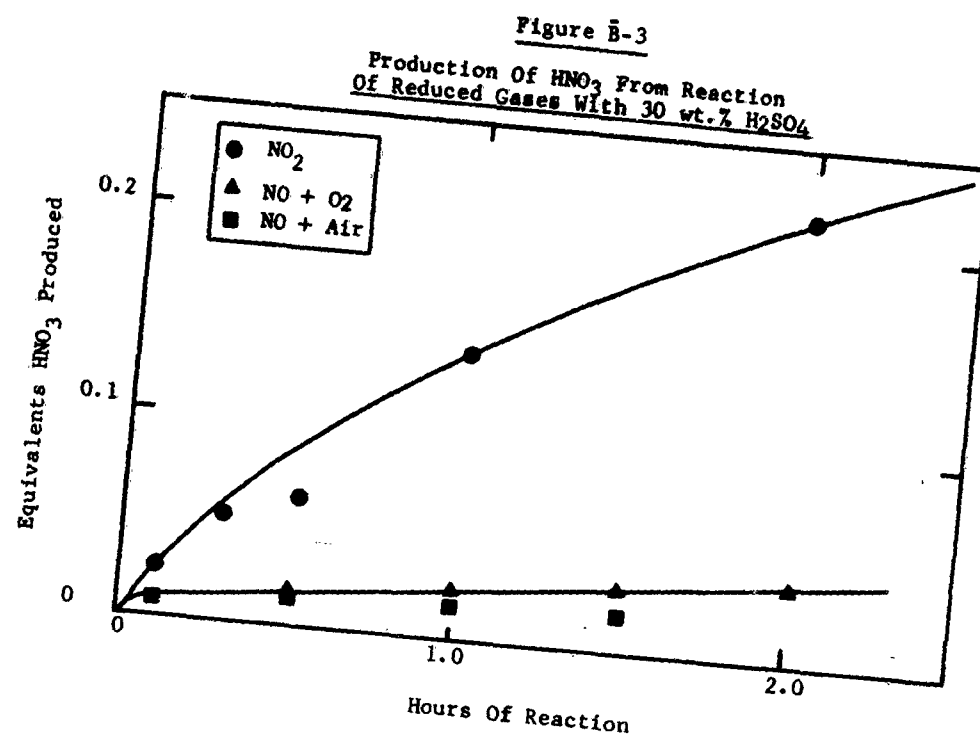
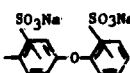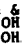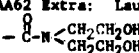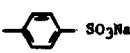## HNO₃ REGENERATION WITH SURFACTANTS AT THE AIR ELECTRODE

82°C. 29 wt.% H₂SO₄ 1 wt.% HNO₃ 3 Electron Reaction
Electrodes: Platinized Pt or Nondiffusional Carbon #837

Surfactant Wt.%	Electrode	Flow Rate cc/min	Average Current Density ma/cm²	Coulombs Measured	Regeneration Efficiency Coulombs Coulomb Equiv. to HNO₃ Lost	Amp Hours Gm HNO₃ Fed	Coulombs Coulomb Equivalent to HNO₃ Fed
I. Experiments With Oxygen							
None (for comparison)	plat. pt	30	32	9700	4.2	2.0	1.6
None (for comparison)	Carbon #837	30	27	9200	4.0	2.1	1.6
Benax 2A1[1] 1 wt.%	plat. pt	30	32	23400	16.2	4.9	3.9
Benax 2A1[1] 1 wt.%	plat. pt	50	30	54600	24.0	11.4	9.1
GAFAC RS710[2] 0.5 wt.%	plat. pt	30	32	17400	7.6	3.6	2.8
GAFAC RS710[2] 1 wt.%	plat. pt	50	32	19000	8.3	3.9	3.1
GAFAC RS710[2] 1 wt.%	plat. pt	40	33	24200	10.5	5.1	4.0
GAFAC RS710[2] 1 wt.%	plat. pt	40	33	18600	8.1	3.9	3.1
GAFAC RS710[2] 1 wt.%	plat. pt	40	33	19900	8.6	4.2	3.3
Kelzan[3] 0.5 wt.%	plat. pt	30	32	17400	7.6	3.6	2.8
Kelzan 0.5 wt.% GAFAC RS710 1 wt.%	plat. pt	30	31	37500	14.0	7.9	6.1
TD 90[4] 1 wt.%	Carbon #837	30	30	24000	10.5	5.4	4.3
TD 90[4] 1 wt.%	plat. pt	30	31	8900	3.9	1.5	1.9
L-1006[5] 0.02 wt.%	plat. pt	10	31	9300	4.0	1.9	1.5
FC-95[6] 0.15 wt.%	plat. pt	30	33	9000	3.9	1.9	1.5
II. Experiments With Air							
None (for comparison)	plat. pt	30	30	4800	2.1	1.0	0.8
None (for comparison)	Carbon #837	30	27	5050	2.2	1.1	0.9
Benax 2A1 1 wt.%	plat. pt	40	31	7300	3.2	1.5	1.2
Benax 2A1 0.5 wt.%	plat. pt	40	33	8900	3.9	1.9	1.5
Benax 2A1 1 wt.%	plat. pt	50	28	12700	>5.5	2.7	2.8
Benax 2A1 1 wt.%	plat. pt	40	29	11900	5.2	2.5	2.0
Benax 2A1 1 wt.%	plat. pt	15	29	10000	4.5	2.3	1.9
GAFAC RS710 1 wt.%	plat. pt	40	33	8900	3.9	1.9	1.5
GAFAC RS710 1 wt.%	plat. pt	40	31	9600	4.2	2.0	1.6
GAFAC RS710 1 wt.%	plat. pt	30	33	10600	3.9	1.9	1.5
Kelzan 1 wt.% + GAFAC RS710 1 wt.%	plat. pt	30	30	4400	1.9	0.9	0.7
TD 90 1 wt.%	plat. pt	20	35	16200	7.1	3.4	2.9
TD 90 0.1 wt.%	plat. pt	40	34	7900	3.4	1.7	1.3
TD 90 0.1 wt.%	Carbon #837	50	30	7000	3.0	1.6	1.3
TD 90 2 wt.%	plat. pt	30	31	10000	4.4	2.1	1.6
TD 120[7] 0.9 wt.% + AA62 Ex.[8] 0.1 wt.%	plat. pt	30	33	5700	2.5	1.2	1.0
TD 150[9] 1 wt.%	plat. pt	25	34	4300	1.9	1.1	0.9
TD 150 1 wt.%	Carbon #837	40	31	8050	3.5	1.8	1.4
Santomer 85[10] 1 wt.%	plat. pt	60	31	8600	3.7	1.8	1.4

Composition of Surfactants:

(1) Benax 2A1 (Dow Chem. Co) anionic sodium dodecylated oxydibenzene disulfonate

(2) GAFAC RS710 (General Aniline & Film Co.) $C_{13}H_{27}(OCH_2CH_2)_{10}-O-P(OH)_2=O$ Monophosphate ester of tridecyl alcohol-ethylene oxide adduct (mole ratio 1:10-11).

(3) Kelzan (Kelco Co.) microbiological polysaccharide derived from glucose and made up from mannose, glucose, and a gluconate salt at a ratio of 2:1:1.

(4) TD 90 Tridecyl alcohol-ethylene oxide adduct at a ratio of 1:9 $C_{13}H_{27}(OCH_2CH_2)_9$-OH.

(5)(6) L-1006, FC-95, Fluorocarbon surfactant (Minnesota Mining & Manufacturing Company).

(7) TD 120: tridecyl alcohol-ethylene oxide adduct at a ratio of 1:12.

(8) Vinol AA62 Extra: Lauric diethanolamide $C_{11}H_{23}-C(=O)-N(CH_2CH_2OH)_2$

(9) TD 150: Tridecyl alcohol-ethylene oxide adduct at a ratio of 1:15.

(10) Santomer 85: Sodium dodecylbenzene sulfonate. $C_{12}H_{25}$—SO₃Na

HNO₃ REGENERATION AT THE AIR ELECTRODE

82°C. 3 Electron Reaction
29 wt.% H₂SO₄ Polarization – 0.2 to 0.4 volts

Electrode	Gas	Flow Rate cc/min	HNO₃ wt.%	Average Constant Current Density ma/cm²	Coulombs Measured	Regeneration Efficiency Coulombs Coulomb Equiv. to HNO₃ Lost	Amp Hours Gm HNO₃ Fed	Coulombs Coulomb Equiv. to HNO₃ Fed
(1) Standard Runs For Comparison:								
plat. pt	O₂	30	1	32	9700	4.2	2.0	1.6
plat. pt	Air	30	1	30	4850	2.1	1.0	0.8
(2) Influence Of Flow Rate and Gas Type:								
Carbon #837	O₂	5	1	37	3660	2.7	1.4	1.1
plat. pt	O₂	5	1	35	7600	3.5	1.7	1.4
Carbon #837	O₂	10	1	39	5100	2.5	1.3	1.0
plat. pt	O₂	10	1	35	3200	3.1	1.5	1.2
plat. pt	O₂	30	1	32	9700	4.2	2.0	1.6
plat. pt	Air	30	1	30	4800	2.1	1.0	0.8
Carbon #837	Air	30	1	27	5050	2.2	1.1	0.9
plat. pt	Air	200	1	32	2700	1.1	0.5	0.4
Carbon #837	Air	200	1	29	3200	1.2	0.8	0.6
plat. pt	Argon	30	1	35	3200	1.3	0.6	0.5
Carbon #837	O₂	30	1	27	9200	4.0	2.1	1.6
(3) Influence of Current Density:								
plat. pt	O₂	30	1	12.5	15800	5.3	3.3	2.6
plat. pt	O₂	30	1	12.5	14600	4.0	2.8	2.2
Carbon #A-50	Air	20	1	16	6600	1.7	1.5	1.2
(4) Influence of Initial Concentration of HNO₃:								
plat. pt	O₂	30	1.5	38	4700	4.1	1.9	1.5
Carbon #837	O₂	30	1.6	26	22200	4.0	3.2	2.6
Carbon #837	O₂	30	1.6	37	25400	4.6	3.7	2.9
Carbon #837	O₂	30	1.1	31	12800	4.3	2.7	2.1
Carbon #837	O₂	30	1.1	31	12800	4.3	2.7	2.1
(5) Influence of Electrode Structure:								
nonporous Carbon	O₂	5	1	35	4500	2.2	1.1	0.9
plat. pt	O₂	5	1	35	1600	3.5	1.7	1.4
Carbon #837	O₂	5	1	27	3600	2.7	1.4	1.1
Carbon A-50	O₂	20	1	31	50300	18.2	11.4	7.3
Carbon A-50	Air	20	1	31	5200	1.9	1.1	0.9
Carbon A-50	Air	20	1	31	3800	1.4	0.9	0.7
Proprietary	O₂	30	1	30	4000	1.7	0.8	0.6
Proprietary	O₂	30	1	30	8700	3.1	1.8	1.4

HNO₃ REGENERATION AT THE AIR ELECTRODE

82°C. 3 Electron Reaction
29 wt% H₂SO₄ Polarization - 0.2 to 0.4 volts

Electrode	Gas	Flow Rate cc/min	HNO₃ wt.%	Average Constant Current Density ma/cm²	Coulombs Measured	Regeneration Efficiency Coulombs Coulomb Equiv. to HNO₃ Lost	Amp Hours Gm HNO₃ Fed	Coulombs Coulomb Equivalent to HNO₃ Fed
(6) Results With Different Nitrate Sources								
plat. pt	O₂	30	NaNO₃*	34	7300	3.1	1.5	1.2
plat. pt	O₂	30	NH₄NO₃*	30	3900	1.7	0.8	0.6
plat. pt	O₂	30	NH₄NO₃*	30	2500	1.1	0.6	0.4
(7) Results Without Membranes								
plat. pt	O₂	30	1	34	5400	2.3	1.1	0.9
plat. pt	O₂	30	1	31	6400	2.8	1.3	1.1
(8) Influence of Glass Wool								
plat. pt	O₂	30	1	31	27000	7.3	3.6	2.8
plat. pt	Air	30	1	31	20400	4.4	2.1	1.7

* Equivalent to 1 wt.% HNO₃

EFFECT OF HNO_3 ON CH_3OH
PERFORMANCE IN ABSENCE OF REDUCTION PRODUCTS

Methanol Conc. M/L	Current ma/cm^2	Polar. Volts From Theory	cc 30% HNO_3	Wt.% HNO_3
0.5	3.25	.535	None	0
0.5	3.25	.535	2	.2
0.5	3.25	.535	4	.4
0.5	3.25	.525	6	.6
0.5	3.25	.530	8	.8
0.5	3.25	.530	10	1.0
0.5	3.25	.530	12	1.2
0.5	3.25	.530	14	1.4
0.5	3.25	.535	16	1.6
0.5	3.25	.535	18	1.8
0.5	3.25	.535	20	2.0
0.5	3.25	.535	22	2.2
0.25	3.25	.540	None	0
0.25	3.25	.535	2	.2
0.25	3.25	.535	4	.4
0.25	3.25	.530	6	.6
0.25	3.25	.530	8	.8
0.25	3.25	.535	10	1.0
0.25	3.25	.540	12	1.2
0.25	3.25	.545	14	1.4
0.25	3.25	.555	16	1.6
0.25	3.25	.560	18	1.8
0.25	3.25	.570	20	2.0
0.25	3.25	.570	22	2.2
0.5	6.5	.565	None	0
0.5	6.5	.560	2	.2
0.5	6.5	.560	4	.4
0.5	6.5	.555	6	.6
0.5	6.5	.555	8	.8
0.5	6.5	.550	10	1.0
0.5	6.5	.550	12	1.2
0.5	6.5	.555	14	1.4
0.5	6.5	.555	16	1.6
0.5	6.5	.560	18	1.8
0.5	6.5	.570	20	2.0
0.5	6.5	.580	22	2.2
0.5	6.5	.575	24	2.4
0.5	6.5	.590	26	2.6
0.5	6.5	.595	28	2.8
0.5	6.5	.605	30	3.0
0.5	6.5	.605	31	3.1

## MATHEMATICAL ANALYSIS OF THE FUEL ELECTRODE DESIGN

I. The Effect Of Electrochemical
    Oxidation On Methanol Concentration
    Near The Surface Of An Electrode

The electrochemical oxidation of methanol at the surface of a catalytic electrode produces a gradient in the concentration of methanol in the electrolyte. This gradient results in a lower average concentration of methanol in a porous electrode. In part I, the effect of the electrochemical reaction on the methanol concentration at steady-state is explained in a simple geometry at a flat plate electrode. These principles are then extended to a cylindrical pore as representative of a porous structure in part II. In part III, the transient behavior of a particular porous electrode structure is discussed.

The steady-state electrochemical oxidation of methanol at a flat plate electrode is described by one dimensional binary diffusion of methanol through a stationary liquid electrolyte film (0 to z_1).
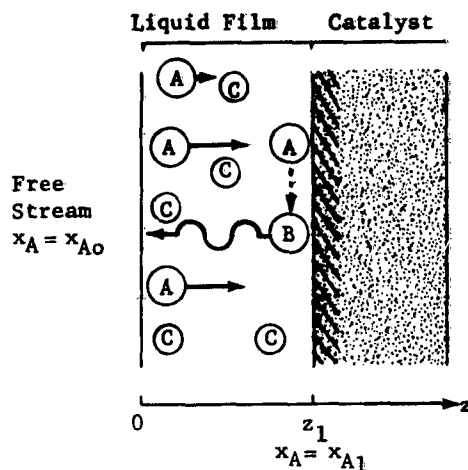
The concentration of methanol, species A, in the free stream at $z = 0$ is denoted by the mole fraction x_{Ao} which is assumed constant. Methanol diffuses through electrolyte C in the film and is adsorbed on the catalyst surface at $z = z_1$ where it reacts to form insoluble CO_2, species B. The concentration of methanol at the interface is x_{A1}, which is assumed constant for a given overall reaction rate.

The assumptions in the mathematical treatment are summarized as follows:

(1) The diffusion flux of methanol is measured relative to the stationary catalyst electrolyte interface.

99

(2) Concentration of B in AC = $x_B = 0$ and therefore the flux of B in AC = $N_{Bz} = 0$

(3) Flux of C in AC = $N_{Cz} = 0$

(4) One dimensional binary diffusion

(5) Steady-state

(6) Concentrations at the boundaries are constant and determined by perfect mixing at $z = 0$ and the overall reaction rate at $z = z_1$

(7) c, D_{AC}, T, P, are assumed constant.

Based on this model, the problem is formulated in terms of the total molar flux of methanol which is equivalent to the overall reaction rate at steady-state.

(I-1)
$$N_{Az} = - \frac{cD_{AC}}{1 - x_A} \frac{dx_A}{dz}$$

where
N_{Az} = molar flux of methanol in the z direction
c = total molar concentration
x_A = mole fraction of methanol
D_{AC} = binary diffusion coefficient
z = Cartesian coordinate

The differential equation is

(I-2)
$$\frac{d}{dz} \left[\frac{1}{1 - x_A} \frac{dx_A}{dz} \right] = 0$$
with boundary conditions

$$x_A = x_{Ao} \quad \text{at} \quad z = 0$$
$$x_A = x_{A1} \quad \text{at} \quad z = z_1$$

The solution of this boundary value problem is straightforward and gives the resulting concentration profile.

(I-3)
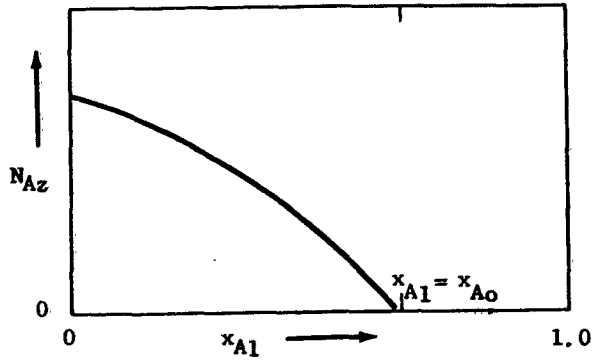$$\frac{1 - x_A}{1 - x_{Ao}} = \left(\frac{1 - x_{Ao}}{1 - x_{A1}} \right)^{- \frac{z}{z_1}}$$

The flux or overall reaction rate is derived from the concentration profile by differentiating the above equation and evaluating at $z = z_1$.

(I-4)
$$N_{Az} = - \frac{cD_{AC}}{z_1} \ln \left(\frac{1 - x_{Ao}}{1 - x_{A1}} \right)$$

The flux varies inversely as the concentration at the interface as shown in Figure C-1. For $x_{A1} = x_{Ao}$, i.e. no gradient, the flux is zero.

Figure C-1

Effect of Interfacial Concentration
on Overall Reaction Rate

$$N_{Az} = - \frac{cD_{AC}}{z_1} \ln\left(\frac{1 - x_{Ao}}{1 - x_{A1}}\right)$$

For $x_{A1} = 0$, the flux is equivalent to the diffusion limited overall reaction rate

(I-5) $$N_{Az_L} = - \frac{cD_{AC}}{z_1} \ln\left(1 - x_{Ao}\right)$$

and the concentration profile is given by

(I-6) $$1 - x_A = \left(1 - x_{Ao}\right)^{1 - \frac{z}{z_1}}$$

The net effect of the reaction of methanol at the surface $z = z_1$ is to decrease the concentration from x_{Ao} through the liquid film 0 to z_1. The average concentration, x_{Aav}, over this film is defined as

(I-7) $$x_{Aav} = \frac{\int_0^{z_1} x_A \, dz}{\int_0^{z_1} dz}$$

Using the relationship for $x_A(z)$ from equation I-3, equation I-7 may be integrated to

(I-8) $$x_{Aav} = 1 + \frac{x_{Ao} - x_{A1}}{\ln\left(\frac{1 - x_{Ao}}{1 - x_{A1}}\right)}$$

The average concentration is a monotonic increasing function of x_{A1}. This follows from the definition of x_{Aav} and the mean value theorem. It is also seen from

(I-9) $$\frac{dx_{Aav}}{dx_{A1}} = - \frac{1}{\ln\left(\frac{1 - x_{Ao}}{1 - x_{A1}}\right)} \left[1 + \frac{x_{Ao} - x_{A1}}{1 - x_{A1}} \frac{1}{\ln\left(\frac{1 - x_{Ao}}{1 - x_{A1}}\right)} \right]$$

101

where

$$\frac{1-x_{Ao}}{1-x_{A1}} < 1$$

and

$$\ln\left(\frac{1-x_{Ao}}{1-x_{A1}}\right) < 0$$

Thus if

$$(I-10) \quad \left|\ln\left(\frac{1-x_{Ao}}{1-x_{A1}}\right)\right| > \frac{x_{Ao}-x_{A1}}{1-x_{A1}}$$

it follows that

$$\frac{dx_{Aav}}{dx_{A1}} > 0$$

for all values of x_A. The inequality in I-10 is seen to be true by expanding the ln function in the left member

$$\left|\ln\left(\frac{1-x_{Ao}}{1-x_{A1}}\right)\right| = 2\left\{\frac{\left(\frac{x_{Ao}-x_{A1}}{1-x_{A1}}\right)}{\left(\frac{1-x_{Ao}}{1-x_{A1}}\right)+1} + \frac{1}{3}\left[\frac{\left(\frac{x_{Ao}-x_{A1}}{1-x_{A1}}\right)}{\left(\frac{1-x_{Ao}}{1-x_{A1}}\right)+1}\right]^3 + \cdots\right\}$$

where

$$\frac{2}{\left(\frac{1-x_{Ao}}{1-x_{A1}}\right)+1} > 1$$

and the proper convergence exists for

$$0 < x_{A1} < 1$$

$$0 < x_{Ao} < 1$$

Since x_{A1} decreases monotonically with increasing N_{Az}, it follows that $x_{Aav} = f(N_{Az})$, shown in equation I-11, also decreases monotonically with increasing N_{Az}.

$$(I-11) \quad x_{Aav} = 1 - \frac{cD_{AC}}{z_1 N_{Az}}\left(1-x_{Ao}\right)\left(e^{\frac{z_1 N_{Az}}{cD_{AC}}} - 1\right)$$

Thus x_{Aav} varies inversely with the overall rate N_{Az}. This is also seen from equation I-12.

$$(I-12) \quad \frac{dx_{Aav}}{dN_{Az}} = \frac{cD_{AC}}{z_1 N_{Az}^2}\left(1-x_{Ao}\right)\left[e^{\frac{z_1 N_{Az}}{cD_{AC}}}\left(1-\frac{z_1 N_{Az}}{cD_{AC}}\right) - 1\right]$$

where for

$$(I-13) \quad \frac{z_1 N_{Az}}{cD_{AC}} > 1 \quad, \quad \frac{dx_{Aav}}{dN_{Az}} < 0$$

102

and for

$$(\text{I-14}) \quad \frac{z_1 N_{Az}}{c D_{AC}} < 1 \ , \quad \frac{dx_{Aav}}{dN_{Az}} < 0 \quad \text{if} \quad e^{\frac{z_1 N_{Az}}{c D_{AC}}} \left(1 - \frac{z_1 N_{Az}}{c D_{AC}} \right) < 1$$

This last inequality (I-14) is true, thus

$$e^{\frac{z_1 N_{Az}}{c D_{AC}}} = 1 + \frac{z_1 N_{Az}}{c D_{AC}} + \frac{1}{2!}\left(\frac{z_1 N_{Az}}{c D_{AC}}\right)^2 + \cdots$$

$$\left(1 - \frac{z_1 N_{Az}}{c D_{AC}}\right)^{-1} = 1 + \frac{z_1 N_{Az}}{c D_{AC}} + \left(\frac{z_1 N_{Az}}{c D_{AC}}\right)^2 + \cdots$$

where the proper convergence exists for $1 > \frac{z_1 N_{Az}}{c D_{AC}}$. The derivative, $\frac{dx_{Aav}}{dN_{Az}}$, at $N_{Az} = 0$ is evaluated from l'Hospital's rule and is zero.
The functional behavior of I-11 is illustrated in Figure C-2.

Figure C-2
Effect of Overall Reaction Rate on Average Concentration in Fluid Film
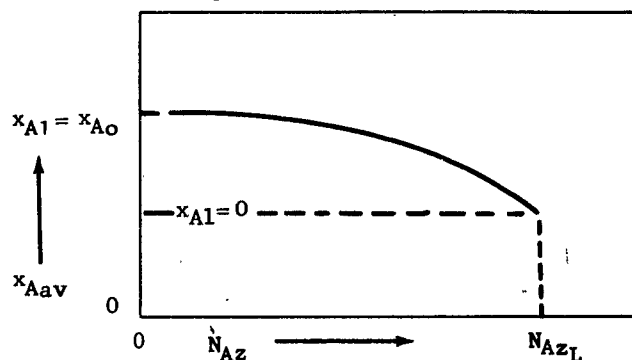
$$x_{Aav} = 1 - \frac{c D_{AC}}{z_1 N_{Az}}\left(1 - x_{Ao}\right)\left(e^{\frac{z_1 N_{Az}}{c D_{AC}}} - 1\right)$$

Equation I-11 can be applied in the case of the electrochemical oxidation of methanol to CO_2 at a flat plate catalytic anode where it is assumed that

$D_{AC} = 10^{-5} \ cm^2/sec$ at $20°C$. and 1 atm
$x_{Ao} = 0.02 = $ mole fraction of methanol at $z = o$
$c \quad = 0.052$ moles/cc
$N_{Az} = 0.173 \times 10^{-8} \ i$
$i \quad = $ milliamps/cm^2
$z_1 \quad = 10^{-2}$ cm

The relationship between N_{Az} and i assumes a 6 electron change for the oxidation process. The concentrations x_{Ao} and c correspond to a 1 molar methanol solution in 30% sulfuric acid. The film thickness, z_1 , is assumed constant. This is based on the CO_2 evolution at the surface which provides efficient stirring action at current densities above 10 milliamps/cm^2 and should reduce z_1 to a minimum value

reported in several studies to be approximately 0.01 cm.

Results are shown in Figure $\overline{C}$- 3 and Table $\overline{C}$- 1, The diffusion limited current is calculated from equation I-5 and is approximately 600 milliamps/cm^2.

Figure $\overline{C}$- 3
Effect Of Overall Reaction Rate On Average
Methanol Concentration In Fluid Film
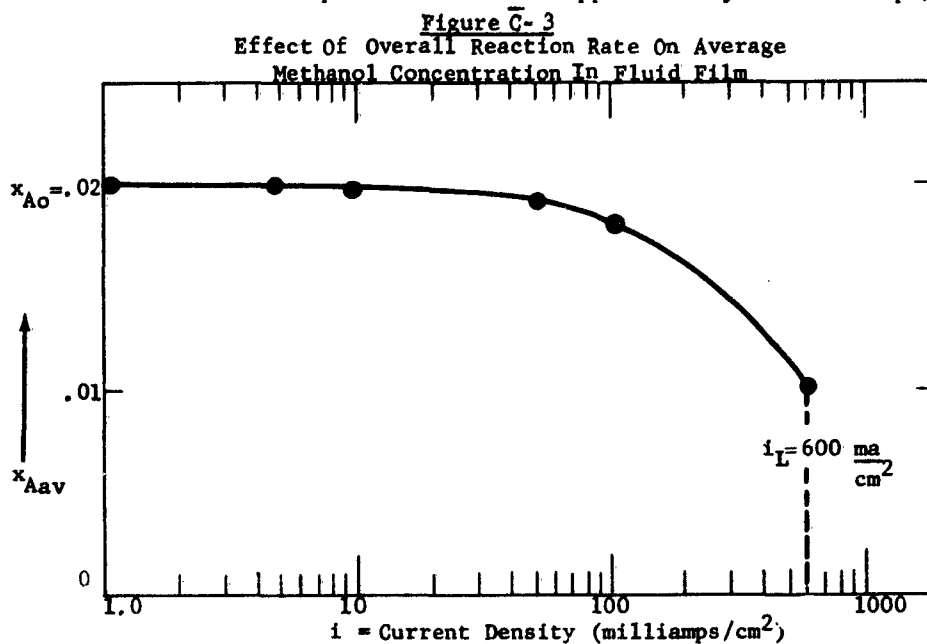
TABLE $\overline{C}$-1

i Milliamps/cm^2	$\dfrac{1 - x_{Aav}}{1 - x_{Ao}}$	x_{Aav} (for x_{Ao}= 0.02)
1	1.000017	0.01998
5	1.000083	0.01992
10	1.000167	0.01983
50	1,000834	0.01919
100	1.00168	0.01833
600	1.0101	0.01013

A partial verification of the mathematical model has been made by measuring limiting currents as a function of methanol concentration, x_{Ao} , and comparing to predicted values from equation I-5. The tests were made at 80°C. and 1 atmosphere absolute pressure in 30% H$_2$SO$_4$ electrolyte where it is assumed that

$$D_{AC} = 1.3 \times 10^{-5} \text{ cm}^2/\text{sec}$$
$$z_1 = 10^{-2} \text{ cm.}$$

The results in Figure $\overline{C}$- 4 show excellent agreement between theory and experiment.

104

Figure C̄- 4

Limiting Currents for Methanol Solutions

$T = 80°C$
$P = 1$ atm

x_{A_o}

● Experiment

▲ Theory
  $z_1 = 10^{-2}$ cm
  $D_{AC} = 1.3 \times 10^{-5} \frac{cm^2}{sec}$

i_L = Limiting Current Density (ma/cm^2)

105
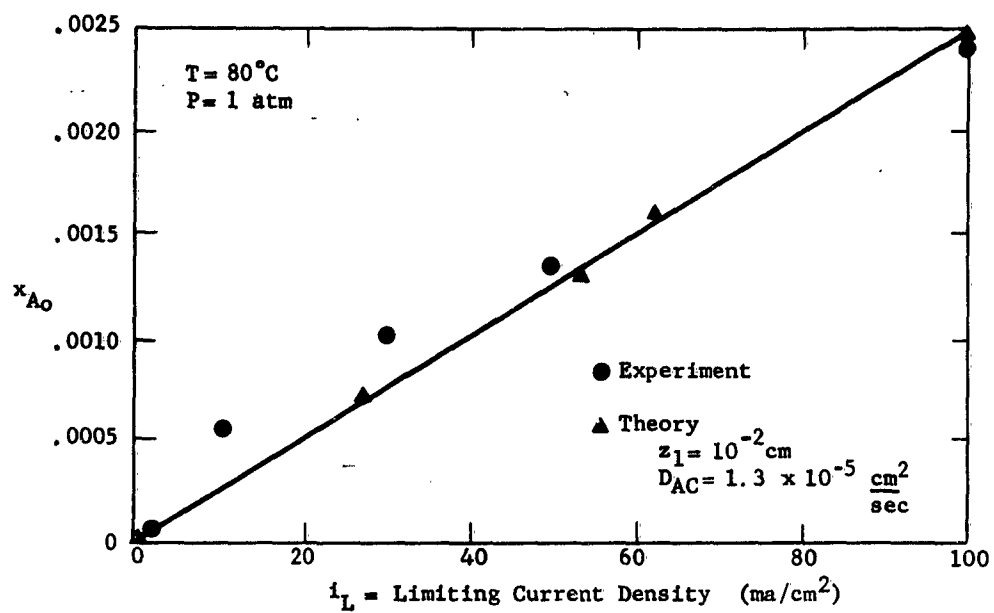
II. The Effect Of Electrochemical Oxidation On
The Radial Methanol Concentration Gradient

        The basic physical model described in part I for Cartesian coordinates can also be applied to a polar geometry as in a cylindrical pore. The results for this type of configuration are representative of other 3 dimensional shapes such as square or irregular pores. The physical picture at the surface is exactly the same as described previously for a flat plate. However, in this case the diverging area in the direction of the flux can account for an additional decrease in concentration at a given reaction rate. This is seen as follows.
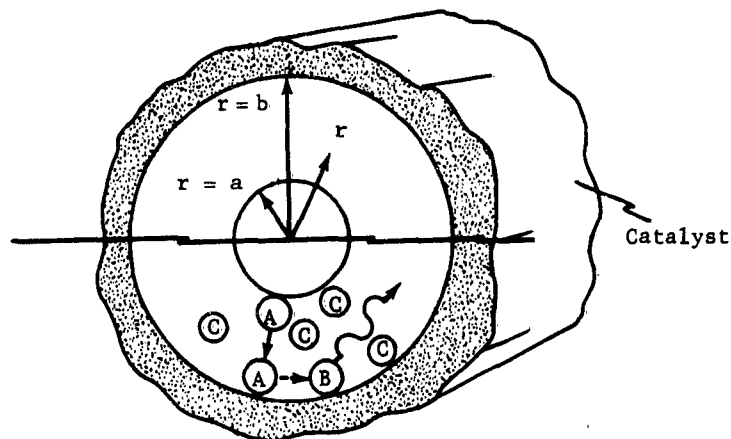
Methanol, A, diffuses from a well mixed free stream at r = a through electrolyte C to the catalyst surface at r = b where it reacts to form an insoluble component. The equation for the radial flux of methanol is

$$(\text{II-1}) \quad N_{Ar} = -\frac{cD_{AC}}{1-x_A} \frac{dx_A}{dr}$$

where

$\quad\quad\quad N_{Ar}$ = radial molar flux of methanol
$\quad\quad\quad c$ = total molar concentration
$\quad\quad\quad x_A$ = mole fraction of methanol
$\quad\quad\quad D_{AC}$ = binary diffusivity
$\quad\quad\quad r$ = radial coordinate

The steady-state differential equation for mass transport in this case is

(II-2) $\quad \dfrac{d}{dr}\left[\dfrac{r}{1-x_A}\dfrac{dx_A}{dr}\right]=0$

with boundary conditions

$$x_A = x_{Ao} \quad \text{at} \quad r = a$$
$$x_A = x_{A1} \quad \text{at} \quad r = b$$

The solution of this boundary value problem is

(II-3) $\quad x_A = 1 - \left[r^{\frac{\ln\left(\frac{1-x_{Ao}}{1-x_{A1}}\right)}{\ln\frac{a}{b}}} \cdot a^{\frac{\ln\left(1-x_{A1}\right)}{\ln\frac{a}{b}}} \cdot b^{-\frac{\ln\left(1-x_{Ao}\right)}{\ln\frac{a}{b}}}\right]$

which represents the concentration profile across the film from a to b. The steady-state flux at the surface, i.e. the overall reaction rate, is derived by differentiating II-3, evaluating at $r = b$, and combining with II-1.

(II-4) $\quad N_{Ar} = \dfrac{cD_{AC}}{b}\dfrac{\ln\left(\dfrac{1-x_{Ao}}{1-x_{A1}}\right)}{\ln\frac{a}{b}}$

This flux is compared with the flux to a flat plate, from equation I-4, in Figure C-5 where the pore radius, b, is assumed to equal the film thickness, z_1[1].

Figure C-5

Effect Of Interfacial Concentration
On Overall Reaction Rate

$$N_{Ar} = \frac{cD_{AC}}{b}\frac{\ln\left(\dfrac{1-x_{Ao}}{1-x_{A1}}\right)}{\ln\frac{a}{b}}$$

---
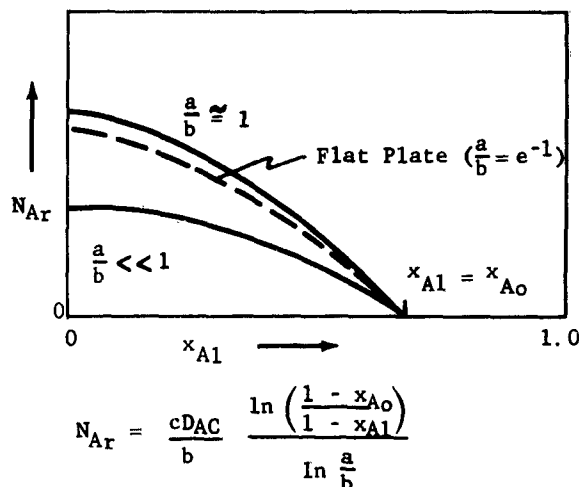
(1) The flat plate with film thickness z_1 is comparable to the cylinder of radius $b = z_1$, with film thickness $\left(1-\frac{1}{e}\right)z_1$. Therefore the comparison actually reflects a change in film thickness as well as geometry. However, for small values of $\frac{a}{b}$ this discrepancy is minimized.

107

For small values of $\frac{a}{b}$ at constant N_{Ar}, the interfacial concentration x_{AI} and therefore the average concentration decreases. Thus the average concentration in the film within a pore will be less than at a flat plate with the same overall reaction rate and approximate film thickness provided $\frac{a}{b}$ for the pore is small enough.

The concentration is averaged over the film thus

$$(II\text{-}5) \quad x_{A\text{-}av} = \frac{\displaystyle\int_a^b x_A \, r \, dr}{\displaystyle\int_a^b r \, dr}$$

This equation is integrated using the concentration profile II-3

$$(II\text{-}6) \quad x_{A\text{-}av} = 1 - \frac{2}{1-\left(\frac{a}{b}\right)^2}\left[(1 - x_{AI}) - (1 - x_{Ao})\left(\frac{a}{b}\right)^2\right]\left[\frac{1}{\dfrac{\ln\left(\dfrac{1-x_{Ao}}{1-x_{AI}}\right)}{\ln\frac{a}{b}} + 2}\right]$$

which is combined with equation II-4 in order to transform to the form $f(N_{Ar})$.

$$(II\text{-}7) \quad x_{A\text{-}av} = 1 - \frac{2(1-x_{Ao})\left(\frac{a}{b}\right)^2}{1-\left(\frac{a}{b}\right)^2}\left[\frac{1}{\dfrac{N_{Ar}b}{cD_{AC}} + 2}\right]\left[\left(\frac{a}{b}\right)^{\left(\frac{bN_{Ar}}{cD_{AC}} + 2\right)} - 1\right]$$

This average concentration is a monotonic decreasing function of the overall reaction rate. This is seen by differentiating equation (II-7) to give

$$(II\text{-}8) \quad \frac{dx_{A\text{-}av}}{dN_{Ar}} = \left[\frac{-2(1-x_{Ao})\left(\frac{a}{b}\right)^2}{1-\left(\frac{a}{b}\right)^2}\right]\left[\frac{b}{cD_{AC}}\right]\left[\frac{1}{\dfrac{bN_{Ar}}{cD_{AC}} + 2}\right]^2\left[\left(\frac{a}{b}\right)^{\left(\frac{bN_{Ar}}{cD_{AC}} + 2\right)}\right]$$

$$\left[-1 - \left(\ln \frac{a}{b}\right)\left(\frac{bN_{Ar}}{cD_{AC}} + 2\right) + \left(\frac{a}{b}\right)^{\left(\frac{bN_{Ar}}{cD_{AC}} + 2\right)}\right]$$

Since the last factor is always positive, i.e.

$$\sum_{n=2}^{\infty} \frac{\left[\left(\frac{bN_{Ar}}{cD_{AC}} + 2\right)\left(\ln \frac{a}{b}\right)\right]^n}{n!}$$

converges and is positive for all values of $\left(\frac{bN_{Ar}}{cD_{AC}} + 2\right)$ when $\frac{a}{b} < 1$, the derivative $\frac{dx_{A\text{-}av}}{dN_{Ar}}$ is always negative.

Equation II-7 can be applied to the case of methanol oxidation considered in part 1, where

$$D_{AC} = 10^{-5} \text{ cm}^2/\text{sec at } 20°C. \text{ and } 1 \text{ atm.}$$
$$x_{Ao} = 0.02 = \text{mole fraction of methanol at } r = a$$
$$c = 0.052 \text{ moles/cc}$$
$$N_{Ar} = 0.173 \times 10^{-8} \text{ i}$$
$$i = \text{milliamps/cm}^2$$
$$b = 10^{-2} \text{ cm}$$
$$\frac{a}{b} = 10^{-2} \text{ or } K = b - a = \text{film thickness} = .0099 \text{ cm}$$

Results are shown in Figure $\overline{C}$-6 and Table $\overline{C}$-2. The limiting current is calculated from II-4 setting $x_{A_1} = 0$.

Figure $\overline{C}$-6

Effect Of Overall Reaction Rate On Average
Methanol Concentration In Fluid Film
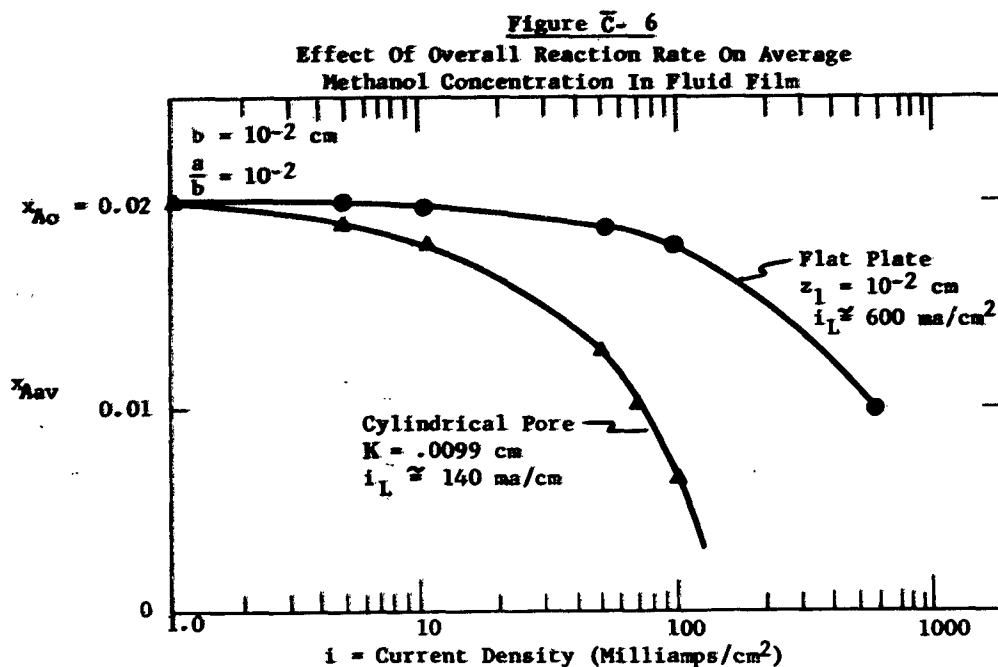
TABLE $\overline{C}$-2

i Milliamps/cm^2	$\dfrac{1-x_{Aav}}{1-x_{Ao}}$	x_{Aav}
0	1.000	0.020
5	1.001	0.019
10	1.002	0.018
50	1.007	0.013
70	1.010	0.010
100	1.013	0.007

109

In order to show the effect of free stream concentration, calculations for x_{Ao} values of 0.02 and 0.01 are compared in Figure C-7.
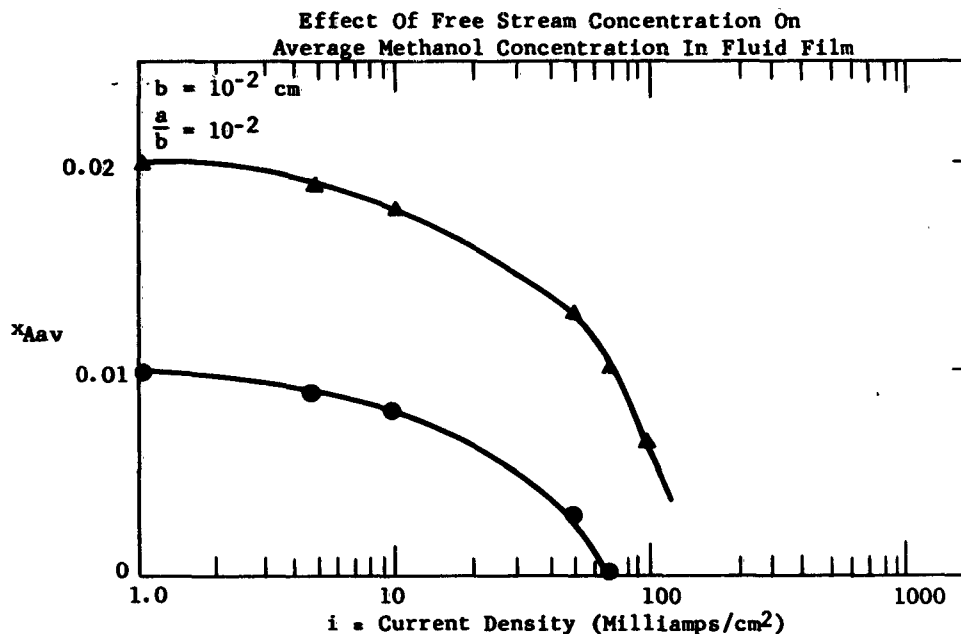
Figure C-7

Effect Of Free Stream Concentration On
Average Methanol Concentration In Fluid Film

i = Current Density (Milliamps/cm²)

TABLE C-3

i Milliamps/cm²	$\dfrac{1 - x_{Aav}}{1 - x_{Ao}}$	x_{Aav}
0	1.000	0.010
5	1.001	0.009
10	1.002	0.008
50	1.007	0.003
70	1.010	0.0003

Since it is difficult to know the exact value of $\frac{a}{b}$ in the previous example, it is necessary to consider its effect on the calculation. This is done in Figure C-8 for overall reaction rates of 50 and 100 milliamps/cm² assuming a constant pore radius of 10^{-2} cm and x_{Ao} = .02 . The decrease in x_{Aav} is more pronounced for smaller values of $\frac{a}{b}$. It is generally of interest to know the value of the concentration averaged over the entire pore diameter instead of just the fluid film. However, for small values of $\frac{a}{b}$ where the effective decrease in concentration is appreciable, the contribution to the total cross-sectional area by the free stream is negligible, e.g. 1% or less for $\frac{a}{b}$ < 0.1.

Effect Of Free Stream Radius On Average
Methanol Concentration In Fluid Film
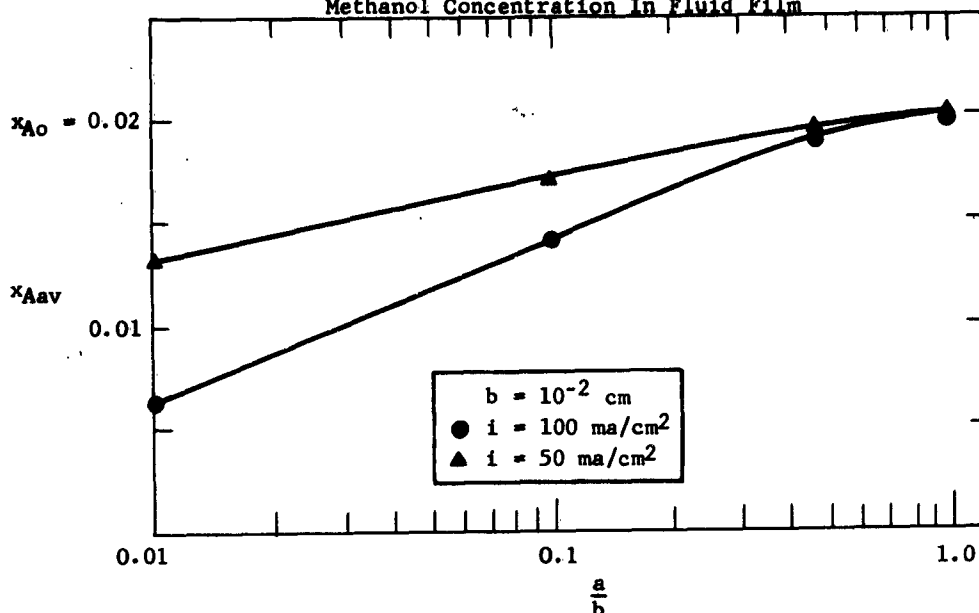
The effect of pore size on methanol transport and oxidation can also be predicted from equation II-7. As discussed in part I, the copious quantities of insoluble CO_2 released at the catalyst surface provide efficient stirring so that the film thickness $K = b - a$ is assumed to be a constant minimum value. Using this assumption, the average film concentration is expressed as a function of pore size, b, as follows.

$$(II-9) \quad x_{Aav} = 1 - \frac{2(1 - x_{Ao})(1 - \frac{K}{b})^2}{2\frac{K}{b} - \left(\frac{K}{b}\right)^2} \left[\frac{1}{\frac{bN_{Ar}}{cD_{AC}} + 2} \right] \left[\left(1 - \frac{K}{b}\right)^{-\left(\frac{bN_{Ar}}{cD_{AC}} + 2\right)} - 1 \right]$$

This function is plotted in Figure $\bar{C}$-9 assuming an overall reaction rate of 100 ma/cm^2, $x_{Ao} = 0.02$, and $K = 0.01$ cm. [1]

As pointed out previously, it is actually the average pore concentration, X_{Aav}, rather than the average film concentration, x_{Aav}, which is often of interest. The average pore concentration is given by

$$(II-10) \quad X_{Aav} = x_{Aav} + \left(\frac{a}{b}\right)^2 (x_{Ao} - x_{Aav})$$

and is also plotted in Figure $\bar{C}$-9. Note that effective reduction of concentration of methanol in the pore is achieved for $b < 0.016$ cm where $X_{Aav} \simeq x_{Aav}$.

_____

[1] Note that at $b = 0.01$ cm, K is assumed to be 0.0099 cm. for purposes of calculation.

111
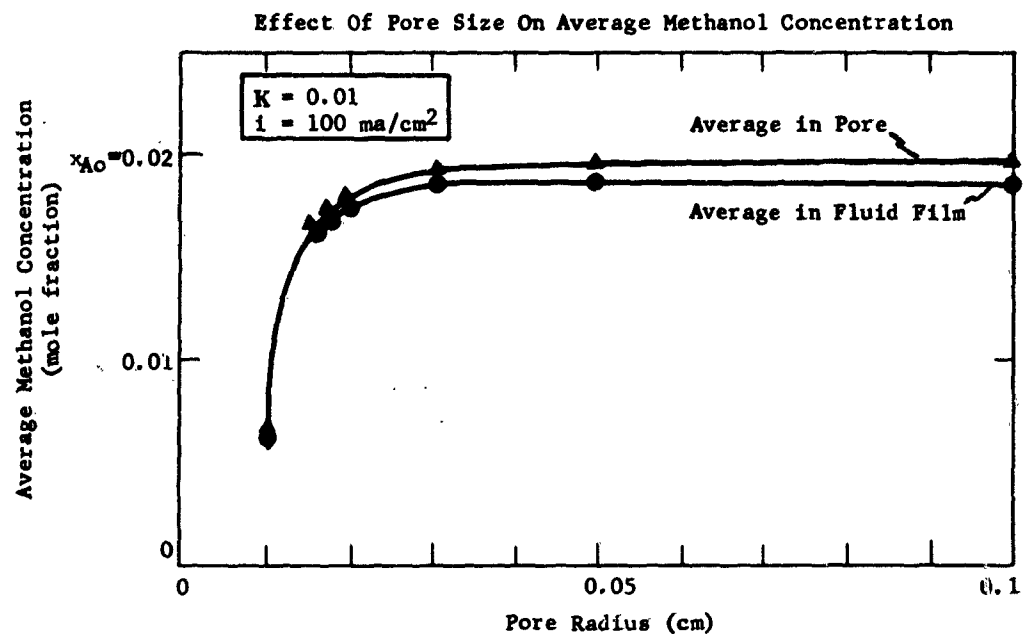
III. Transient Longitudinal
Methanol Diffusion In An
Operating Electrode Structure

The reaction of methanol at the catalyst interface in a porous electrode can be used to decrease the average concentration of methanol within the electrode structure at steady-state. This was explained in parts I and II. In order to complete the analysis, it is necessary to consider the transient behavior of such a system, i.e. the approach to steady-state. In addition to the porous catalytic electrode, a membrane is included as part of the overall structure. The small pores of the membrane prevent bulk mixing of the fluid on either side of the electrode by agitation due to CO_2 evolution and limit the transport mechanism to diffusion.
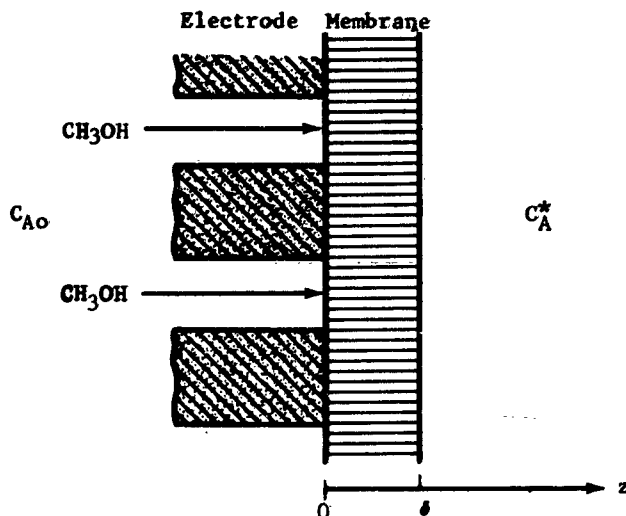
The methanol diffuses through the electrolyte filled pores of the electrode where some of it is reacted to form CO_2. The remainder passes through the very small pores of the membrane.

It is assumed that steady-state in the electrode pores is achieved rapidly and the transient problem is reduced to diffusion through the small pores of the membrane with a constant methanol concentration at $z = 0$. This concentration depends on the electrode structure and the reaction rate and is described in equations II-7 and II-10. This treatment is valid when the pore radius is greater than 10^{-2} cm and the length to diameter ratio is approximately unity. For very small diameters or very long pores, appreciable time is required to reach steady-state in the electrode. In this case, the transient problem is one of diffusion through the membrane with a concentration at $z = 0$ which increases gradually from zero to the final steady-state value within the electrode. An analysis of this problem is _not_ presented.

113

The molar flux of methanol through the membrane is

(III-1) $\quad N_{Az} = -\bar{D}_{AC} \dfrac{\partial c_A}{\partial z}$

where equimolar countercurrent diffusion of methanol and electrolyte is assumed and

c_A = $x_A c$ = molar concentration of methanol within the membrane.
c = total molar concentration = constant
N_{Az} = molar flux of methanol in the z direction
$\bar{D}_{AC}$ = binary diffusivity of methanol through the electrolyte within the membrane = constant
z = spatial coordinate

The differential equation for mass transport is

(III-2) $\quad \dfrac{\partial c_A}{\partial t} = \bar{D}_{AC} \dfrac{\partial^2 c_A}{\partial z^2}$

During the establishment of a methanol concentration gradient in the membrane, the boundary conditions are

$c_A = c_{Aav}$ at $z = 0$ for $t > 0$
$c_A = 0$ at $z = \delta$ for $t > 0$

with an initial condition

$c_A = 0$ at $t = 0$ for $0 < z < \delta$

This problem has been solved in a number of references (1) to give

(III-3) $\quad c_A = c_{Aav}\left(\dfrac{\delta - z}{\delta}\right) + \dfrac{2}{\pi}\sum_{n=1}^{\infty} \dfrac{c_{Aav} \cos n\pi}{n} \sin \dfrac{n\pi(\delta - z)}{\delta} e^{-\frac{\bar{D}_{AC}n^2\pi^2 t}{\delta^2}}$

It is shown that for values of

(III-4) $\quad \dfrac{\bar{D}_{AC}t}{\delta^2} > 0.5$

the series in equation (III-3) approaches zero and the concentration gradient becomes and remains linear. The total amount of methanol which has diffused through the membrane at this time is given by

(III-5) $\quad Q = 0.34 \; \delta \, c_{Aav}$

where

Q = moles of methanol diffused per unit of open area in the membrane
δ = thickness of the membrane

For most membranes the linear gradient is established rapidly and the amount of methanol diffused in this time is negligible.

(1) See for example: Crank, J., "The Mathematics of Diffusion", pp. 47-49, Oxford Press.

114

After the linear gradient is established, the problem of methanol transport through the membrane into a stirred tank is formulated to give

$$\text{(III-6)} \quad \frac{dc_A^*}{c_{Aav} - c_A^*} = \frac{\overline{D}_{AC}}{\delta} \frac{S}{V} \, dt$$

with initial condition

$$c_A^* = 0 \quad \text{at} \quad t = 0$$

where

c_A^* = concentration of methanol in the stirred tank
S = void fraction of the membrane
V = volume of the stirred tank

The concentrations c_{Aav} and c_A^* are assumed to be equal to the methanol concentrations within the membrane at $z = 0$ and $z = \delta$ respectively.

The solution of this problem is

$$\text{(III-7)} \quad \ln \frac{c_{Aav}}{c_{Aav} - c_A^*} = \frac{\overline{D}_{AC}}{\delta} \frac{S}{V} \, t$$

This equation is shown in Figure C-10 for

$c_{Aav} = 1$ mole/ liter
$\overline{D}_{AC} = 2 \times 10^{-6}$ cm^2/sec
$\delta = 0.016$ cm
$\frac{S}{V} = 0.022$ (cm)$^{-1}$

The membrane constants are calculated for a commercially available membrane(1). From equations III-4 and III-5, the time required for establishing the linear gradient is calculated to be 75 seconds and the concentration c_A^* at that time is .0001 moles/liter.

Figure C-10

Transient Diffusion of Methanol Through A Membrane
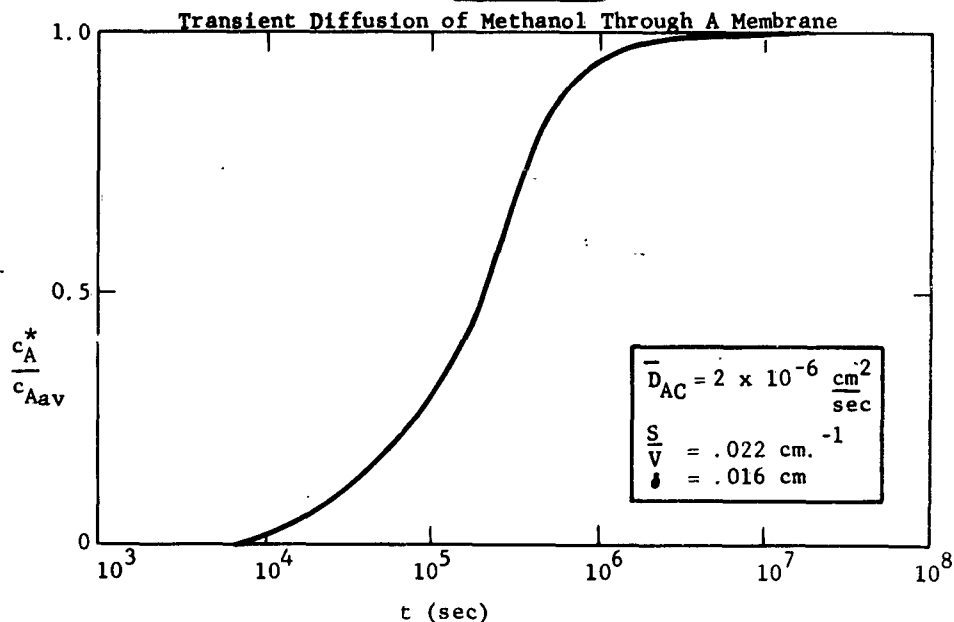
(1) AMFion C313

SUMMARY OF DATA FROM FUEL CELL
RUNS WITH THE CH3OH FUEL AND AIR-HNO3 REDOX SYSTEM

	3579-87	3579-93A	3579-93B	3579-100	3579-106	3579-110A	3579-110B	3579-118
Notebook And Page No.								
Pressure, atm. abs.				----1.0----				
Temperature, °C.	60-77	71-81	77-85	73-77	73-75	82-84	77	79-82
Cell Specifications								
Thickness of Sections:								
Anolyte, mils	875	------137------		137	137	------137------		137
Electrolyte, mils	250	------62------		22[1]	5.6[1]	----5.6[1]----		68[2]
Catholyte, mils	1250	------875------		875	875	------1125------		1000
Cathode To Air Louver, mils	375	----------None----------				------250------		125
Anode								
No. of Pt Screens	3	--------3--------		3	3	--------3--------		3
Mesh of Pt Screens	52	--------52--------		80	80	--------80--------		80
mg Pt Black/cm²	8	--------8--------		8	8	--------8--------		8
Cathode								
No. of Pt Screens	1	--------3--------		3	3	--------3--------		3
Mesh of Pt Screens	80	--------80--------		80	80	--------80--------		80
mg Pt Black/cm²	8	--------8--------		8	8	--------8--------		8
Membranes			----AMP C313 (5.6 mil thickness)[3]----					
No. of Membranes Used	2	--------2--------		4[4]	1	--------1--------		1
Anolyte, M/L of CH3OH in 30 wt.% H2SO4	0.25	0.20	0.50	0.25	0.25	0.25	0.25	0.25
Catholyte, wt.% HNO3 in 30 wt.% H2SO4	1.0	1.0	1.0	1.0	1.0	1.0	1.0	1.0
Hours Operation Before Sharp								
Activity Loss At Anode		9[5]	------55------		20	13	------12------		4
Electrical Performance								
Current Density, ma/cm²	30	39	44	14	54	58	79	38
Volts Polarization At:								
CH3OH Anode	0.57	0.58	0.56	0.49	0.48	0.52	0.60	0.51
Air-HNO3 Cathode	0.27	0.26	0.27	0.19	0.22	0.21	0.21	0.19
IR Drop	0.05	0.13	0.10	0.41	0.32	0.30	0.30	0.36
Observed Cell Voltage	0.32	0.24	0.28	0.12	0.19	0.18	0.10	0.15
Efficiency, %	25	19	22	10	15	14	8	12
Power, mwatts/cm²								
Ex. IR	11.1	14.4	16.7	7.4	27.5	27.8	31.6	19.3
Observed	9.6	9.3	12.3	1.7	10.2	10.4	7.9	5.7
Ohmic Resistance In Cell	0.02	0.04	0.03	0.35	0.07	0.06	0.04	0.11
Feed Utilization								
Run Hours Represented	6	7[9]	6.5[8]	-	-	6.5	-	4
CH3OH Conversion, %	50.0	44.5	14.5	-	-	63.0	-	38.4
% Of Reacted CH3OH Used								
Electrochemically	86.7[6]	92.1	78	-	-	96	-	97.4
Chemically At Cathode	13.3	7.9	22	-	-	4	-	2.6
Feed Rate, Stoichiometric Ratio To Current:								
O2 In Air	1.5	1.5	1.8	-	-	0.6[10]	-	0.9
Air Feed Into	Cell	----Glass Bead Packed Column[7]----				Cell & Glass Bead Packed Column		
O2 Consumed, % of Stoichiometric	76	60	125	-	-	51	-	65
% Of O2 Fed That Reacted	51.4	40.0	68.5	-	-	86.7	-	71.2
% Of Reacted O2 Used For:								
HNO3 Regeneration	84.8	100	80.2	-	-	100	-	100
Oxid. NO To NO2 Lost	15.2	0	19.8	-	-	0	-	0
HNO3 Regeneration, Coulombs Measured/								
Coulomb Equiv. To HNO3 Consumed	2.9	2.5	2.7	-	-	2.0	-	2.9

(1) Thickness of membranes between the electrodes.
(2) Thickness of membrane plus a 1/16" Teflon slotted spacer.
(3) Preconditioned in electrolyte solution at 82°C. prior to installation.
(4) Gas buildup between the four membranes caused high resistance and poor performance.
(5) Shutdown due to leaks.
(6) Actually a small fraction (say 0.2%) could be lost as vapor in water removal at 82°C.
(7) Catholyte recycled into top of 3/4" dia. glass helices packed column countercurrent to air fed into bottom, temp. = 30-37°C.
(8) In a 25 hour period at 8.5% CH3OH conversion 28.6% of reacted CH3OH was used chemically at cathode (current was 7.4 ma/cm²).
(9) In a 24 hour period at 33% CH3OH conversion 12.4% of reacted CH3OH was used chemically at cathode (current was 29 ma/cm²).
(10) The glass helices packed column was operated at 40 to 57°C. with 38% of the air through the cell and 62% through the column.

ACTIVITY LOSS DURING RUN 3579-93

Figure C-11
Polarization At Methanol Anode

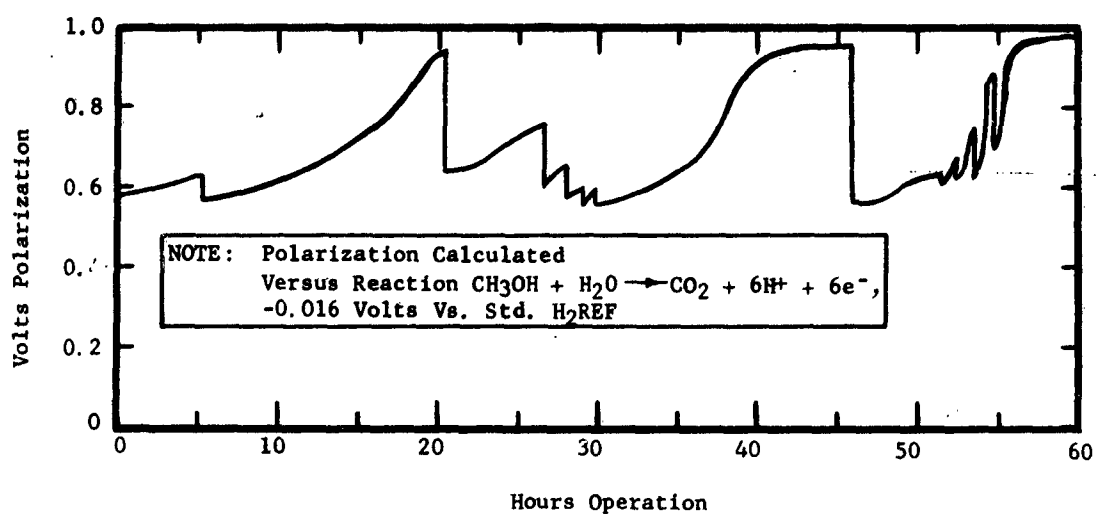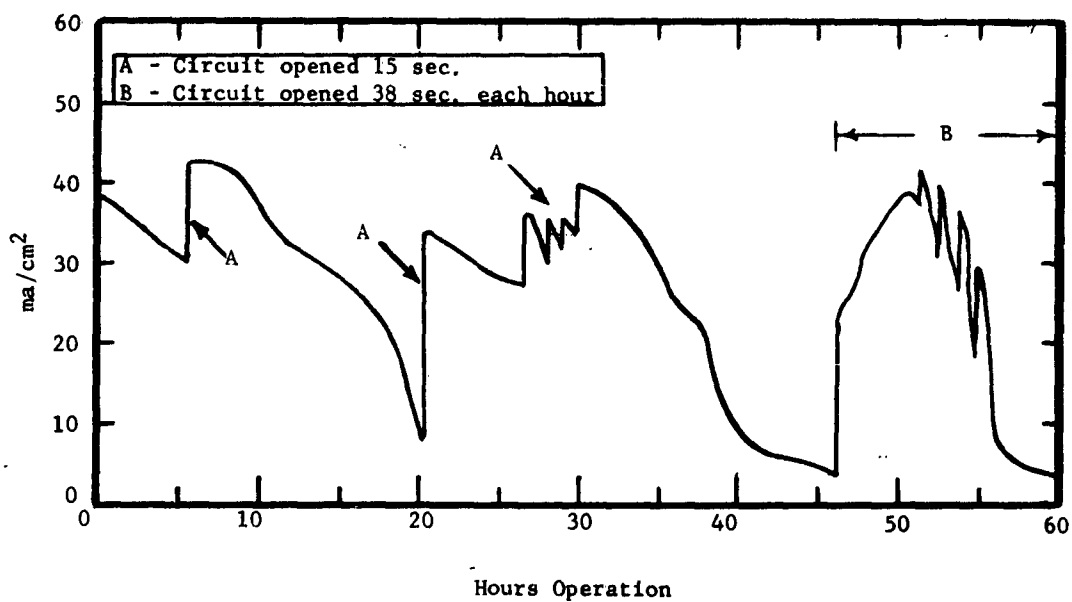NOTE: Polarization Calculated
Versus Reaction $CH_3OH + H_2O \longrightarrow CO_2 + 6H^+ + 6e^-$,
-0.016 Volts Vs. Std. H_2REF

Hours Operation

Figure C-12

Current Density

A - Circuit opened 15 sec.
B - Circuit opened 38 sec. each hour

Hours Operation

117

NOMENCLATURE

α: charge transfer coefficient
a: free stream radius
b: pore radius
c: total molar concentration
c_R: molar concentration of R
c_A: molar concentration of A
c_A^*: molar concentration of A in volume V
δ: membrane thickness
D: diffusion coefficient
D_{AC}: binary diffusion coefficient of A in C in the bulk fluid
$\overline{D}_{AC}$: binary diffusion coefficient of A in C within the membrane
E: potential
F: Faraday's constant
i: current density
K: film thickness within a pore = b-a
k^o: specific rate constant
N_{Az}: molar flux of A in the z direction
N_{Ar}: molar flux of A in the r direction
n: number of electrons in overall process
n_a: number of electrons in limiting step
P: pressure
Q: total moles of methanol diffused per unit open area of membrane
R: gas constant
r: radial coodinate
S: void fraction of the membrane
τ: transition time
t: time
T: temperature
V: volume
x_A: mole fraction of A
x_{Aav}: film average mole fraction of A
X_{Aav}: pore average mole fraction of A
z: Cartesian coordinate
z_1: film thickness at a flat plate
ln: natural logarithm
e: base of the natural logarithm

Subscripts and Superscripts

L: diffusion limited value
o: free stream or bulk value
1: interfacial value

AD-

Div.

Esso Research and Engineering Company,
Linden, New Jersey
SOLUBLE CARBONACEOUS FUEL-AIR FUEL CELL, by Carl
E. Heath, Barry L. Tarmy, and others. First semi-
annual report, 1 Jan. 1962-30 June 1962. 118p.
incl. illus. tables. (Rept. No. 1; PR&C No.
62-ELP/R-4306)
(Contract DA 36-039 SC-89156) Unclassified report

Studies are under way aimed toward the ultimate
development of a fuel cell using a partially
oxidized hydrocarbon as the fuel and air as the
oxidant at moderate temperatures and pressures.
Included are work carried out on the effects of
fuel type, catalyst composition, and other major
operating variables on the design and operation
of the fuel electrode, experiments performed to
improve the overall efficiency of the HNO3 redox
air electrode and tests designed to evaluate the
(over)

1. Power supplies-Fuel
   cells
2. Electrolyte-Soluble
   carbonaceous fuel
3. Acid electrolyte
4. Electrodes
I. Heath, C. E.
   Tarmy, B. L.
II. U.S. Army Signal
   Research and
   Development
   Laboratory
III. Contract DA 36-039
   SC-89156

AD-

Div.

Esso Research and Engineering Company,
Linden, New Jersey
SOLUBLE CARBONACEOUS FUEL-AIR FUEL CELL, by Carl
E. Heath, Barry L. Tarmy, and others. First semi-
annual report, 1 Jan. 1962-30 June 1962. 118p.
incl. illus. tables. (Rept. No. 1; PR&C No.
62-ELP/R-4306)
(Contract DA 36-039 SC-89156) Unclassified report

Studies are under way aimed toward the ultimate
development of a fuel cell using a partially
oxidized hydrocarbon as the fuel and air as the
oxidant at moderate temperatures and pressures.
Included are work carried out on the effects of
fuel type, catalyst composition, and other major
operating variables on the design and operation
of the fuel electrode, experiments performed to
improve the overall efficiency of the HNO3 redox
air electrode and tests designed to evaluate the
(over)

1. Power supplies-Fuel
   cells
2. Electrolyte-Soluble
   carbonaceous fuel
3. Acid electrolyte
4. Electrodes
I. Heath, C. E.
   Tarmy, B. L.
II. U.S. Army Signal
   Research and
   Development
   Laboratory
III. Contract DA 36-039
   SC-89156

AD-

Div.

Esso Research and Engineering Company,
Linden, New Jersey
SOLUBLE CARBONACEOUS FUEL-AIR FUEL CELL, by Carl
E. Heath, Barry L. Tarmy, and others. First semi-
annual report, 1 Jan. 1962-30 June 1962. 118p.
incl. illus. tables. (Rept. No. 1; PR&C No.
62-ELP/R-4306)
(Contract DA 36-039 SC-89156) Unclassified report

Studies are under way aimed toward the ultimate
development of a fuel cell using a partially
oxidized hydrocarbon as the fuel and air as the
oxidant at moderate temperatures and pressures.
Included are work carried out on the effects of
fuel type, catalyst composition, and other major
operating variables on the design and operation
of the fuel electrode, experiments performed to
improve the overall efficiency of the HNO3 redox
air electrode and tests designed to evaluate the
(over)

1. Power supplies-Fuel
   ells
2. Electrolyte-Soluble
   carbonaceous fuel
3. Acid electrolyte
4. Electrodes
I. Heath, C. E.
   Tarmy, B. L.
II. U.S. Army Signal
   Research and
   Development
   Laboratory
III. Contract DA 36-039
   SC-89156

AD-

Div.

Esso Research and Engineering Company,
Linden, New Jersey
SOLUBLE CARBONACEOUS FUEL-AIR FUEL CELL, by Carl
E. Heath, Barry L. Tarmy, and others. First semi-
annual report, 1 Jan. 1962-30 June 1962. 118p.
incl. illus. tables. (Rept. No. 1; PR&C No.
62-ELP/R-4306)
(Contract DA 36-039 SC-89156) Unclassified report

Studies are under way aimed toward the ultimate
development of a fuel cell using a partially
oxidized hydrocarbon as the fuel and air as the
oxidant at moderate temperatures and pressures.
Included are work carried out on the effects of
fuel type, catalyst composition, and other major
operating variables on the design and operation
of the fuel electrode, experiments performed to
improve the overall efficiency of the HNO3 redox
air electrode and tests designed to evaluate the
(over)

1. Power supplies-Fuel
   cells
2. Electrolyte-Soluble
   carbonaceous fuel
3. Acid electrolyte
4. Electrodes
I. Heath, C. E.
   Tarmy, B. L.
II. U.S. Army Signal
   Research and
   Development
   Laboratory
III. Contract DA 36-039
   SC-89156

AD-

UNCLASSIFIED

operability of the fuel cell components in a
complete cell. These tests demonstrate the
feasibility of combining the cell components in a
compact cell without severe losses in efficiency
due to their interaction.

UNCLASSIFIED

UNCLASSIFIED

AD-

operability of the fuel cell components in a
complete cell. These tests demonstrate the
feasibility of combining the cell components in a
compact cell without severe losses in efficiency
due to their interaction.

UNCLASSIFIED

AD-

operability of the fuel cell components in a
complete cell. These tests demonstrate the
feasibility of combining the cell components in a
compact cell without severe losses in efficiency
due to their interaction.

AD-

operability of the fuel cell components in a
complete cell. These tests demonstrate the
feasibility of combining the cell components in a
compact cell without severe losses in efficiency
due to their interaction.

UNCLASSIFIED

UNCLASSIFIED

Commanding Officer
U.S.A. Signal Research and Development
  Laboratory
Fort Monmouth, New Jersey
  ATTN: Logistics Division
       (MARKED FOR PROJECT
       ENGINEER) (2)
  ATTN: SIGRA/SL-P (1)
  ATTN: Dir of Research/Engineering (1)
  ATTN: Technical Document Center (1)
  ATTN: Technical Information Div
     (UNCLASSIFIED REPORTS ONLY
     FOR RETRANSMITTAL TO
     ACCREDITED BRITISH AND
     CANADIAN GOVERNMENT
     REPRESENTATIVES) (3)

OASD (R&D), Rm 3E1065
ATTN: Technical Library
The Pentagon
Washington 25, D.C. (1)

Chief of Research and Development
OCS, Department of the Army
Washington 25, D.C. (1)

Chief Signal Officer
ATTN: SIGRD
Department of the Army
Washington 25, D.C. (1)

Chief Signal Officer
ATTN: SIGRD-4a
Department of the Army
Washington 25, D.C. (1)

Director
U.S. Naval Research Laboratory
ATTN: Code 2027
Washington 25, D.C. (1)

Commanding Officer & Director
U.S. Naval Electronics Laboratory
San Diego 52, California (1)

Commander
Air Force Command and Control
  Development Division
ATTN: CRZC
L. G. Hanscom Field
Bedford, Massachusetts (1)

Commander
Rome Air Development Center
ATTN: RAALD
Griffiss Air Force Base, New York (1)

Commanding General
U.S.A. Electronic Proving Ground
ATTN: Technical Library
Fort Huachuca, Arizona (1)

Commanding Officer
Diamond Ordnance Fuze Laboratories
ATTN: Library, Room 211, Bldg. 92
Washington 25, D.C. (1)

Commanding Officer
U.S.A. Signal Equipment Supply Agency
ATTN: SIGMS-ADJ
Fort Monmouth, N.J. (1)

Deputy President
U.S. Army Security Agency Board
Arlington Hall Station
Arlington 12, Virginia (1)

Commander
Armed Services Technical Information
  Agency
ATTN: TIPCR
Arlington Hall Station
Arlington 12, Virginia (10)

Chief
U.S. Army Security Agency
Arlington Hall Station
Arlington 12, Virginia (2)

Commander
Astronautical Systems Division
ATTN: ASAPRL
Wright-Patterson Air Force Base
Ohio (1)

AFSC Liaison Office
Naval Air Research and Development
 Activities Command
Johnsville, Pennsylvania (1)

Commander
Air Force Cambridge Research
 Laboratories
ATTN: CRO
L. G. Hanscom Field
Bedford, Massachusetts (1)

Commander
Air Force Command and Control
 Development Division
ATTN: CCRR (1)
ATTN: CCSD (1)
L. G. Hanscom Field
Bedford, Massachusetts

Liaison Officer, LAA
U.S.A. Signal Research and Development
 Laboratory
75 South Grand Ave., Bldg. 13
Pasadena, California (1)

Power Information Center
Moore School Building
200 South Thirty-Third Street
Philadelphia 4, Pennsylvania (1)

Army Research Office
Office, Chief Research & Development
Department of the Army
Room 3D442, The Pentagon
Washington 25, D.C.
ATTN: Dr. Sidney J. Magram (1)

Director Advanced Concepts Division
Bureau of Ships (Code 350)
Washington 25, D.C.
ATTN: LCDR, Frank W. Anders (1)

Office of Naval Research (Code 429)
Department of the Navy
Washington 25, D.C.
ATTN: Mr. James R. Patton, Jr. (1)

Commander
Aeronautical Systems Division
Wright-Patterson Air Force Base
Ohio
ATTN: Mr. George W. Sherman (1)

Assistant Director, Material Sciences
Advanced Research Projects Agency
The Pentagon, Room 3E153
Washington 25, D.C.
ATTN: Mr. Charles F. Yost (1)

Advanced Research Projects Agency
The Pentagon, Room 3E157
Washington 25, D.C.
ATTN: Dr. John H. Huth (1)

National Aeronautics & Space
 Administration
1520 H. Street, N.W.
Washington 25, D.C.
ATTN: Mr. David Novik (1)

National Aeronautics & Space
 Administration
1512 H. Street, N.W.
Washington 25, D.C.
ATTN: Mr. Ernst M. Cohn (RPP) (1)

Equipment & Supplies Division
Office of Ordnance
Office, DODR&L
The Pentagon
Washington 25, D.C.
ATTN: Mr. G. B. Wareham (1)

Director
Advanced Research Projects Agency
Washington 25, D.C. (6)

Chief Signal Officer
Department of the Army
Washington 25, D.C. (8)

U.S. Army R&D Liaison Group
  (9851 DV)
APO 757
New York, New York
ATTN: Dr. B. R. Stein   (1)

Director
U.S. Army Engineer Research and
  Development Laboratory
Fort Belvoir, Virginia
ATTN: Dr. D. Looft   (1)

Chief of Ordnance
Department of the Army
Washington 25, D.C
ATTN: Mr. J. Crellin (ORDTB)   (1)

Engelhard Industries, Inc.
Military Service Department
113 Astor Street
Newark 2, New Jersey
ATTN: Mr. V, A. Forlenza   (1)

Union Carbide Corporation
Union Carbide Consumer Products Co.
270 Park Avenue
New York 17, New York
ATTN: Mr. R. B. Klopfenstein   (1)

United Aircarft Corporation
Pratt & Whitney Aircraft Division
East Hartford 8, Connecticut
ATTN: Mr. J. M. Lee   (1)

General Electric Company
Research Laboratory
Schenectady, New York
ATTN: Dr. H. Liebhafsky   (1)

University of Pennsylvania
John Harrison Laboratory of
  Chemistry
Philadelphia 4, Pennsylvania
ATTN: Dr. J. Bockris   (1)

Speer Carbon Company
Research Laboratory
Packard Road @ 47th Street
Niagara Falls, New York
ATTN: Dr. W. E. Parker   (1)

Dr. H. D. Gregor
150 Lakeview Avenue
Leonia, New Jersey   (1)

General Dynamics Corporation
General Atomic Division
P.O. Box 608
San Diego 12, California
ATTN: Library (L)   (1)